phantastica: a gene required for dorsoventrality of leaves in *Antirrhinum majus*

Richard Waites

Doctor of Philosophy

The University of Edinburgh

1995

This thesis has been composed by myself and unless otherwise stated all work presented here is my own.

Abstract

Leaves have three striking morphological features. Firstly, they are much longer and wider than thick, secondly they are produced laterally from the stem axis and thirdly, they exhibit dorsoventrality. To understand better the mechanisms that lead to dorsoventrality in the lateral organs of plants the morphology of mutants of the *phantastica (phan)* locus of *Antirrhinum majus* were characterised. The leaves, bracts, and petal lobes of *phan* mutants showed varying degrees of reduction in dorsal tissues, indicating that *phan* is required for establishing dorsal cell identity. Each *phan* mutant produces a similar variety of different leaf morphologies, but has a characteristic and relatively constant floral phenotype. In several different forms of *phan* mutant leaves and petal lobes, novel boundaries between dorsal and ventral cell types form ectopic axes of growth, suggesting that *phan*-dependent dorsal identity is required for lateral growth of the wild-type leaf and petal lobe. Comparisons between the development of wild-type and mutant petals or leaves reveal that *phan* acts early in development of these lateral organs.

To allow molecular characterisation of the *phan* gene an attempt to isolate the locus was undertaken. Stable *phan* mutant lines were crossed to transposon active lines and 18,000 F1 progeny screened for a new *phan* mutant allele. One new mutant allele, *phan*-522, was identified and this showed the genetic instability characteristic of transposon-induced mutations. A new insertion of the transposon Tam 4 was identified that appeared to be responsible the *phan*-552 mutation. It was present in the *phan*-552 mutant, but not in eight wild-type siblings and had been lost in 31 *Phan*$^{+}$ revertants in nine families produced by back-crossing the *phan*-552 mutant to its stable mutant parent. This copy of Tam 4 was isolated and DNA flanking the transposon shown to include part of the *phan* transcription unit.

CONTENTS

CHAPTER 1 INTRODUCTION

1.1 Leaves

Leaves have at least two striking features. Perhaps most remarkable is their shape. Most leaves are much longer and wider than thick. This shape is probably an adaptation to their role in photosynthesis where they present a large surface area for incidence with light, release of O_2 and absorption of CO_2. Much attention is paid to water loss from leaves, yet shape is only compromised for reduced water loss in extreme conditions and presumably at a cost to photosynthesis. This suggests the functional importance of leaf shape.

Secondly, the formation of a leaf represents a dramatic change in the pattern of development as a leaf is produced laterally from the stem and is flattened usually in a plane more-or-less perpendicular to the stem axis. This suggests novel processes are required for leaf development.

The shape of leaves is perhaps more remarkable because plant cells lack mobility. They divide by laying down a new cell wall internally and, as a result, daughter cells share the new cell wall and are unable to move apart. Therefore the mature shape of the leaf is entirely the result of polarised cell growth and division. In contrast, after an animal cell divides the daughter cells are relatively free to move. Animal cells are also not constrained by walls. Therefore, cell movement, internal cytoskeletal structures and contact with other cells can contribute to determination of animal form.

Another interesting feature of the leaf is that it may represent a developmental pattern from which other lateral organs of the plant evolved.

1.2 Leaf development

1.2.1 Leaves initiate from the vegetative meristem

A leaf initiates on the flanks of the apical meristems as a bulge of cells. The site of initiation may reflect the arrangement of cells within the meristem. The organisation of the meristem has been examined and two patterns have emerged. Firstly, three regions showing differences in rates of cell division and morphology have been identified. The central region, at the most apical point of the meristem has been defined by cells that divide less frequently and have more prominent nuclei than cells elsewhere in the meristem (Rembur and Nougarede, 1977; Nougarede and Rembur, 1978; Steeves and Sussex, 1989; Lyndon, 1990). This central region is thought to function as a source of cells for the remainder of the apical meristem (Ruth *et al.*, 1985). The second region, termed the rib region, lies at the transition between rapidly dividing cells of the meristem and the elongating, slower dividing cells of the shoot. Because of its position, this region has been attributed with organising functions in shoot development (Sachs, 1991). The third region lies at the periphery of the meristem. Cells of this peripheral region arise from the central region and extend radially towards the outer surface of the meristem (Buvat, 1952; Catesson, 1953). Secondly, evidence from periclinal chimeras has demonstrated that cells of the meristem are also arranged in three layers which reflect another level of meristematic organisation. The L1 and L2 layers are each a single cell thick and surround the central L3 core. The three layers remain distinct because divisions in L1 and L2 are almost entirely anticlinal, whereas divisions in L3 are both anticlinal and periclinal. Each of these layers contributes to the leaf (Satina *et al.* 1940; Satina and Blakeslee, 1941). The leaf epidermis is derived from the outermost layer, L1 and the internal tissues from both L2 and L3.

The central, rib and peripheral regions of the meristem contain cells of each cell layer (Essau, 1970; Steeves and Sussex, 1989; Lyndon 1990). The leaf initiates from cells of all three layers

within the peripheral region. Clonal analysis has shown that in tobacco and maize about 100 to 200 cells in all cell layers will give rise to the leaf primordium, the first point at which the leaf is morphologically distinguishable (Poethig and Sussex, 1984a, b; Poethig, 1984).

1.2.2 Leaf initiation

A number of factors have been implicated in the swelling that represents primordial initiation. The primordial bulge appears to be produced by localised shifts in the polarity and rate of cell division, and a change in the pattern of cell growth, although the relative importance of these processes is disputed.

Initiation of the leaf primordium of *Solanum tuberosum* is associated with a localised increase in the rate of cell divisions and specific changes in the pattern of cell division in at least three layers of cells (Sussex, 1955). In the surface layer of the initiation site, cells divide only anticlinally whereas in the underlying cells both anticlinal and periclinal divisions occur.

In the pea, *Pisum sativum*, changes in the polarity and rate of cell divisions have also been linked to the presumptive site of the incipient primordium (Lyndon, 1970). An increase in the rate of cell division was identified about one and a half plastochrons before emergence of the primordium. A plastochron is the unit of developmental time that separates initiation of successive leaf primordia. Changes in polarity were also noticed later as the proportion of periclinal divisions rose half a plastochron before the primordium appeared.

Further evidence for a change in the growth pattern as the primordium initiates was demonstrated by Foard (1971). *Triticum* seeds were irradiated with a dose of γ rays sufficient to stop cell division. After germination each "gamma plantlet" produced an outgrowth, as cells in the surface layer enlarged, where the next primordium was expected. This suggests that cell enlargement also has a role in leaf initiation, and that it may be sufficient for initiation in the absence of cell division.

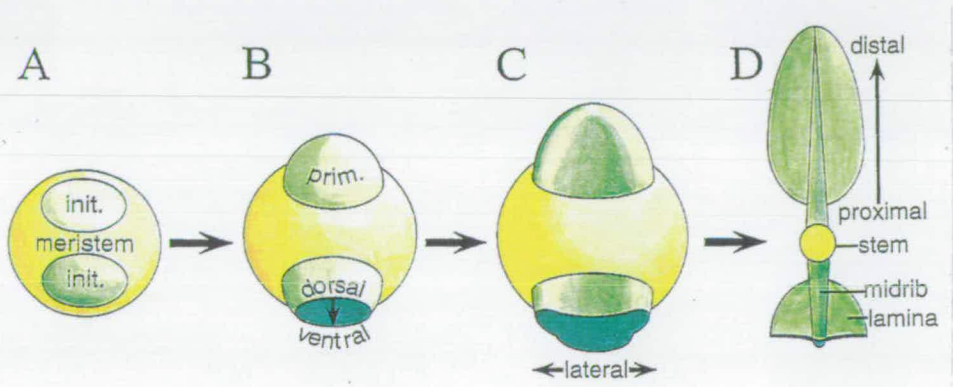

Figure 1 Leaf initiation

Successive stages in leaf initiation at the vegetative apex are represented as viewed from above. (**A**) Two groups of leaf initials (init.) destined to form leaf primordia are shown within the flanks of the vegetative meristem. (**B**) Each group of initials subsequently forms a primordium (prim.) with an axis of growth away from that of the apical meristem. (**C**) Lateral proliferation in the dorsal part of the primordium forms the laminae, and the leaf therefore shows dorsoventral asymmetry which becomes more pronounced in mature leaves (**D**).

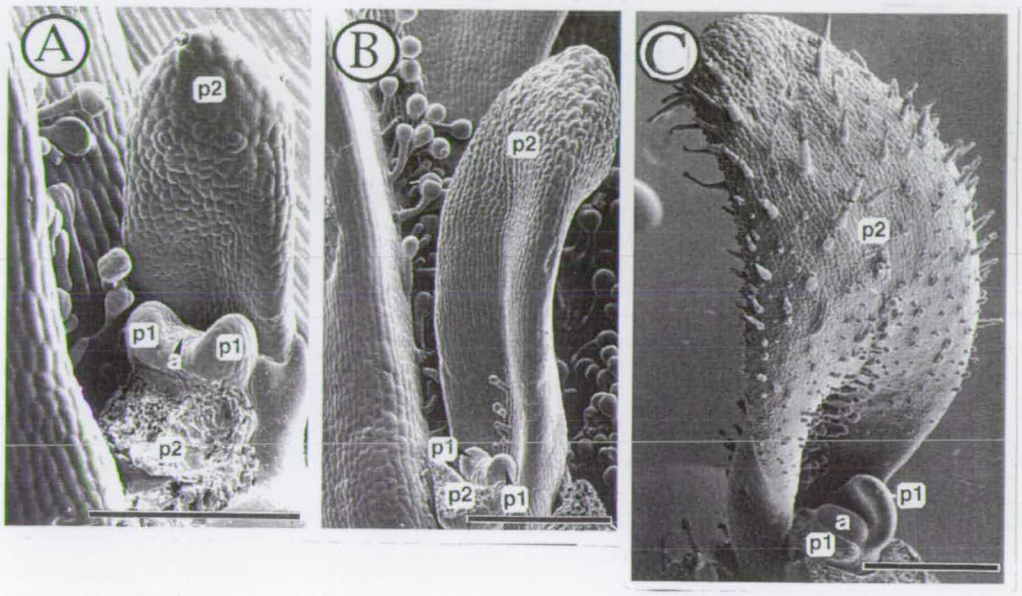

Figure 1.1. Morphogenesis of wild-type leaves of *A. majus*.

(**A**) A wild-type apex late in vegetative development. Two newly initiated leaf primordia (pl) flank the apical meristem (a). One of the older pair of leaves (p2) has been removed. At this stage, p2 shows obvious dorsoventral flattening. Subsequent growth rapidly extends the leaf axis and also increases flattening to the stage shown in **B**. (**C**) A wild-type apex early in development. The first true leaf of the plant is the largest shown (p2).

Therefore changes in the polarity and rate of cell division and cell growth have been associated with primordial initiation. Clearly all these processes may have a role in production of a leaf.

1.2.3 Early growth of the primordium

After initiation, the leaf primordium develops as a peg-like outgrowth from the summit of the original bulge of cells. A detailed study of primordial growth has been made in *Solanum tuberosum* (Steeves and Sussex, 1989). Meristematic cells next to the primordium appear to contribute to its growth as it enlarges over the surface of the apex. At initiation, the primordium of *Solanum tuberosum* is radial in transverse section (Sussex, 1954 and 1955). However, the side facing the meristem flattens as the primordium widens. As a result, the primordium becomes bilaterally symmetrical before the laminae develop.

1.2.4 Expansion of the leaf primordium

Once the primordial bulge has been formed by localised changes in growth and division of meristematic cells, the primordium enters its most dramatic period of growth. This appears to occur through a generalised pattern of cell division and expansion, which is dominated by growth in two axes. One shift in the polarity of cell division results in proliferation of the axis representing the length of the leaf and the second shift accounts for the width. The definition of the length of the leaf appears to be established early with the differentiation of the midrib and the distal tip where cells vacuolate.

The width of the leaf is established next. The most proximal part of the leaf shows little lateral expansion and becomes recognisable as the petiole. The laminae expand through a general pattern of growth involving an increased rate of cell division (Poethig and Sussex, 1985a, b). The highest rate of cell division was identified in an area between the midrib and the margin (Dubuc-Lebreux and Sattler, 1980). The margin itself does not have a meristematic function in forming the width of

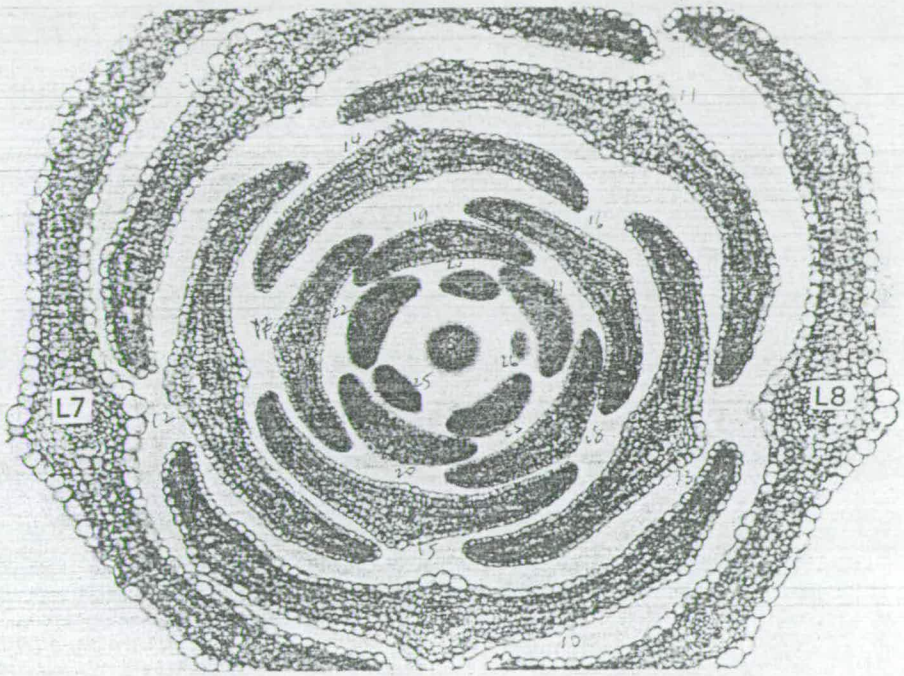

Figure 1.2 Transverse section through the apex of a 15 day old flax plant.

This details the early development of leaf primordia. 19 leaf primordia are shown and range from the youngest (26), which lacks dorsoventrality, to later stages where leaf structures such as the lamina, midrib and leaf edge have been defined.

(Adapted from The Shoot Apex and Leaf Growth, A Study in Quantitative Biology, R. F. Williams, Cambridge University Press, 1974)

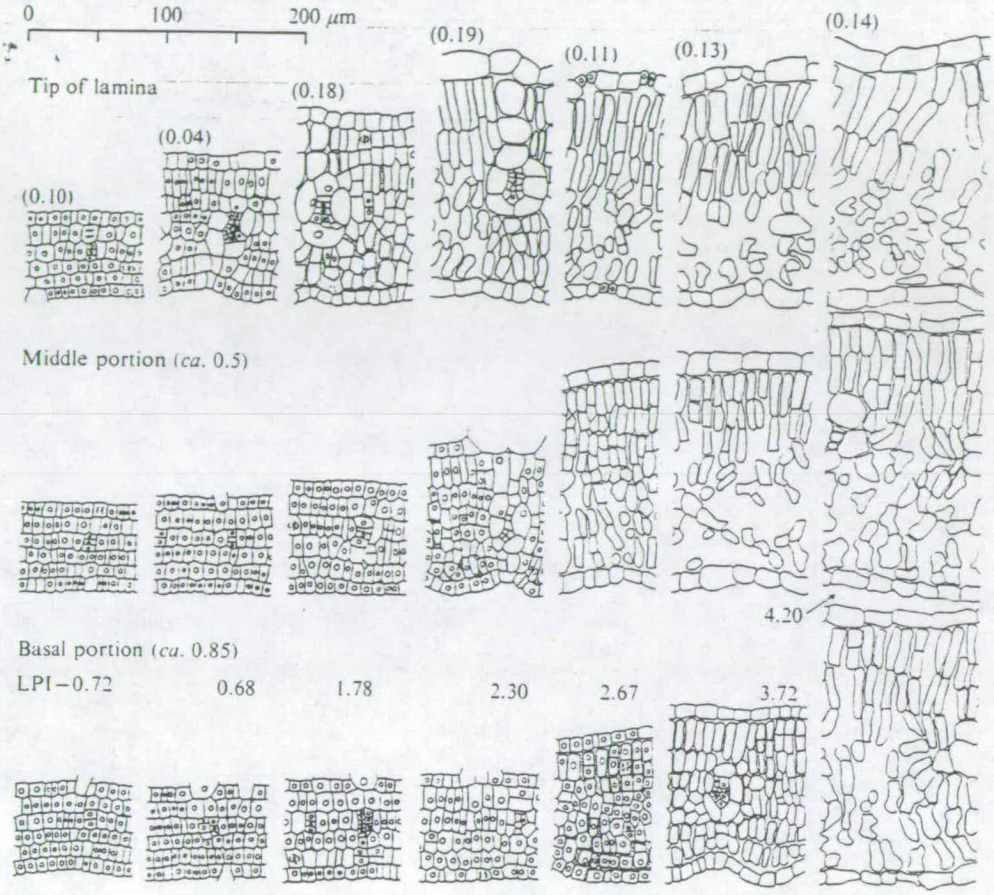

Figure 1.3 Various stages of lamina development of tip, middle and basal portions of the leaf of *Xanthium pennsylvanicum*. The numbers represent the relative positions of leaf sections from the tip.

These stages of leaf development correspond to a later period than those shown in Figure 1.2 and detail the development of different cell types which occurs after the leaf structures described in Figure 1.2 have been determined. (Adapted from Analysis of Leaf Development, R. Maksymowych, Developmental and Cell Biology Series, Eds. M. Abercrombie, D. R. Newth and J. G. Torrey, Cambridge University Press, 1973)

the leaf (Maskmowych, 1963). In tobacco, cell divisions appear to continue until the lamina is half to three-quarters its mature size (Steeves and Sussex, 1988). Proliferation ceases first at the distal end of the leaf, but continues for slightly longer in proximal areas. The rest of leaf growth is largely the result of cell expansion.

1.2.5 Positional information determines the identity of cells in leaf development

The shape of the mature leaf appears to reflect regional differences in the rate and polarity of cell division and cell expansion. Therefore it appears that cells of the developing leaf have position-dependent identities which determine their patterns of growth and division, and later specify cell types. The question remains as to how position and therefore ultimately leaf shape is defined.

1.2.6 Leaf shape and the determination of form

One possibility is that after the primordium has been established cell lineage directs subsequent growth of the leaf. However, the pattern of clones generated by irradiating tobacco leaves soon after initiation (Poethig and Sussex, 1985a, b) indicates that the contribution of initial cells is variable. Once the primordium has initiated, the position of a cell does not determine the position of its daughter cells. Because daughter cells can be displaced by divisions into a neighbouring layer and acquire the fate appropriate to their new position it appears that the fates of cells inherited from the L1, L2 and L3 layers of the apex are also not dependent on lineage. Either, the cells appear to be undetermined or they may require a constant positional signal with which their identity is maintained. If this signal is broken, for example when a cell is displaced, a new identity is established by another signal specific to the new position (Dermen, 1953; Stewart and Burk, 1970; Stewart and Dermen, 1975; Szymkowiak and Sussex, 1992 and reviewed by Dawe and Freeling, 1991).

A more appealing possibility is that the cells of a developing leaf determine their identity by responding to as yet unknown positional signals.

1.3 Objectives

Because of their size and sensitivity to wounding leaf primordia are unsuited to surgical and biochemical studies. As a result little is known about the mechanisms responsible for the determination of leaf form. An alternative approach to study early developmental processes has been to exploit mutants in which the fate of meristems and organ primordia have been disrupted. This has largely been done in three species *Antirrhinum majus* (reviewed by Coen and Carpenter, 1993), *Arabidopsis thaliana* (reviewed by Weigle and Meyerowitz, 1994) and maize (Delong *et al.*, 1993; Smith *et al.*, 1992; Vollbrecht *et al.*, 1991). The major advantage of these species is that genes that have been identified by their mutant phenotypes may be isolated. For example, in *Antirrhinum* and maize this has been achieved through transposon induced mutations that allow gene cloning by transposon tagging (Shepherd, 1988).

The role of an isolated gene can be examined in a number of ways. For example, sequence analysis may suggest the biochemical function of its product. In the case of genes involved in determination of meristem and floral organ identity, most have been found to encode transcription factors. The pattern of gene expression can be examined by *in situ* hybridisation to mRNA and compared with the domain of gene action determined from mutant phenotypes. Molecular epistasis experiments can be carried out to determine the relationship between genes in a developmental pathway. For example, the effect of a second mutation on expression of the isolated gene can be determined by *in situ* hybridisation to plants mutant for the second gene. Gene isolation also allows the effects of mis-expression to be determined in transgenic plants. Application of these approaches to floral development in *Antirrhinum* and *Arabidopsis* has lead to its becoming the best characterised

developmental system in plants (reviewed by Coen and Carpenter, 1993; Weigle and Meyerowitz, 1994).

This approach has not been fully applied to leaf development. Numerous leaf shape mutations have been identified in *Antirrhinum* (Baur, 1933; Stubbe, 1966). These may provide a way to examine the processes that determine the shape of leaves.

1.3.1 Transposon tagging and mutagenesis in *Antirrhinum*

Transposon tagging and mutagenesis strategies are discussed in the introduction to Chapter 3. Transposons in *A. majus* are described here.

1.3.2 Transposons of *Antirrhinum*

Antirrhinum was adopted as a model species for genetic analysis partly because it showed great variation in floral pigmentation. In 1890, De Vries described the inheritance of a variegated floral phenotype which has since been shown to be due to the presence of a transposon in a gene required for anthocyanin biosynthesis (Coen *et al.*, 1989). By exploiting existing pigmentation mutations, several genes encoding enzymes of anthocyanin biosynthesis, such as *nivea*, *pallida* and *incolorata*, and a regulator of this pathway, *delila*, have been isolated along with four different transposons, Tam 1, Tam 2, Tam3 and Tam 4, responsible for mutations in these loci (Sommer *et al.*, 1988a; Almeida *et al.*, 1989; Coen *et al.*, 1989; Luo *et al.*,. 1991; Goodrich *et al.*, 1992). Of the ten different transposons isolated, four have been characterised in some detail. Tam 1, Tam 2, and Tam 4 are related. All have 13 bp terminal inverted-repeats that are identical and all share a conserved 700 bp sub-terminal region. Because the terminal repeats end in the sequence 5'-CACTA-3' these related elements have been termed the CACTA family. Only Tam 1 appears capable of encoding a protein necessary for transposition (transposase), and therefore transposition of the other CACTA elements is assumed to require

the presence of an active copy of Tam 1 in the genome to provide transposase. Tam 1 shows homology to the *Spm* and *En* transposons of maize in both the transposase-coding and over 12 out of 13 bp of the terminal inverted repeats (Bonas *et al,* 1984; Upadhyaya *et al.,* 1985). Related CACTA elements have also been identified in a variety of species (Bureau and Wessler, 1994; Inagaki *et al.*, 1994). All appear to transpose by a similar mechanism that involves excision from a donor site, almost always leaving a sequence footprint, and insertion at a recipient site that generates a 3 bp direct duplication of host DNA. Additional CACTA elements have also been identified in *Antirrhinum*: Tam5 and Tam 6 (E. S. Coen and S. Doyle, pers. comm.) and Tam 7, Tam 8 and Tam 9 (Zs. Schwarz-Sommer, pers. comm.). They appear to be different on the basis of restriction maps, cross hybridisation studies and limited sequence analysis, although their complete nucleotide sequences have not yet been determined.

In contrast, Tam 3 is distinct from the CACTA transposons. It appears capable of encoding a transposase and possesses terminal inverted repeats but shows no homology to the CACTA family. All evidence suggests that there is no interaction between Tam 3 and CACTA elements. Tam 3 shows homology to the well-characterised *Ac* element of maize, with which it shares 7 out of 11 bp of the terminal inverted repeat (Sommer, *et al.,* 1985). Its transposition mechanism appears similar to that of CACTA elements, except that it has a tendency to generate larger sequence alterations on excision, and causes a direct duplication of 8 bp of host sequence upon insertion (Sommer, *et al.,* 1985; Hudson *et al.,* 1990).

All mutations caused by active transposons are characterised by genetic instability. This is illustrated by the *pallida*$^{recurrens-2}$ (*pal*$^{rec-2}$) allele which has an insertion of Tam 3 in the promoter of a gene required for anthocyanin synthesis (Martin *et al.*, 1985). The flowers of homozygous mutants are predominantly ivory but show red wild-type sectors. The sectors are caused by

somatic excision of Tam 3 from the *pal* allele leading to restoration of gene function. The majority of the progeny of the mutant show the parental phenotype, but a significant proportion have red flowers. These wild-type plants can be explained by reversion events which occured in the germline cells of the parent. Therefore transposition events can occur both during the somatic development of the plant, producing clones of wild-type cells and in cells that will give rise to gamates and produce revertant progeny.

1.3.4 *Antirrhinum majus* as a genetic system

Antirrhinum was adopted as a genetic system for similar reasons to those which have made it horticulturally important. Traditionally, plants that showed variation in certain characters, mainly in pigment but also in aspects of plant morphology, were collected as horticultural varieties, and therefore considerable genetic variation was available. It is a true diplod and self-fertile. The flowers contain large amounts of pollen and each can produce over 100 seeds. The size of the flower makes emasculation and cross pollination simple. Vegetative propagation by cuttings and grafting experiments are also possible. Because of these reasons *Antirrhinum* was adopted as a model system for early studies of inheritance, and a linkage map established in the early part of this century (Stubbe, 1966).

The advent of molecular biology allowed exploitation of the classical genetics of *Antirrhinum*. The key proved to be isolation of transposons (see above) which made transposon tagging possible (see Chapter 3). Further advantages of *Antirrhinum* for molecular genetics are that a single plant can provide large amounts of material for extraction of nucleic acids, and relatively large meristems for analysis of gene expression patterns *in situ*. The genome of *Antirrhinum* is also relatively small, making detection of single copy genes by Southern hybridisation and isolation of genomic clones routine.

As a result, *Antirrhinum* became a model system for developmental molecular genetics.

1.3.5 The leaves of *Antirrhinum majus*

The leaves of *Antirrhinum majus* have a simple ovate shape with an entire margin and can therefore be considered representative of many dicot plant leaves. They are arranged initially in a decussate phyllotaxy and during long day conditions (16 hrs light/8 hours dark) six pairs of decussate leaves are typically produced before bracts are formed in a spiral phyllotaxy. In shorter days (which are less inductive for flowering) the transition from decussate to spiral phyllotaxy may occur before bracts are formed, and later leaves therefore occur singly. Variation in leaf shape during development of the plant is slight but consistent: the lower (earlier) leaves are broader and shorter than those produced later, higher up the plant.

1.3.6 *phantastica* mutants

Perhaps the most striking leaf-shape mutants to have been described in *Antirrhinum* are those of the *phantastica* (*phan*) locus (Baur, 1907 and 1926). *phan* mutant leaves may be reduced to needle-like structures, but all mutants show a variety of leaf morphologies from needle-like to broad. Although this variation was originally interpreted as the result of somatic instability of the mutant alleles (Baur, 1926), none of the three mutants available at the start of the work described in this thesis showed germinal instability. Therefore they appeared not to be transposon induced, and somatic excision of transposons could not therefore easily explain variations in leaf morphology.

The *phan* gene was chosen as the subject of this work for several reasons. First, mutations could have a severe effect on leaf morphology, suggesting that *phan* had a fundamental role in determining the shape of leaves. Secondly, all mutants showed variation in leaf phenotype. Therefore comparisons of the development of mutant and wild-type leaves might reveal the function of the *phan* gene in some detail. A further interesting

aspect of the *phan* mutations was that they affected other leaf like organs: bracts and petal lobes. This suggests that the developmental processes in leaves, bracts, and petal lobes were similar. Therefore phenotypic characterisation of *phan* mutants was carried out and a programme of transposon-tagging undertaken to isolate the *phan* locus.

CHAPTER 2 MATERIALS AND METHODS

2.1 *Antirrhinum majus* stock lines

Jl. 75

The wild-type line, Jl. 75, was produced at the John Innes Institute, Norwich, UK from a revertant of a *pallida*^{recurrens}::Tam3 line that showed a high frequency of pale sectors on red flowers, presumably due to transposons inserting into anthocyanin loci (Harrison and Carpenter, 1979).

Jl. 98

Line Jl. 98 was also produced at the John Innes Institute, Norwich, UK. It is homozygous for the mutant *nivea*$^{recurrens-98}$::Tam3 allele (Carpenter *et al.*, 1987; Harrison and Carpenter *et al.*, 1979). Jl. 98 flowers are pink flecked with white and dark red.

Jl. 605

Line Jl. 605 is homozygous for the *olive*-605 allele that has an insertion of Tam 3 in a gene required for a key step of chlorophyll synthesis, the chelation of magnesium by protoporphyrin IX (Hudson *et al.*, 1993). The transposon excises: somatically to produce green patches on predominantly yellow leaves, and germinally at a frequency of about 5% per gamete.

2.1.1 *phan* mutant lines

phan^{ambigua}-250G and *phan*^{antiqua}-249G

The mutants *phan*^{ambigua} (*phan*-250G) and *phan*^{antiqua} (*phan*-249G), originally isolated by Baur (1926) were obtained from Zentralinstitut für Genetik und Kulturflanzenforschung, Gatersleben, Germany, and inbred as homozygous stocks for at least a further three generations. Both lines are homozygous for the semi-dominant *Eluta* mutant allele which limits anthocyanin pigmentation to the floral face and to the region between the upper petal lobes, and also for a mutant *delila* allele which prevents anthocyanin synthesis in the corolla tube.

phan-607

The *phan*-607 mutant arose amongst families produced by self-pollination of line JI. 75, in a programme designed to identify novel transposon-induced mutations (Carpenter and Coen, 1990), and was kindly provided by R. Carpenter and E. S. Coen, John Innes Centre, Norwich, UK. It was shown to carry a single recessive mutation which was unable to complement the *phan*-249G and *phan*-250G mutant alleles.

phan-709

The *phan*-709 mutant also arose in a line derived from JI. 75, in 1993, and was kindly provided of R. Carpenter and E. S. Coen, John Innes Institute, Norwich, UK.

phan-106

The *phan*-106 mutant was also produced at John Innes Institute, Norwich, UK in 1994, from a mixed genetic background. It was kindly provided of R. Carpenter and E. S. Coen.

2.2 Plant culture

Seeds were sown in Levington M3 potting compost under a thin layer of sand and germinated under a fine spray from a misting unit. Young seedlings were transferred to M3 potting compost and repotted once more before they reached maturity.

Vegetative cuttings were taken from mature plants. Healthy shoot tips were removed with a clean cut and larger leaves removed. The cut ends were dipped in hormone rooting liquid (PBI Roota). The cuttings were cultured in sand under a water misting unit in the glasshouse. Typically they rooted in about three to four weeks and were then transplanted to M3 compost.

For self pollinations, pollen from stamens was put onto the stigma of open flowers using fine tipped forceps. Care was taken to wash off unused pollen from the forceps with 70% ethanol, and the forceps were not used until excess ethanol had been shaken off.

For cross pollinations, anthers were removed, using forceps, from young flowers which had not yet opened. Emasculated flowers were then pollinated with pollen grains from another flower soon after the corollas had opened.

Plants for genetic analysis were grown in a greenhouse at an average temperature of 20°C with a minimum of 16 hours light. In winter, daylight was supplemented with light from metal halide lamps. Plants for morphological analysis were grown at 20°C in a 16 hour light - 8hr dark cycle, with illumination of 50 μmol m^{-2} photosynthetically active quanta from metal halide lamps.

2.3 *Escherichia coli* strains

JM101 (*sup*E,*thi*, Δ(*lac-pro*AB)*rps*L, [F', *tra*D36, *pro*AB, *lacI*^{q} lacZΔM15])

JM101 was stored on minimal agar plates for short periods at 4°C and in 50% (v/v) glycerol/L broth at -70°C for longer periods. Cells were taken from storage and gown overnight in minimal broth to ensure the presence of the F' plasmid.

This strain was used where selection of recombinant plasmids, such as pBluescript (Stratagene), was required using *alpha*-complementation. The pBS plasmid contains both the regulatory sequences and the first 146 aa of the β-galactosidase gene (*lac* Z). Included in the coding region is a multiple cloning site (MCS) that does not disrupt the reading frame but adds a few amino acids to the amino-terminal fragment of β-galactosidase. The host carries a mutant copy of *lac*Z that codes for the carboxy-terminal portion of β-galactosidase. Niether host encoded, nor plasmid encoded fragments are themselves active, but both can associate to form an enzymatically active protein a phenomenum named a-complementation. Using the chromogenic substrate X-gal (5-bromo-4-chloro-3-indolyl-β-D-galactoside), bacterial colonies capable of α-complementation hydrolyse the substrate and produce a blue product. Colonies carrying a copy of the plasmid with an insertion in the MCS almost always produce an

amino-terminal fragment incapable of α-complememntation and are therefore white.

C600 (F⁻, *thi*-1, *thr*-1,*leu*B6, *lac*Y1, *ton*A21, *sup*E44)
and C600*hflA*⁻ (F⁻, *thi*-1, *thr*-1, *leu*B6, *lac*Y1, *ton*A21, *sup*E44, *hfl*A150, [*chr*::Tn10]).
The C600 strains were purchased from NBL. Fresh cells were taken from a 10% glycerol stock stored at -70°C. Overnight culture were grown in L broth supplemented with 10 mM $MgSO_4$ and 0.2% maltose. Cells were sub-cultured in the same broth before use.

C600 and C600 *hfl*A⁻ were used as hosts for λgt10 genomic and cDNA libraries. After inserts have been cloned into the *Eco* RI cloning site of the *c*I gene the λ repressor is inactivated. C600 bacterial host cells are permissive to both parental and recombinant molecules and both plaques grow at the same rate: recombinant phage are lytic producing clear plaques whereas parental phage are lysogenic developing turbid plaques. The high frequency of lysogeny mutation (*hfl*A⁻150) allows growth of *c*I parental phage molecules to be repressed to between 50 and 100 fold and therefore only recombinant phages effectively produce plaques. Phage plating cells were prepared from an overnight culture of bacteria in L broth supplemented with 0.2% maltose and 10 mM $MgSO_4$. Cells were pelleted by centrifugation for 5 minutes at 3 600 rpm in an MSE Mistral centrifuge and resuspended in 10 mM $MgSO_4$ to give an absorption of 2.0 at 600 nm in a 1 cm light path.

2.4 λ phage strains

λgt10

λgt10 is a phage insertion vector which was used for the construction of genomic libraries. The vector has a unique *Eco* RI site in the *c*I repressor gene allowing selection of recombinant phage (see 2.3). Purified *Eco* RI-digested λgt10 arms were purchased from Promega.

λ DNA solutions were stored at -70°C. Phage eluates from agar plugs were stored in either 500 μl or 1 ml of phage buffer (20 mM Tris-HCl, pH 7.4, 100 mM NaCl, 10 mM $MgSO_4$ and 0.2 % (w/v) gelatin), with 15 μl or 30 μl of chloroform respectively, at 4°C.

2.5 Bacterial media and antibiotics

L broth and L agar

L broth, used for plating most *E. coli* strains and for the bottom layer of phage plates, contained 10 g bacto tryptone (Difco Laboratories), 5 g bacto yeast extract (Difco), 10 g NaCl per litre. L agar had the same composition as L broth except for the addition of 15 g l^{-1} of Bacto agar (Difco).

Minimal agar

Minimal agar, used for selection of the F' plasmid in strain JM101, contained 200 ml of 5X M9 salts (64 g $Na_2HPO_4.7H_2O$, 15 g KH_2PO_4, 2.5 g NaCl, 5.0 g NH_4Cl), 20 g glucose and 15 g Bacto agar per litre.

BBL top agar

λ phage were plated in BBL top agar, which contained 10 g trypticase (Baltimore Biological Laboratories), 5 g NaCl and 6.5 g Bacto agar per litre.

All media components were sterilised either by autoclaving (120°C, 20 minutes) or by filtration using 0.2 μm pore size Acrodiscs (Gelman Sciences, Michigan).

Antibiotics

Ampicilin was used at a final concentration of 150 μg ml^{-1} from a sterile stock of 100 mg ml^{-1} in water. Tetracycline was used at 10 μg ml^{-1} from a stock solution of 5 mg ml^{-1} in ethanol.

2.6 Nucleic acid extractions

2.6.1 Extraction of genomic DNA from *Antirrhinum*

2 - 5 g of leaf tissue, particularly from the growing tips of lateral shoots, was harvested into aluminium foil packets and frozen in liquid nitrogen. The tissue was ground for about 20

seconds with occasional shaking to a fine, light green powder in a coffee grinder which had been pre-chilled with liquid nitrogen. The powder was then thawed in 20 ml of extraction buffer (150 mM NaCl, 15 mM Na citrate, 100 mM EDTA, pH 8.0, 100 mM Na diethyldithiocarbamate) and 5 ml of 10% SDS (w/v) in a 50 ml screw top plastic centrifuge tube. Chloroform was added to bring the final volume to 50 ml and the tube with the extract was shaken for about 1 minute. The tube was spun for 5 minutes at 3 600 rpm in a bench top MSE Mistral centrifuge. The upper, aqueous, phase was removed and one half volume (12.5 ml) of phenol added to it. The phenol had previously been equilibrated with 10 mM Tris-HCl, pH 7.4. The volume was then again made up to 50 ml with chloroform and the tube shaken and spun as before. The aqueous phase was recovered after centrifugation and a further chloroform extraction performed. Nucleic acids were then precipitated by adding an equal volume of absolute ethanol and pelleted to the bottom of the tube by centrifugation at 3 600 rpm in an MSE Mistral for 10 minutes. They were dissolved in 5 ml of TE (10 mM Tris-HCl, 5 mM EDTA, pH 7.4) with 0.25 μg of RNase A, after the ethanol had been removed. RNA was digested for about 30 minutes, after which the DNA was precipitated by addition of 0.7 ml 5M NaCl and 5.7 ml of CTAB solution (2% (w/v) cetyltrimethylammonium bromide, 10 mM EDTA, 50 mM Tris, pH 8.0). The DNA was pelleted by centrifigation and washed overnight in 70% (v/v) ethanol/0.5 M NaCl. The pellet was air dried and dissolved in between 100 μl and 500 μl of TE.

2.6.2 Poly (A)$^+$ RNA isolation from *Antirrhinum*

Tissue was excised from the shoot tips of healthy plants was put immediately in aluminium foil packets floating in liquid nitrogen. The sachets of 3-4 g of tissue were stored at -70°C. To prepare RNA, the tissue was ground as described for genomic DNA extraction and thawed into 20 ml RNA extraction buffer (50 mM Tris-HCl, 150 mM LiCl, 5 mM EDTA, pH 9.0), 5 ml 10% (w/v) SDS in a 50 ml screw top centrifuge tube. The preparation was extracted twice or three times with phenol/chloroform (1:1,

v/v), until no debris collected at the interface between the phases. A further extraction with chloroform was then made. LiCl was added to the aqueous phase from an 8 M stock to a final concentration of 2 M, and RNA left to precipitate over night at 4°C. Spinning for 10 minutes at 3 600 rpm (MSE Mistral) pelleted the RNA.

The RNA pellet was redisolved in 5 ml of bind solution (0.5 M NaCl, 10 mM Tris-HCl, 1.0 mM EDTA, 0.5% (w/v) SDS, pH 7.5) and heated to 70°C to disassociate any secondary structures. For each preparation, about 0.5 g of oligo dT cellulose (Pharmacia) was added and the mixture cooled on ice. The slurry was loaded onto a 10 ml disposable plastic column (Biorad) and washed with excess bind solution. The column was then washed with several volumes of wash solution (0.15 M NaCl, 10 mM Tris-HCl, 1.0 mM EDTA, 0.5% (w/v) SDS, pH 7.5), and poly $(A)^+$ RNA eluted with repeated 200μl volumes of elute solution (10 mM Tris-HCl, 10 mM EDTA, 0.1% (w/v) SDS, pH 7.5). The eluate was collected in about 16 individual 400μl volumes each of which was precipitated by adjusting to 0.3 M LiCl and adding 2.5 volumes of ethanol. After spinning for 10 minutes at 13 000 rpm in an MSE microfuge, any tubes with a pellet were saved. Pellets were dissolve in 20 μl Northern loading buffer (1X MOPS buffer (see 2.9.1), 25% (v/v) formamide, 5.5% (w/v) formaldehyde) and 2 μl of 10X gel loading buffer (0.25% (w/v) bromophenol blue, 0.25% (w/v) xylene cyanol, 15% (w/v) Ficoll type 400) added. Samples were stored at -80°C, and heated at 85°C for 5 minutes before electrophoresis. To establish the amount of RNA in the samples, 1μl was examined by minigel electrophoresis (see 2.9.3) against standards of known concentration.

2.6.3 Bacterial plasmid minipreps

Bacteria transformed with plasmids were grown overnight with vigorous shaking at 37°C in L broth supplemented with the appropriate antibiotic for plasmid selection.

1.5 ml of the culture was decanted into a 1.5 ml Eppendorf tube and spun briefly at 6 500 rpm in an MSE microfuge to pellet the cells. The medium was removed and cells resuspended in 100 µl of resuspension buffer (50 mM glucose,10 mM EDTA, 25 mM Tris-HCl, pH 8.0). After 5 minutes at room temperature, 200 µl of lysis solution (0.2 M NaOH/1% (w/v) SDS) was added, the tubes inverted 2 or 3 times to ensure all the cells had lysed, and left for 5 minutes to allow DNA to denature. 150 µl of ice-cold KOAc solution (3 M KOAc, 2 M HOAc) was then added to neutralise the alkali allowing plasmid DNA to anneal, and to form K-SDS-protein precipitates. The contents were gently mixed to ensure the pH was similar throughout the tube, and the tubes left on ice for 5 minutes. To remove the precipitate, the tubes were centrifuged for 2.5 minutes at 13 000 rpm in a MSE microfuge, the supernatant recovered and extracted once with phenol/chloroform (1:1, v/v). Nucleic acids were precipitated from the aqueous phase by addition of two volumes of ethanol at room temperature, pelleted by centrifugation and washed briefly in 70% ethanol. The pellet was dissolved in 20 µl TE with 1 µl of RNase A (10 mg/ml) to hydolyse RNA.

Plasmid preparations from 100 ml of overnight culture were used for larger quantities of DNA. Cells were spun down in two 50 ml screw top centrifuge tubes and resuspended in 5 ml of resuspension buffer. After five minutes 10 ml of lysis solution were added and, after a further 5 minutes, 7.5 ml of ice-cold KOAc solution. The tubes were left on ice for 5 minutes and spun for five minutes at 3 600 rpm in an MSE Mistral centrifuge. The supernatant was recovered and filtered through Whatman 3MM paper. After one phenol:chloroform (1:1, v/v) extraction, plasmid DNA was precipitated with 2 volumes of ethanol. After ten minutes at room temperature the tube was centrifuged. The pellet was washed in 70% (v/v) ethanol and redissolved in 250 µl of TE with 15 µl of RNase A (10 mg/ml).

2.6.4 λ lysate cultures and λ minipreps

The agar corresponding to single positive plaque was cored out with a shortened yellow tip and eluted into 500 ml of phage buffer for two hours. A drop of chloroform was then added. 100 μl of the eluate was mixed with the same volume of plating cells and left at 37°C for 20 minutes. The infected cells were added to 5 ml of LB, supplemented $MgSO_4$ (10 mM) and maltose (0.2%), and shaken vigorously at 37°C. Lysis occured overnight. The cultures were then shaken for 30 minutes with 30 μl of chloroform to lyse any remaining intact cells.

For λ minipreps, 1 ml of lysate proved sufficient to prepare enough phage DNA (0.5-1.0 μg) for a single restriction digest. The lysate was spun briefly to remove any large cell debris and incubated with 2 μl of DNase I and RNase A (50 mg ml^{-1} each in 50% (v/v) glycerol) for 30 minutes at 37°C to digest bacterial RNA and DNA. 1 μl of Proteinase K solution (20 mg ml^{-1}) and 50 μl of 0.5 M EDTA were added. Proteinase K breaks down the nucleases and phage proteins which dissociate from phage DNA after Mg^{2+} ions are chelated by EDTA. The reaction was left for 30 minutes at 37°C. 100 μl of 3 M NaOAc and 0.5 ml phenol/chloroform (1:1, v/v) were added and the mixture vortexed for 2 minutes to ensure that all the Proteinase K had been denatured. The tubes were spun for 3 minutes and DNA from 1 ml of the aqueous layer precipitated with 600 μl of iso-propanol. After 10 minutes at room temperature, the DNA was pelleted by centrifugation for 10 minutes. The pellet was washed in 70% ethanol (v/v) and redisolved in 20 μl of TE with 0.1 μg/μl BSA to complex remaining bacterial polysaccharides.

2.7 Manipulating DNA

2.7.1 Estimation of DNA concentration

The absorption of DNA solutions was measured at 260 nm and 280 nm using a quartz cuvette with a light path of 1 cm. For genomic DNA, 10 μl of the DNA preparation was diluted with 1 ml of water before being measured in the spectrophotometer. The amount of DNA was calculated using the following formula:

concentration of DNA (mg ml^{-1}) = (2X(A260-A280)/20) X (1000/10), which partly accounts for the presence of impurities in the sample.

2.7.2 Restriction digests of DNA

Genomic DNA restriction digests for Southern blots

About 5 μg of genomic DNA was digested with each restriction enzyme. Enzymes were purchased from NBL or Boehringer and were supplied with the appropriate 10X buffer. Digests were made in a final volume of 25 μl consisting of 2.5 μl of 10X buffer, 1.5 μl of restriction enzyme (typically 15-18 units), 1.25 μl of 1 μM spermidine chloride and sterile distilled H_2O to 25 μl. The reaction mixtures were incubated at 37°C for at least two hours, after which 3.0 μl of 10X gel loading buffer (section 2.6.2) was added and 2.5 μl aliquots size fractionated in a 0.7% w/v agarose TBE mini-gel to check digestion and DNA concentrations.

Restriction digests of plasmid and phage DNA

Plasmids were digested as described for genomic DNA except that no spermidine was included in the reactions.

2.8 Purifying DNA from agarose gels

2.8.1 Isolation of genomic DNA fragments from agarose gels for construction of genomic libraries

Restriction digested genomic DNA was size fractionated in large gels (20 cm X 20 cm X 0.6 cm) of 0.7% agarose in 0.5X TBE and stained with ethidium bromide (10 μg/ml). A size fraction of DNA was cut from the gel in a thin slice (< 1 cm wide) and two further slices were cut above and below the original slice. The last lane to the right of the top slice and the first lane to the left of the bottom slice were not excised. The remainder of the gel was blotted and the filter hybridized to confirm that the correct size fraction had been removed. Gel slices were stored at -20°C until the DNA was extracted.

A piece of sterile glass paper was put over the end of a 5 ml or 10 ml disposable syringe. The slice of agarose was placed in the syringe and centrifuged at increasingly higher speeds until almost all the liquid had been removed from the agarose.

For construction of the genomic library, DNA was purified using a NACS column (Gibco BRL). The column was washed in excess 2.0 M NaCl in TE and equilibriated with excess 0.5 M NaCl in TE. The agarose eluate was adjusted to 0.5 M NaCl with 5 M NaCl and then allowed to flow through the column. The column with the DNA bound to it was washed with 10 ml 0.5 M NaCl in TE. The DNA was eluted with 200 µl of 2.0 M NaCl in TE and precipitated with two volumes of 100% ethanol at room temperature overnight, washed in 70% ethanol and dissolved in water.

For mapping size fractions of genomic DNA, the agarose eluate was extracted once with phenol/chloroform (1:1, w/v) and DNA precipitated with 1/10 th volume of 3 M NaOAc and 2.5 volumes of 100% ethanol, then washed in 70% ethanol and dissolved in sterile distilled water.

2.8.2 Isolation of plasmid DNA fragments from agarose gels

The required fragment of the plasmid was cut out of the gel and placed in a 0.75 ml Eppendorf on a bed of about 50 µl of glass beads. The tube had a small pin hole in its base. The small Eppendorf was placed in a 1.5 ml Eppendorf and the two then spun at 13 000 rpm in an MSE microfuge for five minutes or until almost all the liquid had been removed from the gel slice. The agarose remained in the smaller Eppendorf and the liquid collected in the larger tube. The eluate was extracted once with phenol:chloroform (1:1 w/v) and was then precipitated with 1/10 th volume of 3 M NaOAc and 2 volumes of ethanol at -20°C. After centrifugation the pellet was washed in 70% EtOH, briefly dried and dissolved in between 20 µl and 50 µl of TE.

2.9 Gel electrophoresis

2.9.1 Gel electrophoresis of genomic DNA

For Southern blotting, genomic DNA was resolved in either large (20 cm X 20 cm X 0.6 cm) or medium-sized (10 cm X 16 cm X 0.6 cm) gels. Agarose gels (0.7% w/v) were prepared with either 1 X or 0.5 X TBE (1X TBE is 2.5 mM EDTA, 90 mM boric acid, 90 mM Tris base). Large gels were run at 1.5 - 2.5 V cm^{-1} for 24 - 72 hours, and medium-sized gels at 2.5 - 3.0 V cm^{-1} overnight.

2.9.2 Gel electrophoresis of RNA

Agarose (0.7% w/v) was melted in 80% of the final gel volume of 1.25X MOPS buffer (200 mM MOPS, 50 mM NaAc, 10mM EDTA). The agarose was allowed to cool to about 60°C with constant stirring, formaldehyde solution (37%) added up to the final gel volume and the gel poured promptly. Before loading, the RNA samples were heated to 85°C for 5 minutes. Gels for Northern blotting were run for several hours at about 8 V cm^{-1} in 1X MOPS buffer with a peristaltic pump to recirculate the buffer between electrodes. After running, the gel was inverted and blotted in the same way as described for Southern gels.

2.9.3 Mini-gel electrophoresis of small amounts of DNA

For small quantities of DNA (e.g. for checking restriction digests and estimating amounts of DNA) small miniscus gels (15 cm X 6 cm X 3 mm) of 0.7% w/v agarose in 0.5X TBE with 10μg/ml ethidium bromide, were poured on thin glass plates. The meniscus gels were run at high voltage, 8 - 15 V cm^{-1} for1 5-30 minutes and then photographed on a UV transilluminator.

2.10 Southern hybridisations

2.10.1 Southern blotting

The agarose gel was stained with ethidium bromide (10 μl/ml) for 15-30 minutes in the same concentration of buffer as used for electrophoresis. The gel was then photographed on a UV transilluminator. The gel was turned upside down and then left shaking in 0.25 M HCl for ten minutes in which time acid depurination leads to nicking of DNA allowing larger fragments

to be blotted more efficiently. The acid was removed and the gel washed briefly in distiled water. The gel was then left gently shaking for about 30 minutes in denaturing solution (1.5 M NaCl, and 0.5 M NaOH) to denature the DNA. This solution was then replaced by neutralising solution (1.5 M NaCl, 0.5 M Tris-HCl, 1 mM EDTA, pH 7.2) and the gel again left shaking for 30 minutes.

The gels were blotted using a wick of three pieces of Whatman 3MM paper supported by three perspex sheets. These were soaked in 20X SSC (1M NaCl, 100 mM Na citrate) and bubbles removed from between the sheets by rolling with a glass rod. The gel was laid upside down on top of the wick and bubbles gently forced out from between the gel and the wick. A piece of Hybond-N nylon filter (0.45 μm, Amersham) was cut to the size of the gel and rinsed in 2X SSC. This was placed on top of the gel and bubbles again removed. About six pieces of Whatman 3MM paper were placed on top of the filter, the first two soaked in 2X SSC to ensure the absence of air bubbles which would hinder DNA transfer. Finally, paper towels were put on top of the Whatman 3MM paper to soak up 20X SSC from the tray through the gel. The gel was blotted for at least 24 hours, after which the filter was washed in 2X SSC and left to air dry. The DNA was fixed to the filter by UV crosslinking using 0.4 J cm^{-2} of UV light from a transilluminator.

2.10.2 Random primer labelling of DNA probes for hybridisation

25 - 50 ng of DNA for probe synthesis was made single stranded by boiling for 5 - 10 minutes in a total volume of 15.5 μl. This was cooled rapidly on ice, and 6 μl oligo labelling buffer (250 mM Tris-HCl, pH 8.0, 25 mM $MgCl_2$, 5 mM β-mercaptoethanol, 2 mM each of dATP, dTTP, dGTP, 1 M HEPES, pH 6.6, 1 mg ml^{-1} random hexamers) and 1.0 μl of BSA (10μg/ml) added. 1.5 μl (1.5 units) of the Klenow fragment of DNA Polymerase I was added, followed by 30 μCi (3μl) of [α^{32}P]dCTP (3 Ci μmole^{-1}, Amersham). The enzyme synthesises labelled single strands using the hexamers present in OLB as primers and the single

stranded DNA as template. The reaction was incubated at 37°C for about 45 minutes.

2.10.3 Purifying labelled DNA probes

Radio-labelled probes were purified from unincorporated labelled nucleotide with a G50-Sephadex (Pharmacia) column. The bottom of the barrel of 1 ml disposable syringe was covered with a piece of sterile glass paper and the syringe filled with TE. After a few drops of TE had run out of the syringe, the G50-Sephadex slurry was added drop by drop to form a column with about 1 cm of TE left at the top of the syringe. The column was stored temporarily under TE with the narrow end of the syringe closed with parafilm.

For purifying the probe, the column was supported by a retort stand and allowed to drain. About 30 μl of 5% (w/v) blue dextran, 0.5% (w/v) orangeG was added to the probe as markers. Blue dextran co-elutes with DNA and orange G with unincorporated nucleotides. The sample was loaded onto the column and allowed to run in to the Sephadex bed. The column was continuously topped up with TE and run off was collected until the orange G marker was about 2 cm from the bottom of the syringe. Typically, about 600 μl of column run-off was collected. The column was disposed of, and the probe denatured by heating to 100°C for 5 - 10 minutes immediately before use.

2.10.4 Hybridisations

Filters were pre-hybridised by gentle shaking at 65°C in large plastic sandwich boxes for at least 15 minutes in 50 ml of hybridisation buffer (41 ml sterile distilled water, 7.5 ml 20X SSC, 0.5 ml 10% (w/v) SDS, 0.5 ml 2% (w/v) Ficoll, 1 ml 2% (w/v) polyvinylpyrollidone) with 0.5 ml of Herring sperm DNA (50 mg ml^{-1}) which had been denatured for 10 minutes at 100°C. The solution was replaced with fresh hybridisation mix containing the denatured DNA probe. The box was covered with Saranwrap (Dow Chemicals) that was depressed in the middle to

return condensed water to the hybridisation solution. The lid was put on and the box left shaking overnight at 65°C.

The next day, the probe solution was poured off and stored at -20°C. The filters were washed with shaking at 65°C in 2X SSC, 0.1% (w/v) SDS for about ten minutes. The wash solution was then replaced with fresh solution and left for a further 5 - 10 minutes. The filters were then dried with paper towels and placed between two pieces of Saranwrap while still damp. A piece of X-ray film (Dupont Cronex) was then exposed to the filter in a light tight cassette with an intensifing screen for a minimum of 24 hours at -70°C.

Filters which still had signal from a previous probe were stripped. This was done in a Pyrex casserole dish containing 0.1% SDS that had brought to the boil in a microwave oven. The filter was added to the solution which was left to cool to room temperature.

Low stringency hybridisations were made at 60°C in 3X SSC and 0.1% (w/v) SDS and the filters were washed at 60°C in 2X SSC and 0.01% SDS.

2.11 Manipulating λ genomic and cDNA libraries

2.11.1 Genomic libraries

The libraries were made using purified *Eco* RI arms of the vector λ gt10 purchased from Promega. These were ligated to a purified 6.0 kb fraction of *Bgl* II digested DNA from the *phan-552* mutant that had been treated in the following way. The 6 kb fraction of DNA was purified using a NACS column (section 2.8.1). The concentration of purified DNA was estimated by gel electrophoresis against standards of a known concentrations. The overhangs of the *Bgl* II sites were filled-in by incubating in a 25 μl reaction consisting of 0.1 units/μl Klenow, IX Klenow buffer (50 mM Tris-HCl, pH 7.2, 10 mM dithiothreitol), 5mM each dNTP and 0.1 μg μl^{-1} BSA, at 20°C for 30 minutes. The reaction was stopped by extraction with phenol:chloroform (1:1 v/v) and

DNA purified by ethanol precipitation. The blunt-ended DNA was ligated with a 50-fold excess of *Eco* RI adaptors (from Pharmacia cDNA synthesis kit) overnight and purified from unligated linkers using spun columns provided with the kit. The 5' cohesive termini of the *Eco* RI sites were treated with polynucleotide kinase to allow ligation into the dephosphorylated vector, according to the instructions provided with the kit. The DNA was then digested with *Eco* RI extracted with phenol:chloroform (1:1 v/v) and co-precipitated with vector. Each precipitation involved 0.1 μg of vector DNA and 0.01 - 0.1 μg of target DNA. The vector and target DNA were dissolved in 8.5 μl of sterile distilled water, to which was added 1 μl of 10X ligation buffer and 0.5 μl (0.5 units) T4 DNA ligase. Ligations were incubated at 16°C overnight.

2.11.2 Packaging λ gt10

λ gt10 was packaged using the Packagene Extract System purchased from Promega. The total volume of each extract was 50 μl and this was usually divided into 3 separate aliquots of 16μl each. The extract, which had been stored at -70°C, was thawed rapidly for use by warmth from fingertips and by gentle stirring with a yellow tip. 16 μl of the extract was then mixed immediately with 2 - 5 μl of the ligation reaction. The packaging reaction was incubated at 22°C for 2 hours.

445 μl of phage buffer and 25 μl of chloroform were added to each packaging reaction and mixed gently by inversion. Reactions were stored at 4°C. Serial dilutions (1 μl of undiluted and 10^{-1} and 10^{-2} dilutions) of each packaging reaction was plated to establish the titre of recombinant phage.

2.11.3 Plating phage

The host cells used were C600 and C600 *hfl*A$^-$. These were stored in a glycerol stock at -70°C. A 5 ml volume of L broth supplemented with 10 mM $MgSO_4$ and 0.2% maltose was inoculated with a wire loop which had been scraped over the surface of a glycerol stock and the culture incubated overnight.

The cells were spun down in their tubes, the medium removed and cells resuspended in 10 mM $MgSO_4$ to give an absorbance at 600 nm of 1.2 in a 1 cm light path. For plating, 100 μl of these cells were incubated with phage for 20 minutes at 37°C, to allow the phage to adsorb to the surface of the cells. Infected cells were plated in 3 ml BBL top agar at 45°C onto L plates that had been dried and pre-warmed in an oven to 37°C.

2.11.4 Genomic library screening

Libraries were plated at plaque density between 5 000-10 000 per 90 mm diameter plate.

2.11.5 Plaque lifts

Plates were chilled for 2 hours at 4°C to harden the top agar. Round nitrocellulose filters (Hybond-C gridded membranes, 0.45 μm pore size, Amersham) were placed on the top of the agar and left for about five minutes. The filter discs were numbered and three pin holes made through the surface of the filter into the agar in a pattern such that the disc could be orientated with respect to the plates later. The discs were then transferred DNA side up onto Whatman 3MM paper soaked in denaturing solution (section 2.10.1) and left for 5 minutes. They were then transfered to Whatman paper soaked in neutralising solution for 5 minutes and then to paper soaked in 2X SSC for 5 minutes. The discs were subsequently air dried on tissue paper for about one hour and the DNA fixed by baking at 80°C under vacuum for 30 minutes.

Filter discs were hybridized in circular plastic containers as described for Southern blots, except that the filters were pre-hybridised for over 1 hour to remove bacterial debris

2.11.6 Screening libraries by hybridisation

The discs from the plating of the library represented the first round screen. After hybridisation, discs were exposed to film and positive plaques identified. The agar that included the positive plaque was then cored out from the plate with the wide end of a yellow tip. The agar core was eluted in 1 ml of phage

buffer. From a 1 X 10^{-5} dilution of this eluate 1 μl was plated with 100 μl of plating cells. This usually produced a plate with about 600 plaques which could be screened for the second round. Individual plaques could usually be identified and isolated as pure positive phages from this round.

2.11.7 cDNA library

A cDNA library in λgt10, made from young wild-type inflorescences was gift from R. Simon and E. S. Coen, John Innes Institute, Norwich, UK. The library was screened at a density of 10 000 plaques per plate, as described for the genomic library.

2.12 Ligations

Ligation into plasmid vectors were made with a ten-fold molar ratio of insert to vector in a small total volume (typically 10 μl) with 1X manufacturer's ligation buffer and 0.05 unit μl^{-1} T4 DNA ligase (NBL).

2.13 Bacterial transformation

2.13.1 Electroporations

For electro-competent cells, a 100 ml culture of JM101 was grown from a fresh overnight in minimal broth supplemented with thiamine until an A_{600} value of 0.5 - 0.7 had been reached. The culture was divided between two 50 ml tubes and spun at 6 500 rpm for 15 minutes at 4°C in an MSE Mistral centrifuge. The cells were resuspended in 100 ml of ice-cold sterile distilled H_2O and then spun again. The cells were then resuspended in 50 ml of ice-cold 10% (v/v) glycerol and spun again. The cells were resuspended in 15 ml of 10% (v/v) glycerol and centrifuged for a final time. The total washed cells were resuspended in 2-3 ml of ice cold 10% (v/v) glycerol and 40 μl aliquots snap frozen in liquid nitrogen and stored at -70°C.

For electroporations, typically 1 μl of a ligation reaction was added to an aliquot of cells which had been allowed to thaw on ice. This was then given a 2 kV pulse in a 1 mm cuvette using a Biorad Genepulser set for 200 Ω resistance and a capacitance of

25 μF. Directly after the shock, 1 ml of L broth was added to the cells in the cuvette which were then transfered to Eppendorf tubes and allowed to recover at 37°C for one hour. Cells were plated out on L agar with appropriate antibiotics. Cuvettes were washed thoroughly in sterile distilled water before reuse.

2.13.2 $CaCl_2$ transformations

1 ml of a fresh overnight of JM101 was used to innoculate 100 ml of L broth. The culture was grown until the cells had reached a A_{600} value of 0.2. The culture was chilled on ice and the cells spun down in 50 ml Falcon tubes at 6 500X*g* for 10 minutes at 4°C. The cell pellet was then gently resuspended in half the original volume of ice-cold 50 mM $CaCl_2$ and incubated on ice for 30 minutes. The cells were spun once more and the pellet resuspended in 1/10 th the original volume of 15% (v/v) glycerol, 50 mM $CaCl_2$. The cell suspension was then divided into 100 μl aliquots which were frozen in liquid nitrogen and stored at -70°C.

1 μl of a ligation reaction was added to an aliquot of cells, which had been allowed to thaw on ice, and left for 20 minutes. They were then given a 90 second heat shock in a waterbath at 42°C and allowed to recover in 750 μl of L broth for one hour at 37°C.

2.14 Polymerase chain reaction (PCR)

2.14.1 Primers

G339 corresponds to the right hand conserved subterminal region of Tam 1, 4, 5, and 6, and the left hand of Tam 2 with its 3' end pointing to the nearer end of each transposon.
RI left and RI right primers flank the *Eco* RI site in λgt10, with their 3' ends towards this site.

2.14.2 Reaction conditions

For polymerase chain reactions (PCR) *Tbr* polymerase (NBL) was used with the manurfacturer's buffer. A typical reaction was carried out in 50 μl consisting of: 1 X reaction buffer, 0.02 units

μl^{-1} of *Tbr* polymerase, 0.2 μM each primer, 2 μM each dNTP, and 0.1 μl of λ miniprep DNA as template.

RI left and RI right primers were used together to amplify inserts cloned in λgt10. The RI left primer was used in combination with G339 to amplify the sequence flanking the right hand end of Tam 4 in the λ clone derived from *phan*-552. DNA was amplified from λ templates using the RI primers in the following temperature cycle: a denaturing step of 94°C for 20 seconds, a primer annealing step of 55°C for 20 seconds and an extension time of 1 minute at 72°C. This cycle was repeated 35 times. About 1/5 th of the reaction product could be visualised by gel electrophoresis.

2.15 Plasmids

2.15.1 Transposon plasmids

Plasmids used as sources of transposon-specific probes are detailed in Table 2.1. They were kindly provided by E. S. Coen and C. Martin, John Innes Institute, Norwich, UK, or by Zs. Schwarz-Sommer, Max-Planck-Institut für Zuchtungsforschung, Cologne, Germany.

2.15.2 Transposon restriction maps

The origins of restriction fragments used as probes for the 10 different *Antirrhinum* transposons are shown with restriction maps of the transposons in Figure 2.1 a, b.

2.16 Microscopy

2.16.1 Replica moulding

Scanning electron microscopy of leaf surfaces was carried out on resin replicas made using a modification of the method described by Green and Linstead (1990). Specimens of plant material were coated in Extrude vinylsiloxane dental impression medium (Kerr UK Ltd.), which polymerised to form moulds. After about 30 minutes, the moulds were removed and infiltrated with Agar 100 epoxy embedding resin for 15 minutes at 70°C under vacuum. The vacuum was then released, the moulds drained of

excess resin, and the remaining resin allowed to polymerise at 65°C for 16-24 hours. Resin replicas were gold coated before examination at ambient temperature in a scanning electron microscope.

2.16.2 Wax embedding

Tissues for histological sectioning were fixed in FAA (4% (w/v) *para*-formaldehyde, 50% (v/v) ethanol, 5% (v/v) acetic acid) overnight at 4°C. They were dehydrated in 75% ethanol (2hours) and twice in 100% ethanol (5 hours and then overnight). Ethanol was replced with Histoclear (Cell Path Ltd) by incubation in 50% (v/v) Histoclear in ethanol for 2 hours and twice in 100% Histoclear (8 hours and overnight). The Histoclear was replaced with parafin wax (BDH Paraplast) by incubation in 50% (v/v) wax in Histoclear for five hours at 58°C, and in two changes of 100% wax at 58°C, each treatment lasting 8 or 16 hours. Tissues were positioned in molten wax in plastic weighing boats, and the wax allowed to solidfy by floating the weighing boats in iced water.

5-10 μm sections were fixed to slides using albumin-glycerol (R. A. Lamb) and stained in 2% (w/v) toludine blue for 2 minutes. Excess stain was removed by rinsing in tap water and slides air dried. Wax was removed using Histoclear, and sections mounted in Entalan (Merk).

Table 2.1

Each transposon is indicated with the plasmid from which the probe was taken. The restriction enzymes are also shown that were used to excise the fragment for labelling.

Transposon	Plasmid	Restriction enzyme/s to cut out fragment	fragment size	Vector
Tam 1 (Sommer,*et al.*, 1988b)	pAM72 pAM532	Hind III Hind III	430 520	pBR322 pBR322
Tam 2 (Upadyaya, *et al.*,1985)	pEHTam2	Hind III/EcoR I	4460	pUC9
Tam 3 (Martin, *et al.*, 1985)	pJAM4	Bgl I	3600	pACYC184
Tam 4 (Luo, *et al.*, 1991)	pJAM600	LH: Hind III RH: EcoRI/Hind III CACTA: Hind III	1030 2610 260	pUC18
Tam 5	pTam5 *	Eco RI	4550	pBS
Tam 6	pTam6 *	Eco RI	4100	pBS
Tam 7	pgli3 +	Hind III	2000	pUC18
Tam 8	p23N +	Eco RI	2720	pUC18
Tam 9	pgloLR4+	Eco RI	1800	pUC18

* E. S. Coen and S. Doyle, pers. comm.

+ Zs. Schwarz-Sommer, pers. comm.

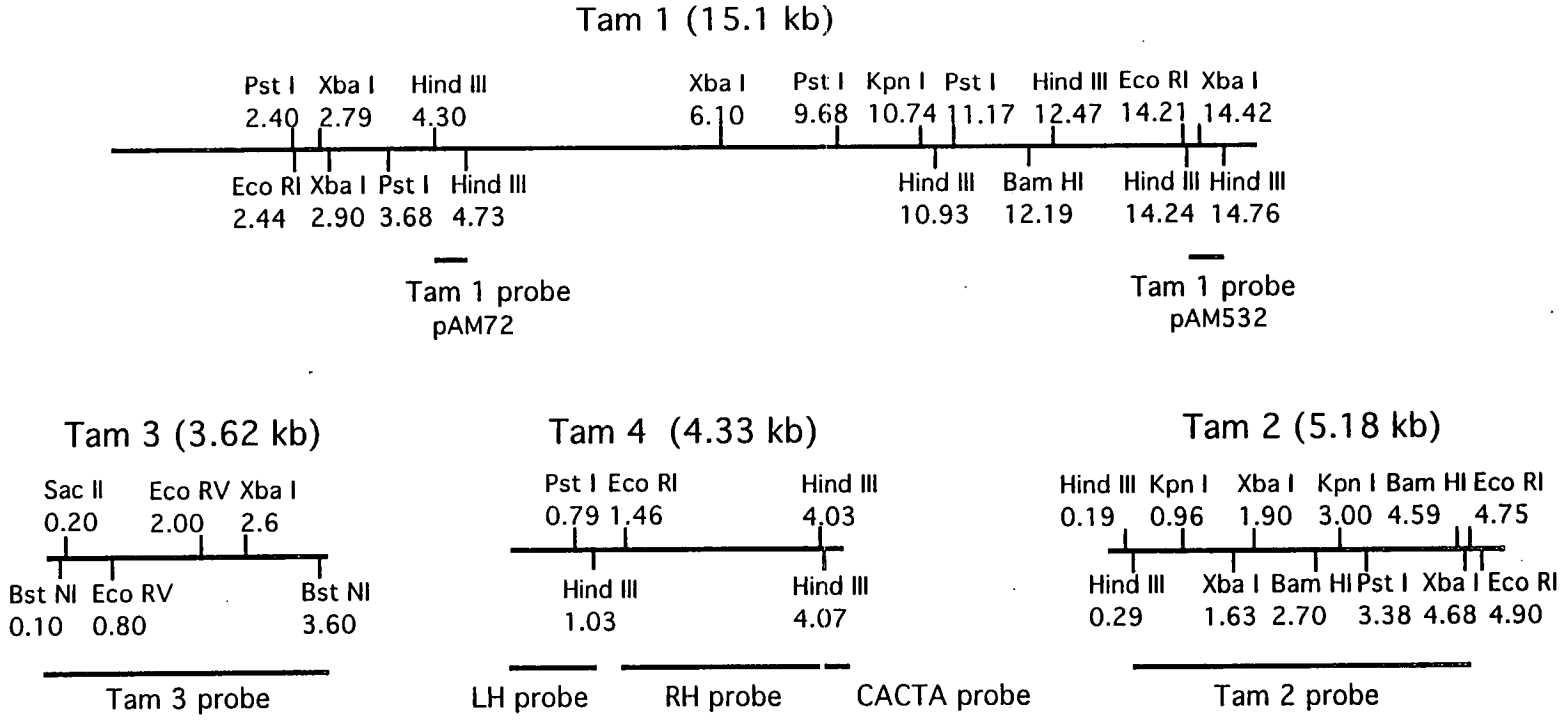

Figure 2.1 a. Restriction maps of Tam 1, Tam 2, Tam 3 and Tam 4.
(see Table 2.1 for further details)

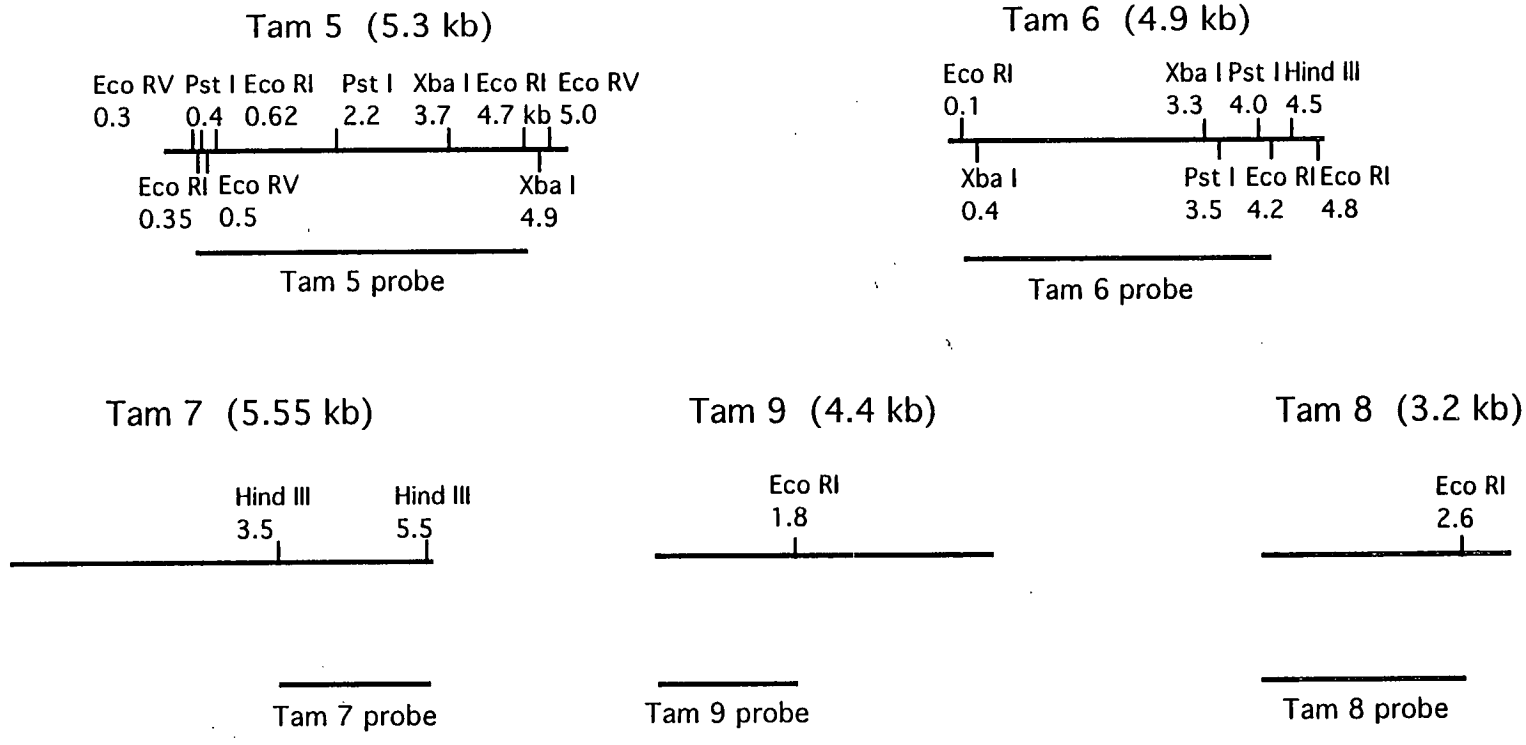

Figure 2.1 a. Restriction maps of Tam 5, Tam 6, Tam7, Tam 8 andTam 9.
(see Table 2.1 for further details)

CHAPTER 3 RESULTS

Mutagenesis and screening for a new *phan* mutation

3.1 Introduction

3.1.1 Mutagenesis programmes

The most successful method to date for isolating transposon tagged mutants in *Antirrhinum majus* has been that developed at the John Innes Institute, Norwich (Carpenter and Coen, 1990). The mutagenesis programme is simple and exploits lines that have been selected for high transposition rates of a number of Tam elements.

For the first generation of the mutagenesis programme, M_0 lines are grown at 15°C to increase the frequency of transposition (Harrison and Fincham, 1964; Harrison and Carpenter, 1973). The important transposition events may occur in germ line cells or may be inherited from somatic ancestors of germ line cells. Self pollination of M_0 plants gives rise to M_1 progeny heterozygous for transposon-induced mutations. Most mutations are recessive and therefore heterozygous M_1 plants are selfed to create the homozygous mutants. The mutants can be identified in the M_2 generation grown in large summer field plots.

This method could have been replicated to find a new *phan* mutant. However, there are several major disadvantages to this approach. Firstly, to identify recessive mutations three plant generations (M_0, M_1 and M_2) have to be grown. With a generation time of about six months this would have taken nearly two years. Secondly, the phenotypes of recessive mutations are not detectable in heterozygous M_1 plants and in the M_2 generation only one in four of the progeny will be homozygous mutants. To have a 95% probability of obtaining homozygous M_2 mutants eleven of the progeny from each M_1 parent would have to be grown.

For these reasons, and because the frequency of transposon mutagenesis is low the John Innes programme involved a

compromise necessary for an economy of labour. Two seed capsules from each of 18 or 30 M_1 plants were pooled. From each pool, 48 or 96 M_2 progeny were grown. Therefore on average there were three progeny from each M_1 parent in an M_2 family. This reduced the probability of detecting recessive mutations to about 60% and many mutants may therefore have gone undetected.

A minor issue is that all mutants detected are homozygous for the same allele. Any severe mutations that have lethal phenotypes when homozygous are therefore undetectable. These mutations may have been viable if heterozygous with a weaker mutant allele of the locus.

However, a major advantage of the method is its potential to reveal mutations in any locus with a viable phenotype. Therefore, the method has been successful in identifying a large number of transposon induced mutants. From an M_1 generation of 13,000 plants a large reserve of pooled mutagenised seed was made. Annually 40,000 M_2 plants have been screened and because M_1 seeds were pooled, these families can be re-screened for further plants with the same mutation. As a result, several of the mutagenised genes have been cloned by virtue of their transposon tags.

3.2 Results

3.2.1 Targeted screen for a new *phan* mutant

Because two stable *phan* mutant lines were available a variation of the basic mutagenesis method was undertaken. This involved crossing the stable mutant lines; *phan*-249G and *phan*-250G, to the John Innes lines, JI. 75, JI. 98 and JI. 605, that had been selected for high transposition rates, and screening the F_1 progeny for mutants with new insertions in the allele derived from the wild-type parent.

There are several advantages to this method. Firstly, only two generations are required to identify new mutants. Secondly, only a single plant is required to detect a single mutation event.

Thirdly, the screen might detect more severe mutants that are lethal when homozygous but might be detectable as heterozygotes with the existing allele.

However, there are also disadvantages. New recessive mutants in alleles other than *phan* will not be identified. When the cross is made there is a possibility of mutants arising by self-pollination of the mutant parent. For this method to be successful, genuine M_1 progeny need to be distinguished from the results of accidental self-pollination.

One way to do this is to use flower colour as a genetic marker. Both the *phan* mutant lines were also homozygous mutants for two unlinked stable flower pigment alleles, *Eluta* (*El*) and *delila* (*del*). The flower petals of homozygous *El/El* mutants have a greatly reduced distribution of anthocyanin pigmentation. The corolla is unpigmented except for small patches of anthocyanin on the floral face and between the upper petal lobes. The coralla tube of homozygous *del* mutants is unpigmented and only the five petal lobes are fully pigmented. The John Innes lines are wild-type with respect to both loci and as a result have full red flowers. The F_1 progeny have the genotype el^+/El^- and Del^+/del^- and can therefore be identified because flowers of heterozygous el^+/El^- plants have an intermediate distribution of anthocyanin. In subsequent generations the segregation of both these markers provided confirmation that the progeny were either the result of cross-pollination to *phan* mutants or of self pollination.

Several hundred crosses had already been made between *phan* mutant and wild-type lines. More crosses were made to create a large seed reserve for F_1 plants. Previously several thousand F_1 seedlings had been screened for new *phan* mutants without success. One reason for failure might have been that these seedlings were germinated on compost. This posed several problems: the seeds are a similar colour to compost and individual germinations were therefore difficult to monitor; seedlings can become quickly overgrown and a potentially

weaker mutant might not have been recognised; the seedlings are in danger from various pests and diseases present in the compost or the greenhouse.

As an alternative, small plastic containers normally used for plant tissue culture were used as germination chambers. From each cross, a family of 120 F_1 seeds from a single capsule were spaced on moist cellulose wadding in a single container. Any remaining seed was saved in case additional wild-type siblings were required following the identification of a mutant. The F_1 seeds germinated after about eight days and the cotyledons were screened after two or three weeks. After about five to six weeks, the seedlings were re-examined when the first pair of leaves had developed. In total about 18,000 F_1 seedlings from 168 different families were screened. In this F_1 generation, 85 putative mutants (putants) were selected on the basis of the morphology of their cotyledons and first leaves. From families where putants were selected a total of 250 wild-type siblings were also isolated for comparison. Putants and wild-type siblings were transplanted to compost, to allow their further development to be monitored.

Over 300 F_1 plants, selected from 77 families, were grown to maturity. All these plants proved to be genuine M_1 progeny, because all had flowers typical of *El-/el+* heterozygotes. All the siblings were confirmed as wild-type because they shared consistent morphological phenotypes with their wild-type parents. The 85 putative mutants were re-examined and one potential new *phan* mutant was selected for further analysis.

The new *phan* mutant was identified in family EB552. The potentially new allele which it carried was therefore named *phan*-552 and the plant numbered 552[1]. The new *phan*-552 mutant was expected to be genotypically heterozygous, *phan*-552/*phan*-249G with one *phan* mutant allele that had been inherited from the mutant parent, *phan*-249G/*phan*-249G, and

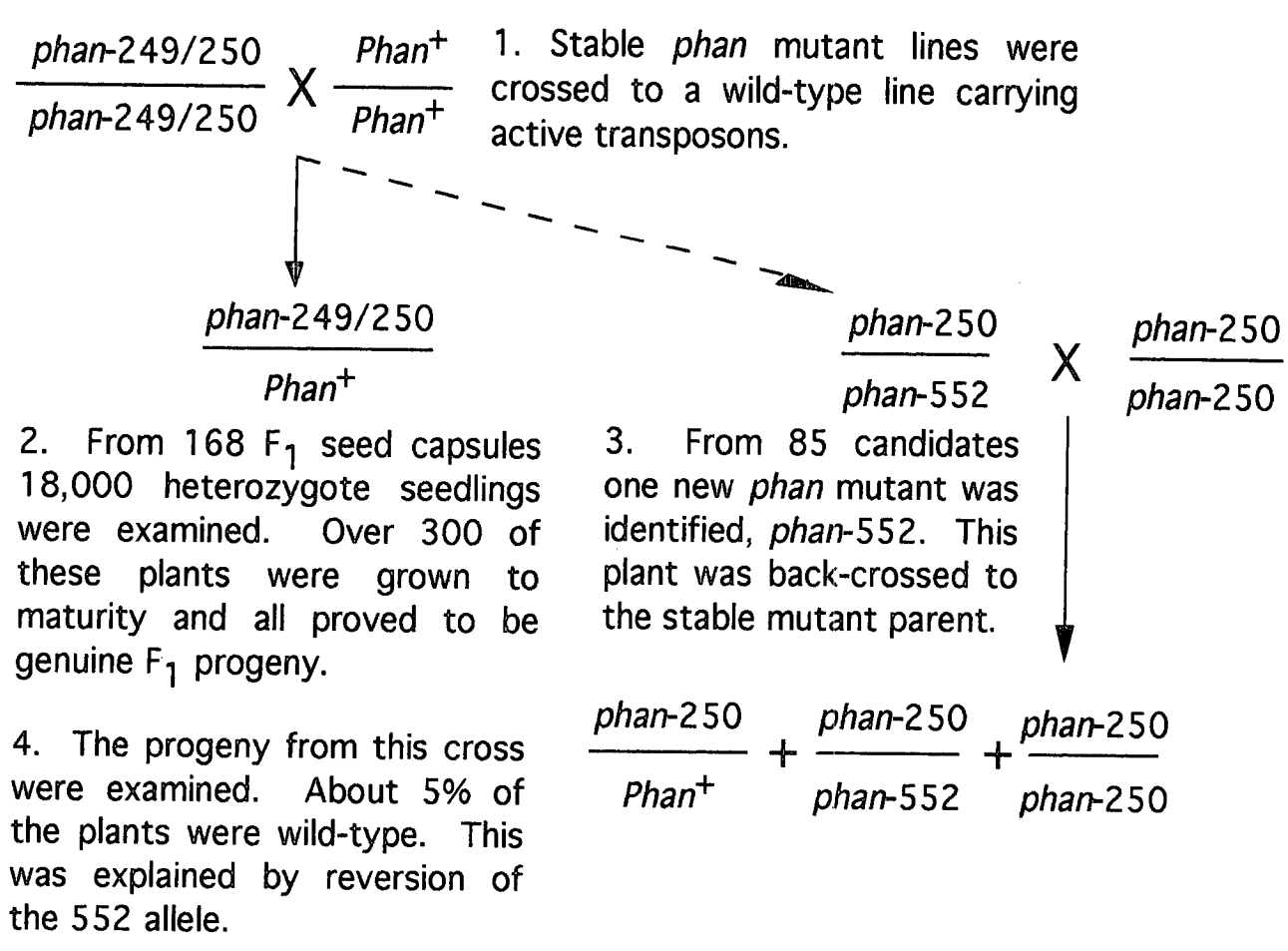

Figure 3a. This digram shows the crosses made in the mutagenesis screen for a new *phan* mutant.

the other as the potentially new transposon insertion in a gamete from the wild-type parent, line Jl. 75.

Further evidence for a transposon being responsible for the new mutant *phan*-552 allele was that after self pollination the *phan*-552/*phan*-249G mutant appeared to be unstable. In a number of families from self-pollination of the mutant about 10% of progeny had a wild-type phenotype (Table 3.1). One explanation for this was that the wild-type plants were the result of reversion due to excision of the transposon from the *phan*-552 allele. The *el* and *del* markers segregated with a frequency consistent with that expected from F_2 progeny from a self pollination.

The *phan*-552/*phan*-249G mutant was back-crossed to the mutant parent, *phan*-249G/*phan*-249G, and also the *phan*-250G/*phan*-250G mutant. Several families, each from a single capsule, were grown. About 5% of plants in these families were wild-type (see Table 3.2), about half of the frequency than in families produced by self-pollination of *phan*-552/*phan*-249G. Because the *phan*-552 allele was twice as common in the progeny of the self than of the cross pollination this frequency was consistent with a reversion frequency of 5%/allele/generation.

To examine the phenotype conditioned by the *phan*-552 allele it was desirable to identify homozygous plants. To do this the *phan*-552/*phan*-249G mutant was back-crossed to the wild-type parent, line Jl. 75, and to other wild-type lines, Jl. 98 and Jl. 605. The F_1 plants, which were either heterozygous *phan*-552/*Phan*$^+$ or *phan*-249G/*Phan*$^+$, were selfed. Each F_2 family contained wild-type and *phan* mutant progeny in the ratio three to one, as expected. The mutant members of half these families were expected to be *phan*-552/*phan*-552 homozygotes.

3.3 Concluding remarks

The targeted transposon mutagenesis programme was successful. A new *phan* mutant allele, *phan*-522, was identified.

Importantly, the new mutation was unstable because revertants appeared in subsequent generations. This indicated the new mutation was probably caused by a transposon that would facilitate cloning the *phan* gene by transposon tagging.

TABLE 3.1 Reversion frequency of the *phan*-552 allele

Families EC500 and ED505: from a self pollination of the *phan*-552/*phan*-249G mutant.

Family no.	No. of plants in family	no of revertants
500	47	4
505	98	9
		Reversion frequency
Total	145	9%

TABLE 3.2 Reversion frequency of the *phan*-552 allele

Families EC501 to EC514: from a backcross of the *phan*-552/*phan*249G mutant to the stable mutant parent *phan*249G/*phan*-249G.

Family no.	No. of plants in family	no of revertants	backcross parent
EC501	39	4	$EA249^{3}$
EC502	42	1	$EA249^{3}$
EC503	53	3	$EA249^{13}$
EC504	57	4	$EA249^{6}$
ED506	112	4	$EA250^{6}$
ED507	32	2	$EC249^{5}$
ED508	48	1	$EC249^{3}$
ED509	24	1	$EC249^{4}$
ED510	110	5	$EC249^{6}$
ED511	110	5	$EC249^{6}$
ED512	120	6	$EC249^{3}$
ED513	24	2	$EC249^{4}$
ED514	70	5	$EC249^{5}$
			Reversion frequency
Total	841	42	5%

CHAPTER 4 RESULTS

Identifying the copy of a transposon that segregates with the new *phan*-552 allele

4.1 Introduction

4.1.1 Identifying transposons responsible for mutations identified in the John Innes mutagenesis programme

When a new mutant is identified in the John Innes mutagenesis programme, it is self-pollinated and back-crossed to the wild-type parent. Selfed seed is sown, and if the new mutation is unstable, revertants should occur at an appreciable frequency. The revertants are self-pollinated, and the progeny should segregate in a ratio of three wild-type plants to one mutant. On average, one of the three wild-type plants will be homozygous for the revertant allele. This can be confirmed by selfing all wild-type plants: the homozygous revertant will produce wild-type progeny after self-pollination.

Homozygous revertants and mutant siblings provide the best range of genetic material for identifying which transposon copy is responsible for the mutation. This transposon should segregate with the mutant allele and have been lost with reversion. Genomic DNA from the homozygous revertants can be compared with DNA from homozygous mutant plants. Southern hybridisations with a probe from one of the nine transposable elements allows transposon copies present in the mutant or wild-type samples to be compared as hybridising bands of different sizes. In this way, bands may be detected which are unique to mutant and therefore represent the mutant allele.

4.2 Results

4.2.1 Identifying a transposon responsible for the new *phan*-552 mutation

To identify a transposon responsible for the new *phan*-552 mutation the John Innes strategy could not be used because the new mutant was heterozygous, *phan*-552/*phan*-249G, and there

was no easy way to distinguish between the different alleles in subsequent generations. Therefore an alternative and more simple strategy was adopted. The *phan*-552 allele is unstable and therefore probably carries a transposon insertion. The quickest method to determine which transposon was potentially responsible was to identify a band in Southern hybridisations present in the original *phan*-552/*phan*-249G mutant and not in its *Phan*$^{+}$/*phan*-249G siblings.

Genomic DNA was therefore extracted from the original *phan*-552/*phan*-249G mutant and from a pool of eight wild-type siblings (*Phan*$^{+}$/*phan*-249G). DNA samples from mutant and wild-type plants were digested with different restriction enzymes with six bp recognition sequences. In total twelve different enzymes were used in various combinations. Using Southern hybridisation, the distribution of each of nine different Tam elements was examined. Bands present in mutant but not wild-type samples were noted and their distribution characterised further. To confirm that bands were unique to the *phan*-552 mutant, DNA was extracted from eight individual wild-type siblings and subjected to digestion and Southern hybridisation. This ruled out the possibility that bands might represent segregating transposons present in only a few of the wild-type siblings, and therefore undetectable in bulked DNA extractions. The possible role of new insertions was tested in a subsequent generation.

Seeds from individual capsules of back-crosses between *phan*-552/*phan*-249G and its mutant parent *phan*-249G/*phan*-249G were sown in separate families. Thirteen back-cross families were grown and all contained revertants. The first four families were numbered 501 to 504, and another eight families were numbered 507 to 511 and 513 (Table 3.2). Additionally, three families that were the result of a backcross of *phan*-552/*phan*-249G to *phan*-250G/*phan*-250G was also grown and were numbered 506, 512 and 514 (Table 3.2).

Mutants in the F_1 generation from a back-cross of the *phan*-552/*phan*-249G mutant to the mutant parent *phan*-249G/*phan*-249G were expected to consist of parental genotypes in a ratio of one to one. About half the mutant plants were therefore expected to carry the transposon responsible for the *phan*-552 mutation. However, this generation also contained *Phan*$^+$/*phan*-249G revertants all of which were expected to lack the transposon. Therefore bands which had been found in the original *phan*-552/*phan*-249G mutant and not in its wild-type siblings were examined in the progeny of the back-cross. From each family, DNA was isolated from a pool of all revertant plants and from a pool of at least thirty different mutants. A transposon present in the *phan*-552 allele was expected to be detected as a band in DNA from mutant plants, but not in DNA from their wild-type siblings.

Bands which occurred in the expected distribution were again examined in further detail. To ensure that all revertants lacked the copy of the transposon present in the mutant pools, genomic DNA was prepared from individual revertants.

After this systematic analysis, only one band was identified which was showed the expected distribution. It was present in the new *phan*-552/*phan*-249G mutant and not in its eight siblings and it was absent from all revertants but present in the mutants of the F_1 back-cross generation. This element was found using a probe derived from Tam 4 which contains a region conserved between all characterised *Antirrhinum* transposons except Tam 3. All elements so far characterised, except Tam 3, share homology in a sub-terminal region, and also in their terminal inverted repeats. Because the repeats end in the sequence CACTA these related transposons are collectively known as CACTA transposons and the sub-terminal probe that is conserved between related elements the CACTA probe. When used at low stringency, this probe is able to detect more bands than a combination of probes from all characterised CACTA elements at high stringency, suggesting that the region is

conserved in as yet uncharacterised transposons. It therefore allows a number of different transposons, including uncharacterised ones, to be screened simultaneously. The probe detected a band unique to *phan*-552, which was only visible in DNA cut with the restriction enzyme *Bgl* II at a size of about 6 kb (Figure 4.1). To discover whether the band corresponded to a previously characterised transposon, Southern hybridisation was carried out at high stringency with 8 probes from the individual CACTA elements: Tam 1, Tam 2, Tam 4, Tam 5, Tam 6, Tam 7, Tam 8 and Tam 9 (Table 2.1 and Figure 2.1 a, b). Two probes from opposite ends of Tam 4, excluding the conserved CACTA region, showed a strongly hybridising band in the same position with the same distribution as detected by the CACTA probe (Figure 4.2 and 4.3). Therefore, the CACTA element appeared to be a copy of Tam 4.

The segregation of the 6 kb *Bgl* II band was examined using the Tam 4 probes in six back-cross families, 506, 507, 508, 509, 510, 511, 512, 513 and 514. In total, all 31 revertants from 9 families had lost the 6 kb band which was still present in the pooled mutant DNA samples (Figure 4.4 and 4.5). From families 501, 502, 503 and 504 DNA was prepared from a pool of eleven revertants and a pool of sixty mutants from the four families. The 6 kb band was present in the mutant DNA sample but not in the revertant pool.

4.3 Concluding remarks

A copy of Tam 4 had be identified that was present in the *phan*-552/*phan*-249G mutant and not the *Phan*$^+$/*phan*-249G siblings suggesting that this was a new transposon insertion. The transposon was shown to be absent from thirty revertants from nine families. The probability of any plant in this generation inheriting a transposon which was heterozygous in its *phan*-552/*phan*-249G parent was 0.5. If every revertant were the result of an independent reversion event the probability of all thirty revertants lacking the copy of Tam 4 by chance would be $(0.5)^{30}$ which is one in 10,737,441,824. However, the *Phan*$^+$

allele carried by several revertants could be the result of early transposon excision which was inherited by a number of gametes. Assuming there was only one reversion per capsule the probability would be $(0.5)^{10}$, that is one in 1024. This strongly suggested that the copy of Tam 4 was associated with the *phan*-552 mutation. Therefore this was taken as sufficient evidence to attempt to clone the tagged *phan*-552 allele using Tam 4 as a probe.

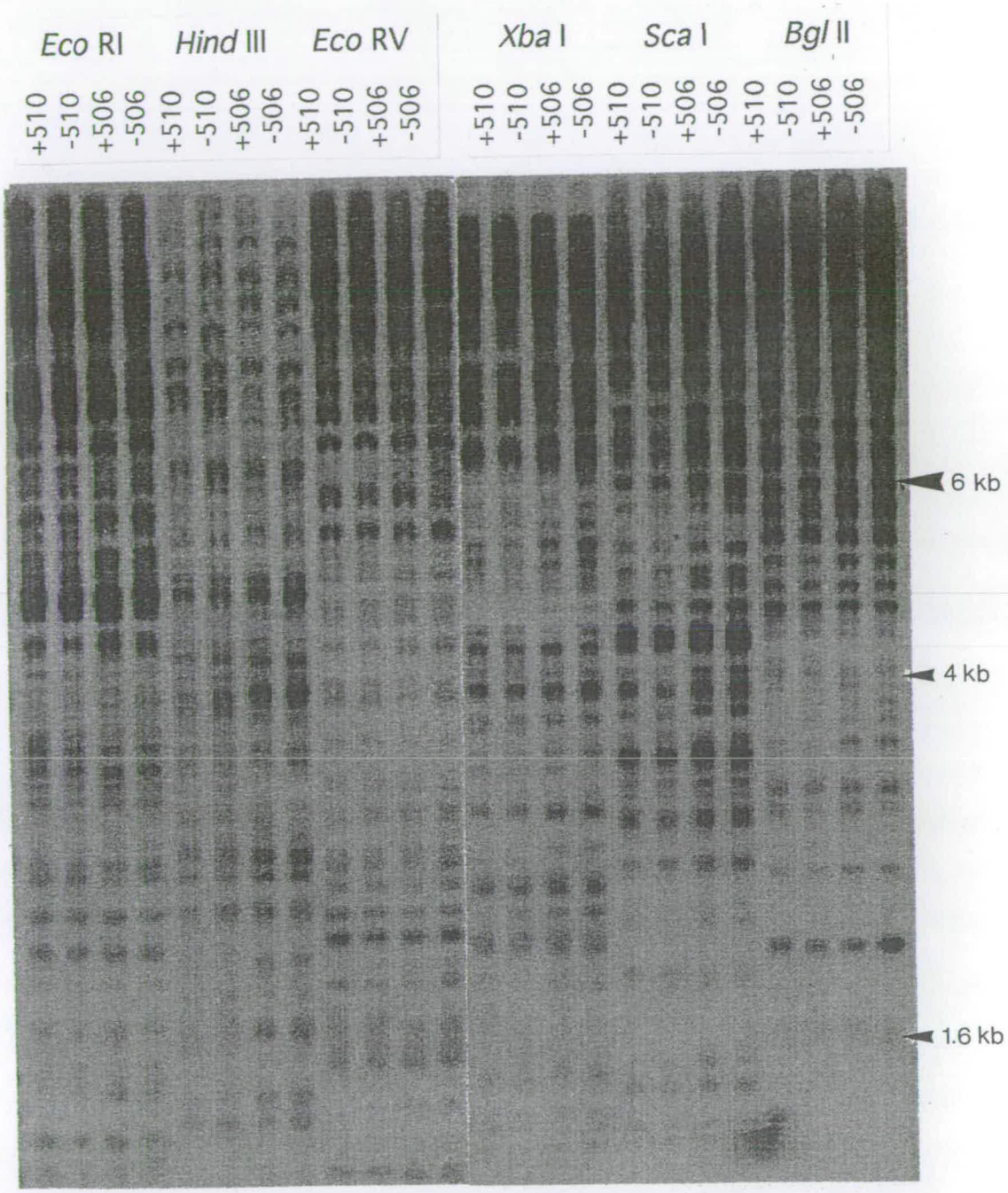

Figure 4.1 Southern hybridisation of revertant (+) and Mutant (-) pools of DNA from the families 510 and 506.
In order to identify a CACTA transposon that segregated with the *phan*-552 allele each pool of DNA was restricted with 12 different enzymes (6 are shown). After hybridisation with the CACTA probe one band was identified that was present in the mutant DNA pools but not the wild-type pools. This band was identified in only DNA cut with *Bgl* II at a position of 6 kb.

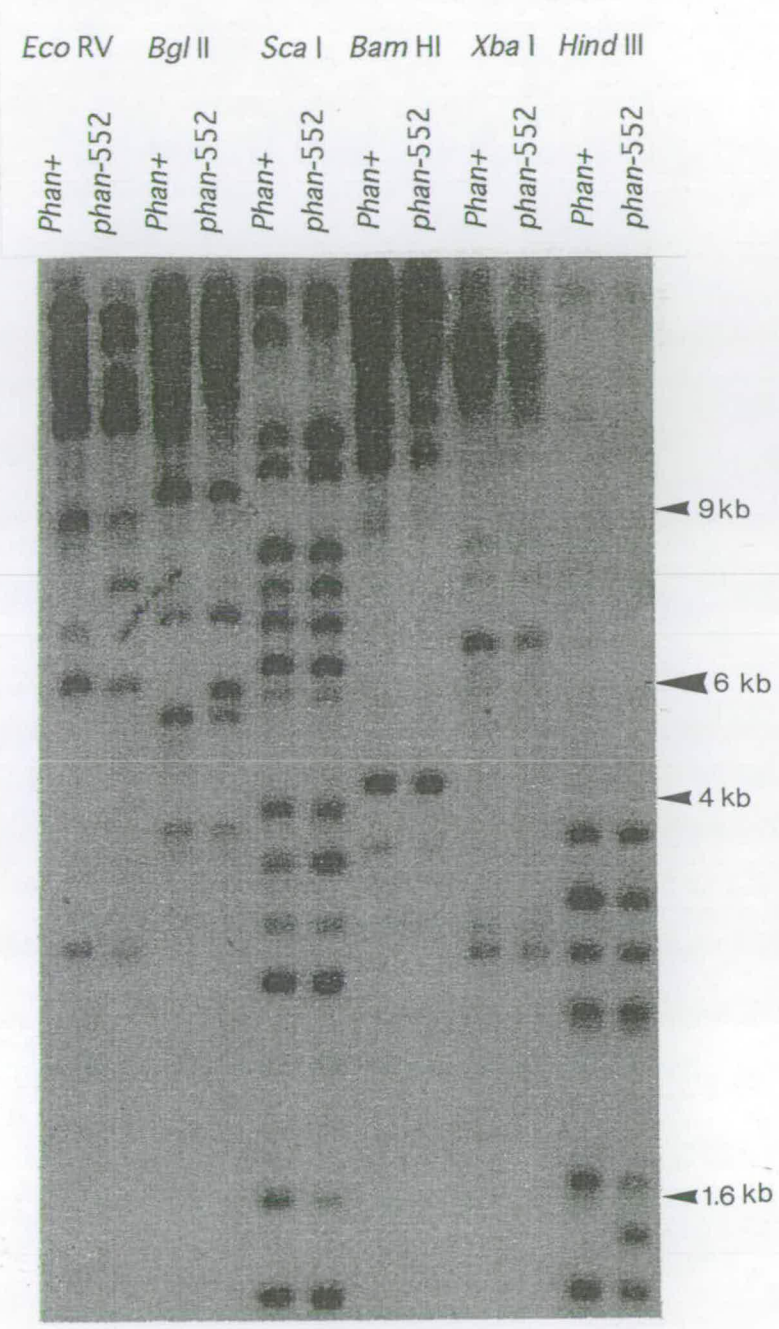

Figure 4.2 Southern hybridisation of DNA from the *phan*-552 mutant and a pool of the eight wild-type siblings.

The CACTA transposon was identified as a copy of Tam 4. After hybridisation with a probe for Tam 4 a band was identified in *phan*-552 mutant DNA samples cut with *Bgl* II at 6 kb. This band was not present in pooled DNA from wild-type siblings.

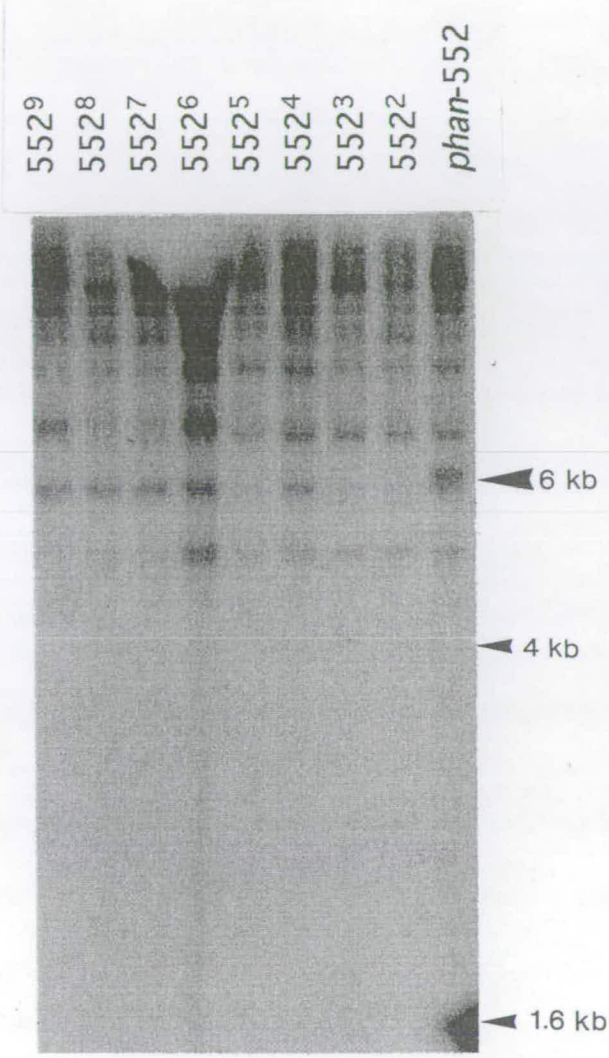

Figure 4.3 Southern hybridisation of DNA from the *phan*-552 mutant and the eight wild-type siblings.
After hybridisation with a Tam 4 probe a copy of the transposon at 6 kb was present in only DNA from the *phan*-552 mutant and not in individual DNA samples from the eight wild-type siblings.

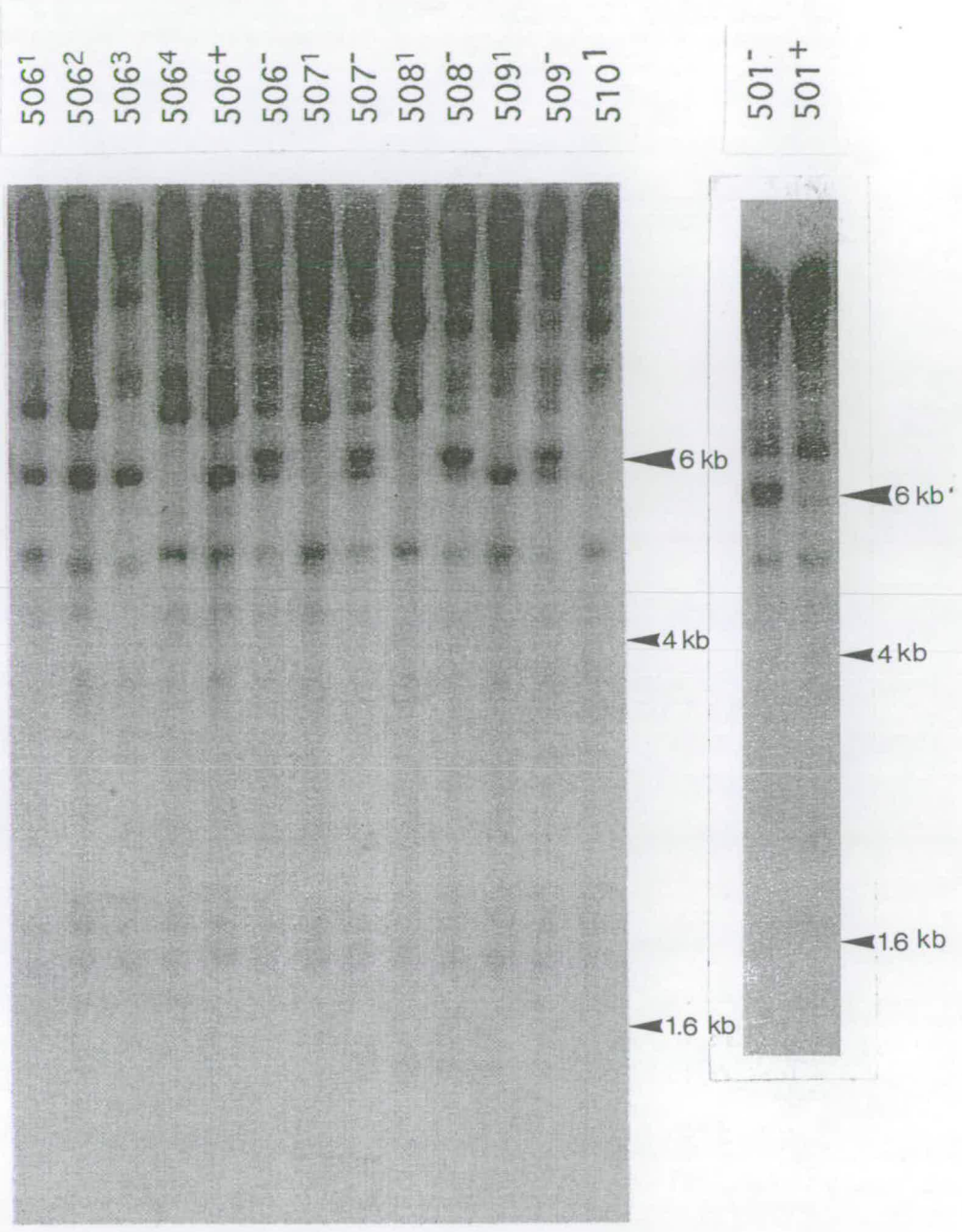

Figure 4.4 Southern hybridisation of DNA from the revertants and pooled mutant plants of the families: 501 to 504, 506, 507 ,508 and 509.

After hybridisation with a probe for Tam 4 a copy of this transposon is present only in the mutant pools of DNA cut with *Bgl* II from each family but not in DNA from any of the revertants. DNA was pooled for the revertants and mutants of families 501 to 504. (the revertant 507^2 is not shown)

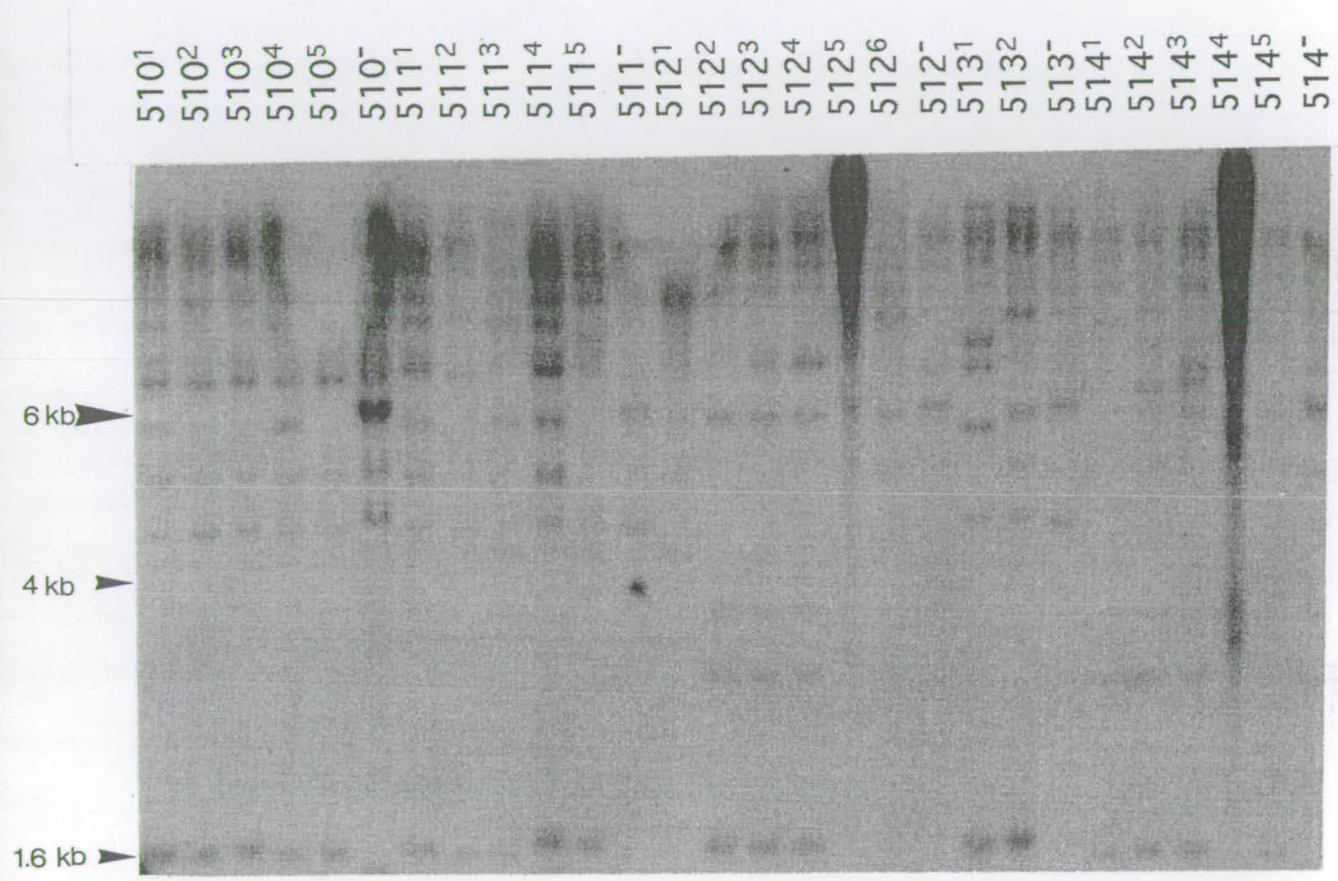

Figure 4.5 Southern hybridisation of DNA from the revertants and pooled mutant plants of the families : 511 to 514.

After hybridisation with a probe for Tam 4 a copy of the transposon was present only in the DNA samples from the mutant pools of each family but not in DNA samples from any of the revertants.

CHAPTER 5 RESULTS

Mapping and cloning the 6 kb *Bgl* II fragment containing Tam 4

5.1 Introduction

A new mutant *phan*-552 had been identified. The mutation, because it was unstable, appeared to be caused by a transposon. A copy of Tam 4, which appeared to be responsible for the mutation had been identified in a 6.0 *Bgl* II fragment. The next step was to isolate this fragment.

5.2 Results

5.2.1 Genomic mapping and cloning the *phan*-552 allele

Choice of λ cloning vector

The simplest strategy to clone the copy of Tam 4 would have been to screen a genomic library made from a 6.0 kb *Bgl* II fraction of DNA from the *phan*-552 mutant. Production of such a library presented several problems. The 6 kb fragments proved too small for the replacement vector λEMBL4 which has a compatible *Bam* HI cloning site. Although the frequency of recombinant phages was high when this approach was used, the packaging efficiency of λ molecules of sub-optimal lengths *in vivo* produced plaques which were too small to screen. Although the NM1151 λ insertion vector with a *Bam* HI cloning site was available as an alternative, it was rejected on the grounds that it carried no convenient restriction sites to cut out cloned fragments.

Subsequently, two methods were adopted which used short DNA linkers or adaptors to make the ends of the genomic DNA suitable for cloning into the *Eco* RI site of λ gt10. This insertion vector has a number of advantages. It has a capacity for DNA inserts up to 7.0 kb. The *Eco* RI cloning site is within the *c*I gene, and therefore recombinants are *c*I$^-$ mutants. This allows efficient positive selection of recombinant phages on *hfl*A$^-$ hosts.

The first approach to adding *Eco* RI sites involved two short oligonucleotides (16'mers) which for part of their length (12 bp) had complimentary sequences. When the single strands were annealed a short linker was made with a 4 nucleotide overhang at each end: one a *Bgl* II cohesive end and the other a *Eco* RI cohesive end. In between the two ends was a *Not* I site. This linker was ligated to both complementary *Bgl* II ends of 6 kb fragments. The linkered fragments were then ligated to the arms of the λ gt10 vector. Prior to the second ligation, the *Eco* RI overhang of the linker was phosphorylated to increase the efficiency of vector to linker ligations. Because this method produced recombinant molecules at a low frequency, and also because the limiting step was difficult to assess, it was abandoned.

The second method used small double stranded DNA adaptors designed for cloning cDNA molecules (Pharmacia cDNA synthesis kit) which were blunt at one end, had an *Eco* RI cohesive end at the other and a recognition sequence for a *Not* I between. The *Bgl* II ends of the genomic fraction were filled-in using Klenow and adaptors ligated to the blunt end. Although this method was more successful, yielding 1.75 x 10^4 p.f.u. recombinant phage per μg of target DNA it was too inefficient to produce a useful library. One possible reason was that the efficiency of filling-in and linker-ligation was low.

5.2.2 Cloning and mapping the *phan*-552 allele

An alternative cloning method using the same DNA adaptors was adopted. If *Eco* RI sites were present in the 6 kb fragment then these could have been exploited. One *Eco* RI site was known to be present in Tam 4, about 1.2 kb from the left hand end of the element. To determine whether there were any other *Eco* RI sites in the 6 kb Tam 4 band, it was restriction mapped. A 6.0 kb size fraction of *Bgl* II-cut genomic DNA from the *phan*-552/*phan*-249G mutant, which included the Tam 4 band, was cut with either *Eco* RI, *Hind* III, or both enzymes in a double digest. The products from these digests were examined by Southern

hybridisation with probes from the right and the left side of the *Eco* RI site in Tam 4.

The 6 kb *Bgl* II fraction cut with *Eco* RI and probed with the left end of Tam 4 consistently showed a band at about 1.6 kb (Figure 5.1). The *Eco* RI site in Tam 4 is 1.2 kb from the left end of the transposon. Therefore, 300 bp of genomic DNA appeared to flank the transposon to its left. The same samples of DNA probed with the right hand end of Tam 4 gave a band at 4.4 kb (Figure 5.1) and therefore the right hand genomic flank was expected to be 1.6 kb in length. The observation that the two fragments resulting from *Eco* RI digestion had a combined size of about 6.0 kb suggested that there were either no additional *Eco* RI sites in the flanking DNA or that if *Eco* RI sites were present, that they were close to the *Bgl* II sites.

In order to clone the two smaller fragments, genomic DNA from the *phan*-552/*phan*-249G mutant was cut with *Bgl* II and a size fraction including the 6 kb Tam 4 band isolated. DNA from this fraction was purified and the *Bgl* II sites filled in with Klenow. The adaptors were ligated to the blunt ended fragments and unligated adaptors removed by spun column chromatography. Because the 5' overhang of the *Eco* RI cohesive end carries no phosphate group to prevent concatomerisation of adaptors, the recovered fragments were treated with polynucleotide kinase to allow subsequent ligation to dephosphorylated vector. The DNA was then restricted for a second time with *Eco* RI, purified and ligated into λgt 10. This produced about 7 x 10^5 p.f.u. per μg of target DNA.

Recombinant phages were screened with a probe which included Tam 4 sequences from both the left and right of the *Eco* RI site. About thirty positives were isolated from the first round screen. Of the first ten to be purified two had an insert of 1.6 kb and one an insert of 4.4 kb as expected for the left and right *Eco* RI-*Bgl* II fragments respectively.

Probed with the left hand region of Tam 4.

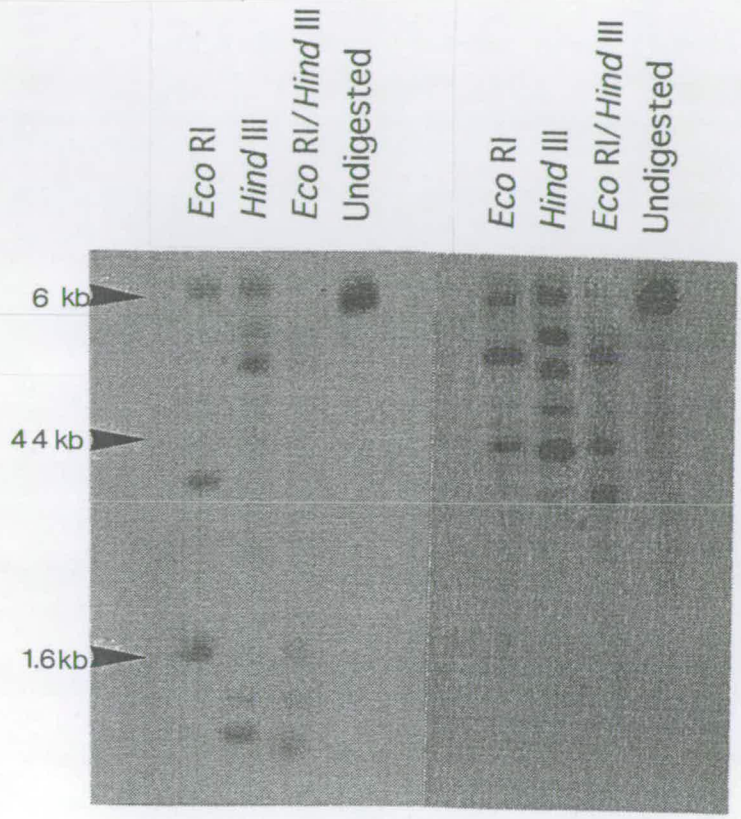

The same filter was probed with the left hand portion of Tam 4.

Figure 5.1 Southern hybridisation of the 6 kb fraction of *Bgl* II DNA from the *phan*-552 mutant.

The size fraction of DNA was cut again with *Eco* RI, Hind III and *Eco* RI/*Hind* III in a double digest. The filter was hybridised with a probe for the left hand region of Tam 4 (see Table 2.1 and Figure 2.1ab) and showed a band at 1.6 kb. After hybridisation of the same filter with a probe for the right hand region of Tam 4 a 4.4 kb was identified.

The other bands represent DNA fragments which include portions of a copy of Tam 4 and therefore hybridise to the Tam 4 probe. These fragments and their copies of Tam 4 were not linked to the *phan*-552 mutation.

The 1.6 kb insert from clone λB13AA was sub-cloned in both orientations into the *Eco* RI site of pBluescript (Stratagene) to make plasmids pBLH1 and pBLH2. The flanking sequence in the 4.4 kb λB2BB clone was amplified using the polymerase chain reaction with a primer at the right hand end of Tam 4 and a primer flanking the *Eco* RI site in λgt10. The PCR product from the right hand flank was 1.6 kb as expected and this was cloned into the *Eco* RV site of pBS to make the plasmid pBRH.

The insert from pBRH, representing the right hand flank to Tam 4, was used as a probe against genomic DNA from the original *phan*-552/*phan*-249G mutant and its wild-type siblings (Figure 5.2), and also the progeny from the F_1 generation of back-crosses of *phan*-552/*phan*-249G to the mutant parent *phan*-249G/*phan*-249G (Figure 5.3 and 5.4). Southern hybridisation produced only a few bands on the autoradiograph indicating that the flank contained sequences that occured only in single copy.

Importantly, only DNA from plants with a *phan*-552 mutant allele had a band at 6 kb. All revertants and wild-type siblings lacked the 6 kb band and instead produced a band at 1.6 kb that was attributable to the wild-type allele. The difference in size between the two bands could be explained by the insertion of Tam 4 which is 4.2 kb in length.

Other bands were present which could be attributed to the other mutant alleles, *phan*-249G and *phan*-250G. These also provided further evidence that the right hand flank contained a part of the *phan* gene. In the families which were the result of back-crosses of the original mutant, *phan*-552/*phan*-249G, to the mutant parent *phan*-249G/*phan*-249G there was a band at 4 kb in both mutant DNA samples (*phan*-552/*phan*-249G) and revertant samples (*Phan*$^+$/*phan*-249G). This band was attributed to the *phan*-249G allele (Figure 5.3).

The original mutant, *phan*-552/*phan*-249G, had also been back-crossed to another *phan* mutant, *phan*-250G/*phan*-250G. The DNA sample from the pooled mutant progeny, *phan*-552/*phan*-250G

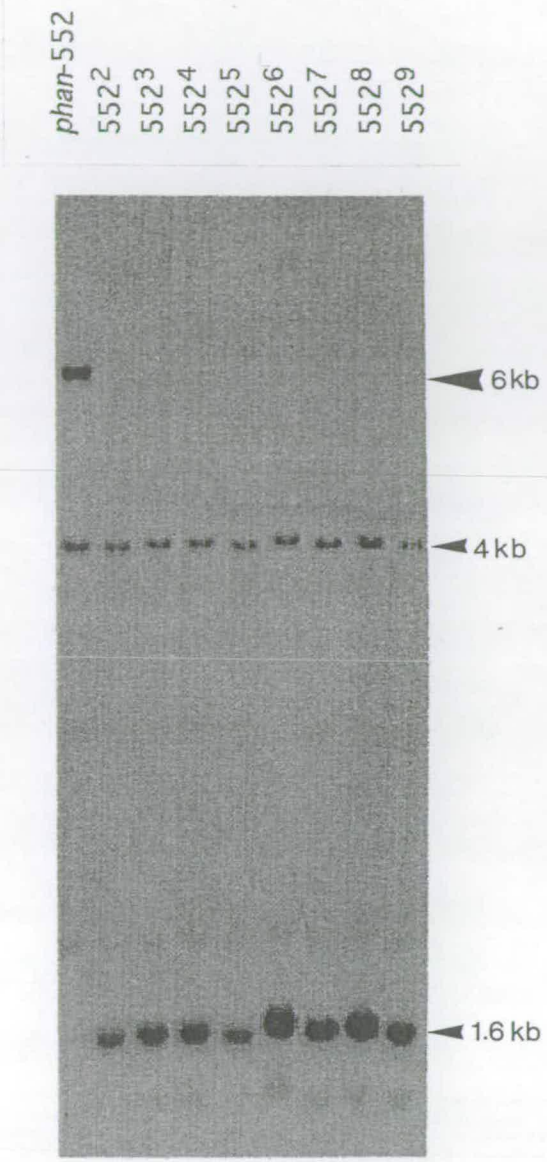

Figure 5.2 Southern hybridisation of DNA from the *phan*-552 mutant and the eight wild-type siblings.
The right hand flank to the insertion of Tam 4 was used as a probe and detected a 6 kb band that was present in DNA from only the *phan*-552 mutant and not in DNA from the individual wild-type siblings.

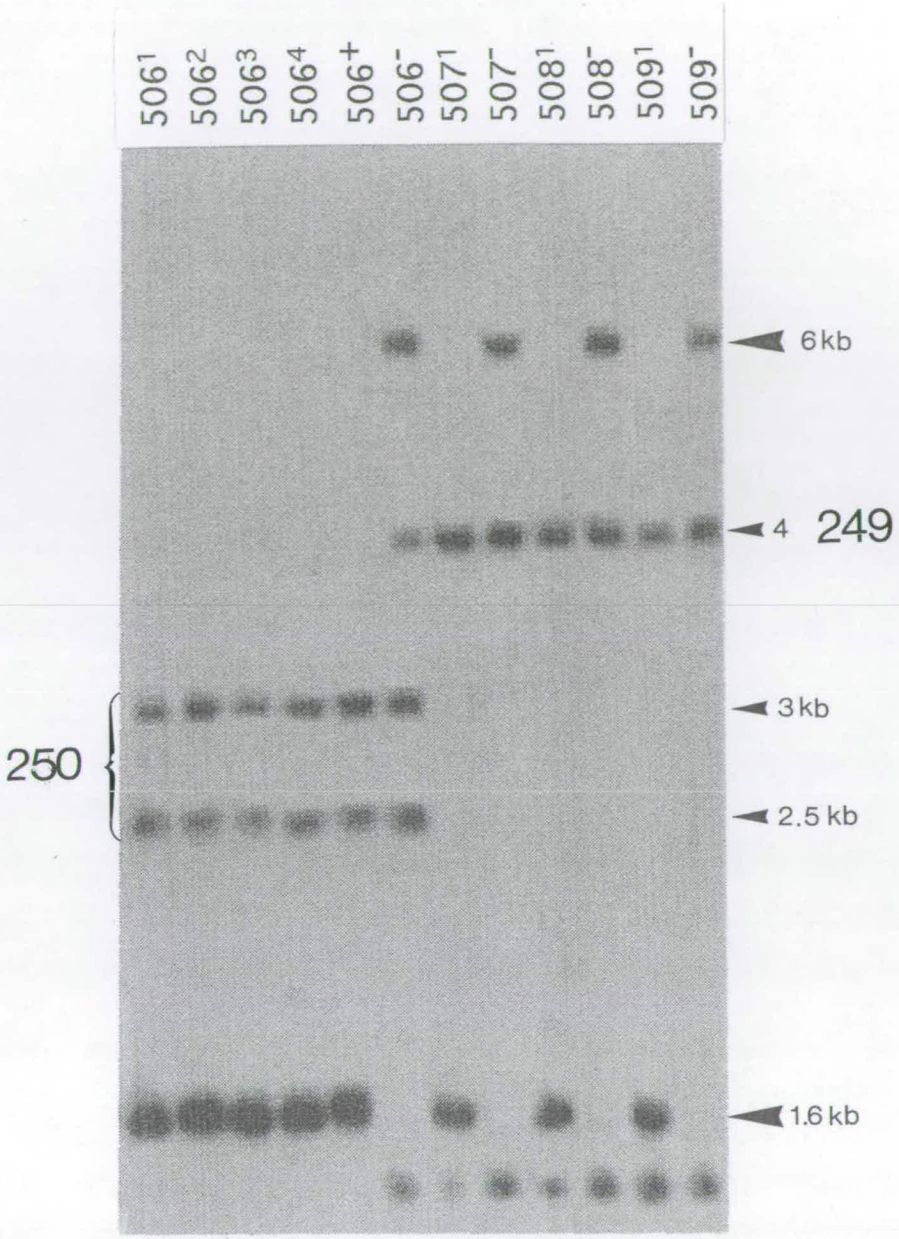

Figure 5.3 Southern hybridisation of DNA from individual revertants and pooled mutant plants of families 506, 507, 508 and 509.

The right hand flank to the insertion of Tam 4 was used as a probe to detect a 6 kb band that was present in only the mutant pools of DNA and not in the DNA from individual revertants (revertant 507^2 is not shown). The alleles attributed to the *phan*-249G and *phan*-250G are indicated. The same filter was used for Figure 4.4.

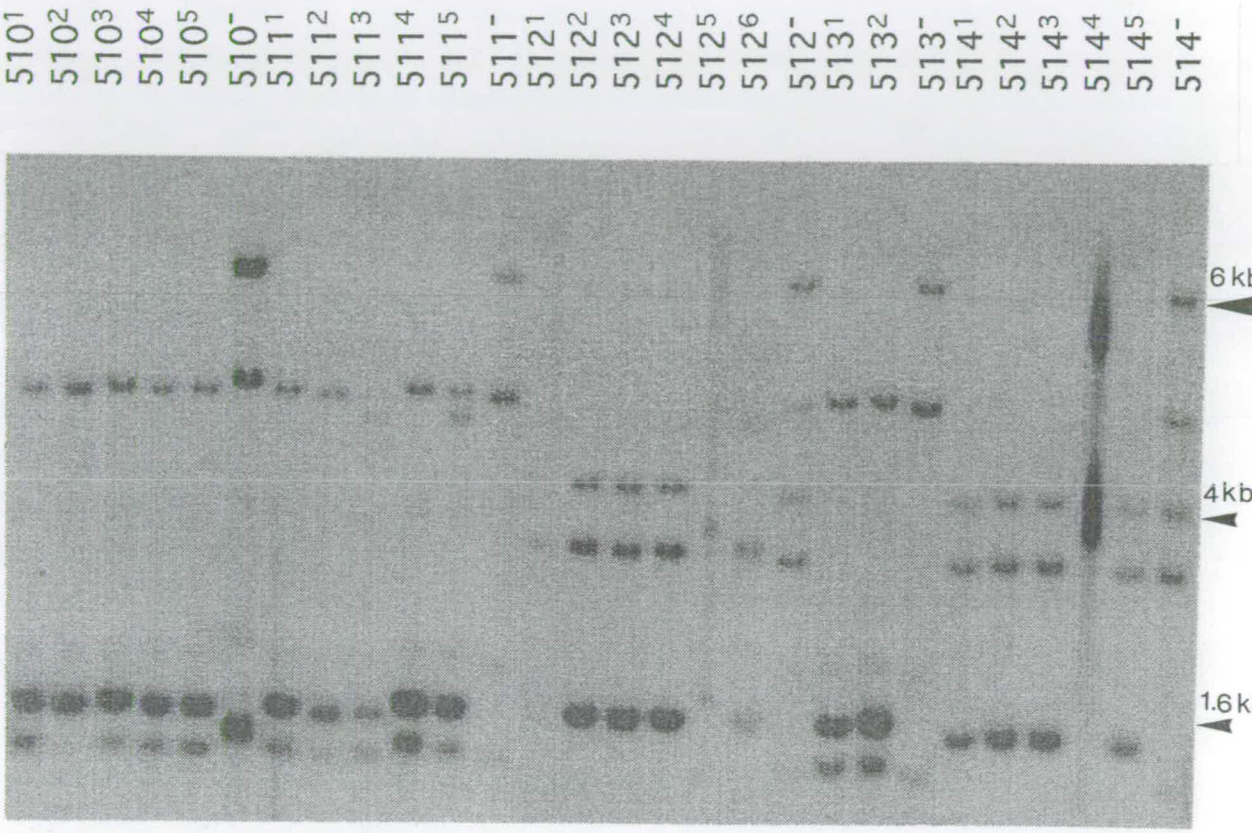

Figure 5.4 Southern hybridisation of DNA from individual revertants and pooled mutant plants of families 510 to 514.

The right hand flank to the insertion of Tam 4 was used as a probe and detected a 6 kb band that was present in only the mutant pools of DNA and not in the DNA from the individual revertants. The same filter were used for Figure 4.5.

and *phan*-250G/*phan*-249G, had four bands; 2.5 kb, 3 kb, 4 kb and 6 kb. The 4 kb band had already been identified as the *phan*-249G allele and the 6 kb as the *phan*-552 allele. Therefore, the other two bands were attributed to the *phan*-250G allele. This was confirmed in the revertant, *Phan*$^+$/*phan*-250G, DNA samples of the same family which had three bands; the *Phan*$^+$ band at 1.5 kb, and the *phan*-250G bands 2.5 kb and 3 kb (Figure 5.3).

5.2.3 *phan*-607 and *phan*-709

DNA samples for two other *phan* mutants were examined to provide further evidence that the flank contained the *phan* gene. These samples were compared to *Phan*$^+$ DNA from wild-type progenitor lines.

The *phan*-607 mutant was compared to its progenitor line JI. 75. After probing with the right hand flank a band was present at 6.5 kb in the *phan*-607 DNA sample which was assigned to the *phan*-607 allele. The sample from the progenitor line JI. 75 had a band at 1.5 kb as expected for the *Phan*$^+$ allele. Again the difference in size between the two bands could be explained by the insertion of a transposon which probably caused the *phan*-607 mutation (Figure 5.5).

During the period of this thesis a single, putative revertant of *phan*-607 was identified. DNA samples from the *phan*-607 mutant, the original revertant (*Phan*$^+$/*phan*-607) were examined. The revertant sample had bands characteristic of both the *phan*-607 and *Phan*$^+$ alleles, but at half the intensity at which they occurred in either the original *phan*-607 mutant or line JI. 75. The simplest explanation for this is that the transposon had excised from one copy of the *phan*-607 allele to give the wild-type restriction fragment length (Figure 5.5).

For confirmation, the *phan*-607/*Phan*$^+$ revertant was back-crossed to the *phan*-250G/*phan*-250G mutant. As expected, half the progeny were wild-type (*Phan*$^+$/*phan*-250G) and half were mutant (*phan*-607/*phan*-250G). From the F_1 generation DNA was prepared from a pool of mutant plants and a pool of *Phan*$^+$ plants.

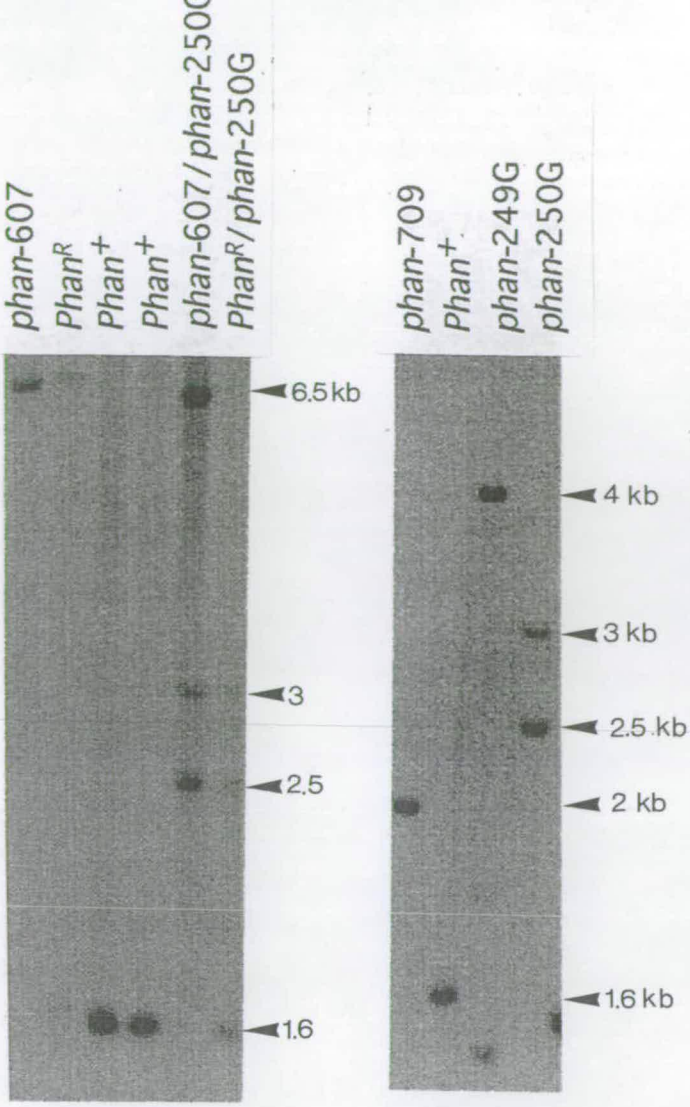

Figure 5.5 Southern Hybridisation of DNA from wild-type and *phan* mutant lines.

DNA from the *phan*-607 and its single revertant were examined after hybridisation with the right hand flank to the insertion of Tam 4 as a probe. The *phan*-607 sample had a single band at 6.5kb. The revertant sample had the same band, but at about half the intensity, as well as a wild-type band, 1.5 kb, also at half the intensity. DNA was examined from the progeny of the backcross of the *phan*-607 revertant to *phan*-250G. *phan*$^-$ progeny had the 6.5 kb band, *Phan*$^+$ progeny the 1.5 kb band and both sets had bands attributed to *phan*-250G. DNA from stock lines was also examined. JI. 75 had only the wild-type 1.5 kb band. *phan*-249G and *phan*-250G showed the bands previously attributed to them. *Phan*$^+$ is the wild-type line JI.75

Also as expected, genomic DNA from mutant plants had a band at 6.5 kb from the *phan*-607 allele, and DNA from the wild-type plants had a band at 1.5 kb derived from the *Phan*$^+$ allele. Both samples had bands which had previously been attributed to the *phan*-250G allele (Figure 5.5).

A fourth *phan* mutant was isolated from the John Innes mutagenesis screen during the work for this thesis. Three mutants were identified in a single family and the allele was numbered *phan*-709. Genomic DNA was examined from the *phan*-709 mutants and their progenitor line JI. 75. Again there was a difference in the size of bands between the two samples. All three mutants with the *phan*-709 allele had a band of about 2.5 kb compared to the 1.5 kb band attributed to the *Phan*$^+$ allele in line JI. 75 (Figure 5.5).

5.2.4 Northern Hybridisation

To confirm whether the right hand flank to the Tam 4 insertion in *phan*-552 allele included a transcribed portion of the *phan* gene, it was used to probe poly (A)$^+$ RNA from *phan* mutants (*phan*-552/*phan*-249) and *Phan*$^+$ plants in a Northern hybridisation. The probe detected a transcript of about 1.2 kb in RNA from wild-type shoot tips. A transcript of this size was not detected in RNA from *phan* mutants, although larger bands were observed at lower intensity (Figure 5.6). This suggested that part of the transcribed region of the *phan* gene was contained within the RH clone, and that the potential transposon insertions in the *phan*-552 and *phan*-249 alleles were within the transcribed region.

5.2.5 cDNA

The flank contained a transcribed region that might have been the *phan* transcription unit. Therefore, for this transcription product to be sequenced a cDNA library (see Materials and Methods) was screened using the right hand flank as a probe. Twenty positives were identified, the majority of which were

about 1.2 kb in size suggesting that they were near full-length cDNAs.

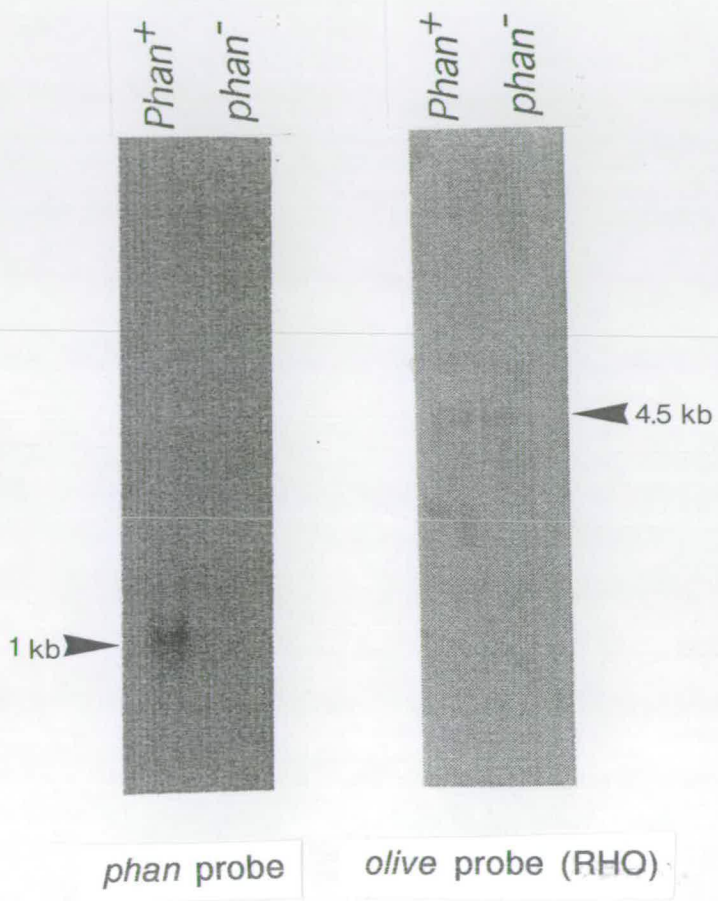

Figure 5.6 Northern hybridisation

10 μg of poly A+ RNA from the shoot tips of wild-type plants and from *phan*-552/*phan*-249G mutants was loaded in adjacent lanes. The filter was probed with the right hand flank to the insertion of Tam 4 and revealed a transcript at about 1 kb in only the wild-type lane. The filter was re-hybridised with a probe (RHO) from the *olive* gene (Hudson *et al.*, 1993) and detected a larger band at about 4.5 kb in both lanes.

CHAPTER 6 RESULTS

Morphology of the *phan* phenotype

6.1 Introduction

Five *phan* mutants had been obtained. All showed a similar vegetative phenotype. The morphologies of wild-type and *phan* mutants leaves were therefore compared to determine the possible role of the *phan* gene in leaf development.

6.2 Results

6.2.1 Dorsoventrality in the wild-type *Antirrhinum* leaf

The morphology of wild-type leaves was examined. The leaves showed dorsoventral asymmetry in two respects (Figure 6.1). Firstly, the laminae, which made the leaf much wider and longer than thick, arose from the dorsal part of the midrib and curved dorsally towards their edges. As a result the leaf possessed one plane of symmetry that ran vertically along the line of the midrib. The dorsal and ventral parts of the leaf were not mirror images of each other. Secondly, the pattern of tissue layers within the leaf also reflected dorsoventrality. For example, in the lamina four distinct cell types were arranged along the dorsoventral axis: dorsal epidermis, palisade mesophyll, spongy mesophyll and ventral epidermis (Figure 6.1). There were distinct differences between the dorsal and ventral epidermis. Ventral epidermal cells were smaller, more complex in outline and also interspersed with stomatal cells that were not present on the dorsal surface (Figure 6.1). The major veins, including the midrib, also showed differences in dorsoventrality. Both had an arc of xylem on the dorsal side of an arc of phloem, with both sets of vascular tissue surrounded by parenchyma (Figure 6.1). Therefore, not only did the arrangement of the vascular tissue reflect the dorsoventral axis, but so did the pattern of cells of within each tissue type. The dorsal and ventral epidermal cells of the midrib were also distinct, despite showing a slightly different morphology to those of the lamina. Ventral epidermal cells of the midrib were elongated along the axis of the midrib whereas the dorsal cells were shorter and included hairs (Figure

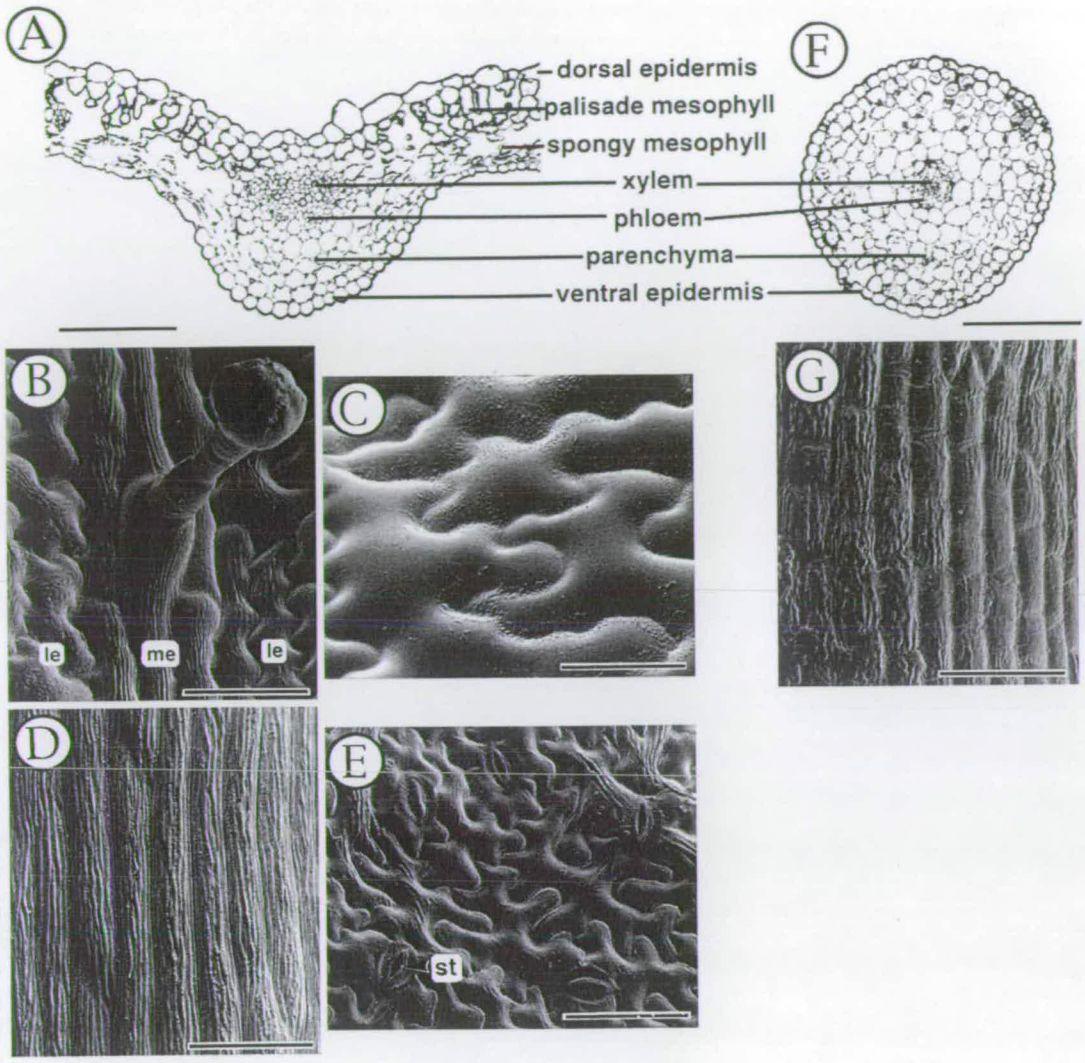

Figure 6.1 Dorsoventrality in the wild-type leaf and the effect of *phan* mutations on leaf anatomy.

(**A**) Transverse section through the midrib and adjacent laminal regions of a wild-type leaf. The epidermal regions are morphologically distinguishable: (**B**) dorsal midrib epidermis (me) and neighbouring dorsal epidermis (le); (**C**) dorsal laminal epidermis; (**D**) ventral midrib epidermis; (**E**) ventral laminal epidermis, including stomata (st). In contrast, needle-like *phan* mutant leaves consist of only ventral types, arranged with radial symmetry (**F**). The epidermis of these leaves resembles that of wild-type ventral epidermis (**G**). Scale bars, 250 μm in **A** and **F**; 50 μm in **B-E** and **G**.

6.1). The petiole showed the same dorsoventral differences as the rest of the leaf despite having a much lower proportion of laminal tissue (data not shown).

6.2.2 Anatomy of *phan* mutant leaves

Mutant leaf morphology varied with the developmental stage of the plant. For example leaves that were produced at and above the fifth node were typically needle-like. They represented a complete loss of dorsventrality. In cross section these leaves were radial, lacking laminae and all cell types associated with the dorsal portion of the wild-type leaf (Figure 6.2). The epidermis was similar to the ventral epidermis of wild-type leaves, most noticeably stomata were present (Figure 6.1). Internally, needle-like leaves consisted entirely of ventral tissue types: parenchyma, phloem and xylem, arranged in concentric cylinders (Figure 6.2).

In contrast, the cotyledons and the first three pairs of leaves of *phan* mutants were more heart-shaped than their wild-type equivalents (Figure 6.3 E and F). Characteristically, patches of ventral epidermis, including stomata, were present on their dorsal surface (Figure 6.4 A). The boundaries of these ectopic patches of ventral epidermis and the surrounding dorsal epidermis formed ridges arranged on an axis perpendicular to the surface of the leaf (Figure 6.4 B). In cross-section these ridges resembled the edge of a wild-type leaf (Figure 6.4 D). The side of the ridge covered by dorsal epidermis contained palisade mesophyll and the side covered by ventral epidermis contained spongy mesophyll. Within the ectopic patch the lamina contained ventral epidermis with only spongy mesophyll between (Figure 6.4 C). The shape of larger ectopic patches tended to be elongated parallel to the axis of the leaf reflected by the midrib, whereas smaller patches were more isodiametric. Also, towards the proximal part of the leaf the patches were larger and occured at a higher frequency. Both these characteristics resembled the shape of the clones showing altered levels of chlorophyll in the *olive*-605 mutant (Hudson *et al.*, 1993). The

clones of the *olive*-605 mutant are the result of somatic excisions of Tam 3 during development of the leaf and therefore these patches of cells are clonally related. This suggests that the patches of ventral cells in *phan* mutant leaves were also clonally related.

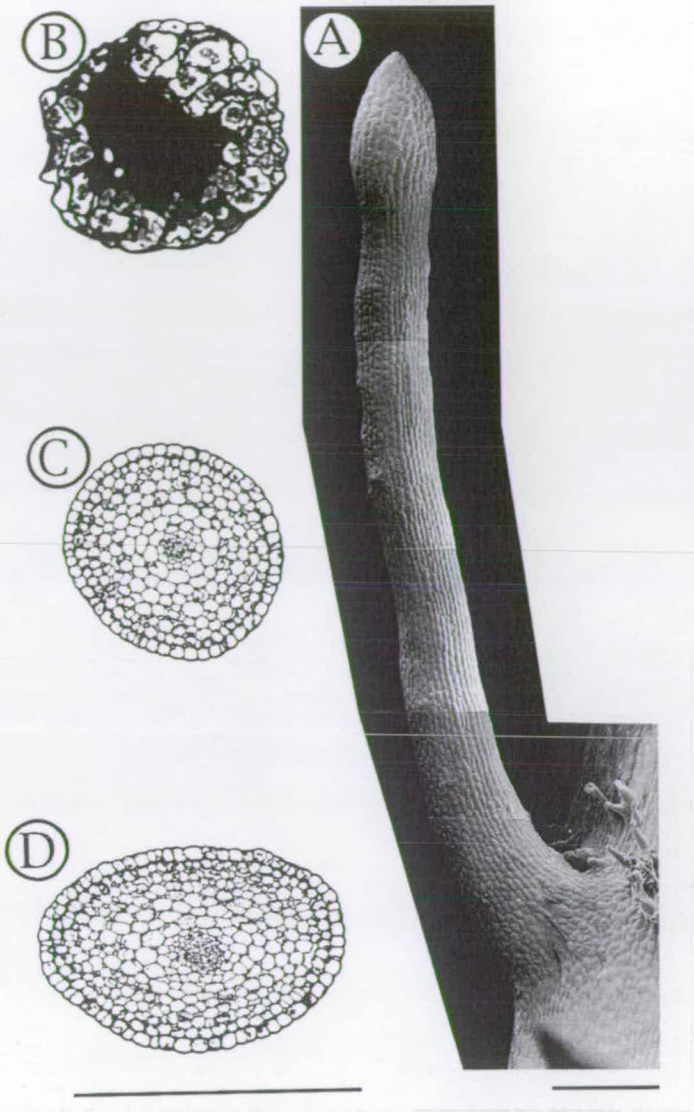

Figure 6.2 A needle-like *phan* mutant leaf.
(**A**) A mature needle-like leaf from a *phan* mutant, and transverse sections cut from the distal (**B**), middle (**C**) and proximal (**D**) parts of the same leaf. Only the most proximal region, derived from the leaf buttress, shows dorsoventral flattening, although it consists of ventral cell types and has radially symmetrical vascular tissue. The darkly staining cells, of unknown function, in the distal region are also found in the tips of wild-type leaves. Scale bars, 250 μm.

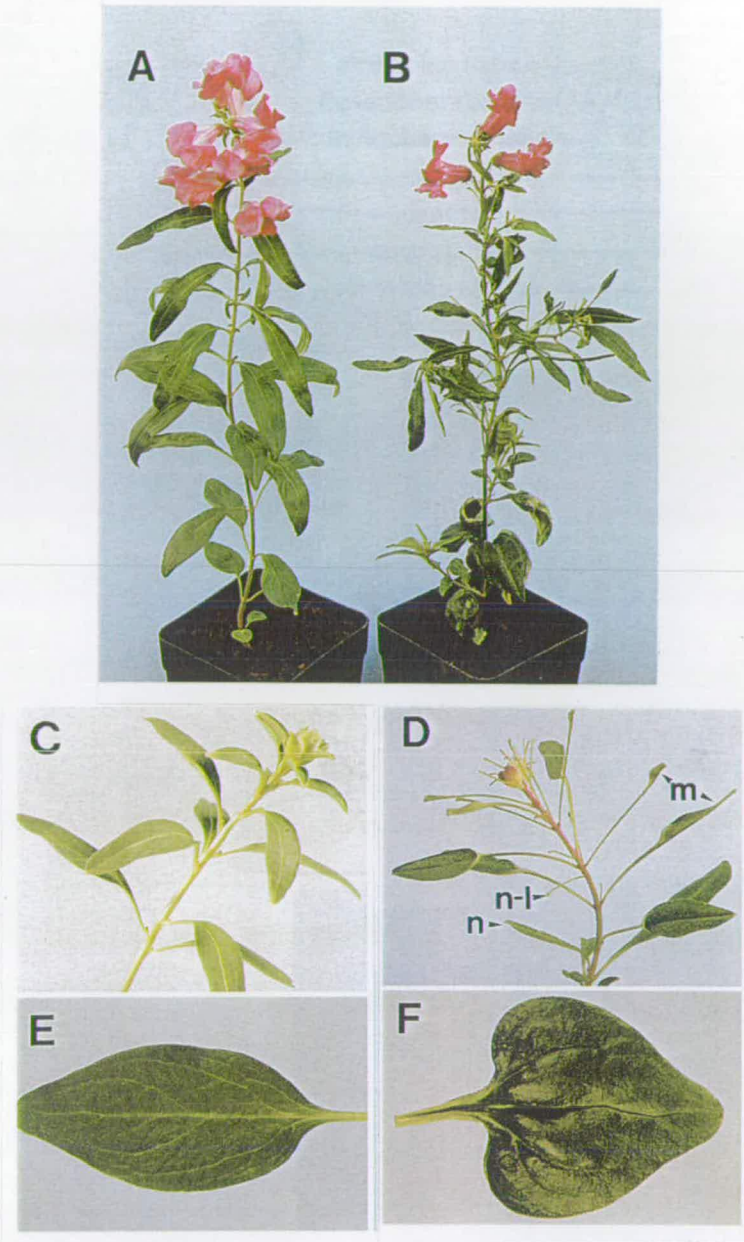

Figure 6.3 Effects of *phan* mutations on morphology.
(**A**) A wild-type plant and (**B**) the *phan*-607 mutant. (**C**) The vegetative shoot of a wild-type plant, and (**D**) the corresponding region of a *phan* mutant with narrow (n), needle-like (n-l) and mosaic (m) leaves. (E) A leaf from the second node of a wild-type plant, and (F) a broad, heart-shaped leaf typical of the equivalent node of a *phan* mutant.

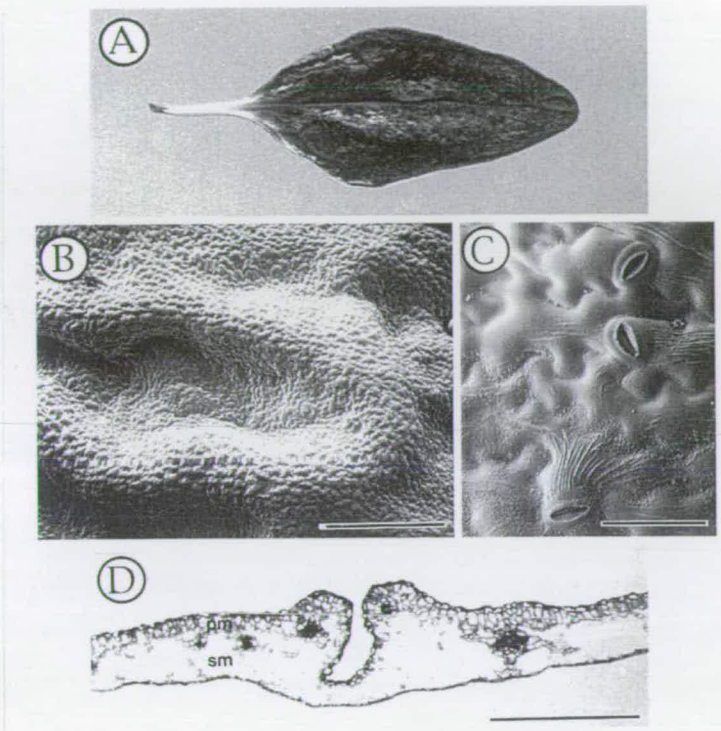

Figure 6.4 Ectopic patches of ventral cell types in *phan* mutant leaves.

(**A**) A leaf from the third node of a *phan* mutant plant. Patches of ventral epidermis tissue appear lighter than the surrounding dorsal epidermis and the leaf surface is uneven due to the presence of frequent ectopic laminal ridges. (**B**) Scanning electron micrograph of an ectopic patch of ventral tissue and the surrounding ectopic ridge. (**C**) Numerous stomata, characteristic of ventral epidermis, are present within the patches. (**D**) A transverse section through a patch of ventral tissue. The region within the ridges lacks palisade mesophyll cells (pm) but retains of the spongy mesophyll (sm). Scale bars, 500μm in **A**, **B** and **D**; 50 μm in **C**.

The transition between the early heart-shaped leaves and later needle-like leaves was rarely abrupt. Leaves at intermediate nodes showed a variety of characteristic mutant phenotypes (Figure 6.3 D). Typically these mutant leaves were narrower than wild-type or were mosaics of needle-like and laminal tissues. The narrower leaves contained fewer cells in cross-section than wild-type and their laminae arose from more dorsal positions on the midrib (Figure 6.5 A). Two types of mosaic leaves were common. In one case the proximal region of the leaf was needle-like and the distal region laminal. In the other example, the reverse occured with needle-like tissue distally and laminal tissue proximally. In both patterns, at the junction between the two tissue types, the lamina formed a novel axis dorsally that also resembles the edge of a wild-type leaf (Figure 6.5 B).

6.3 Discussion

6.3.1 A model for the determination of dorsoventrality in leaves of *Antirrhinum*

Although each *phan* mutant shows a similar variety of leaf phenotypes they suggested a relatively simple model for the determination of leaf dorsoventrality. This involves a dorsalising function (DF), which is expressed in a domain that includes the dorsal most cells of the wild-type leaf primordium (Figure 6.6 A). Soon after primordial initiation cells at the ventral boundary of this domain are induced to change their pattern of division and form the laminae by lateral proliferation. DF expression persists in the dorsal part of the lamina where it is necessary for the determination of dorsal cell types.

The needle-like leaves of *phan* mutants lacked laminae and dorsal cell types. This phenotype suggests a complete loss of DF where no boundary exists for lateral proliferation and expression of DF does not persist for determination of dorsal cell types (Figure 6.6 B).

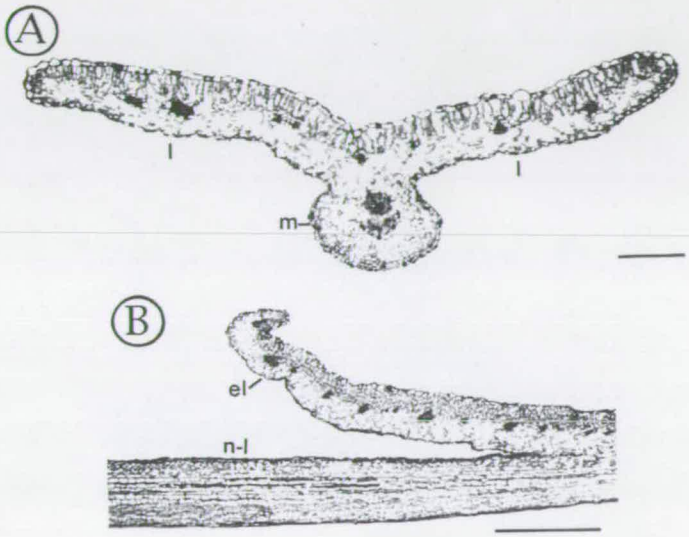

Figure 6.5 Anatomy of *phan* mutant leaves with laminae.

(**A**) Transverse section of a narrow *phan* mutant leaf. The laminae (l) are produced at a more dorsal position on the midrib (m) than in wild-type (compare with Figure 6.1). (**B**) A longitudinal section through a mosaic *phan* mutant leaf at the boundary between laminal and needle-like tissue. In this region, the lamina forms an ectopic dorsal axis (el), distinct from that of the needle-like tissue (n-l). The distal part of the leaf is to the left. Scale bars, 250 μm in A and 500μm in B.

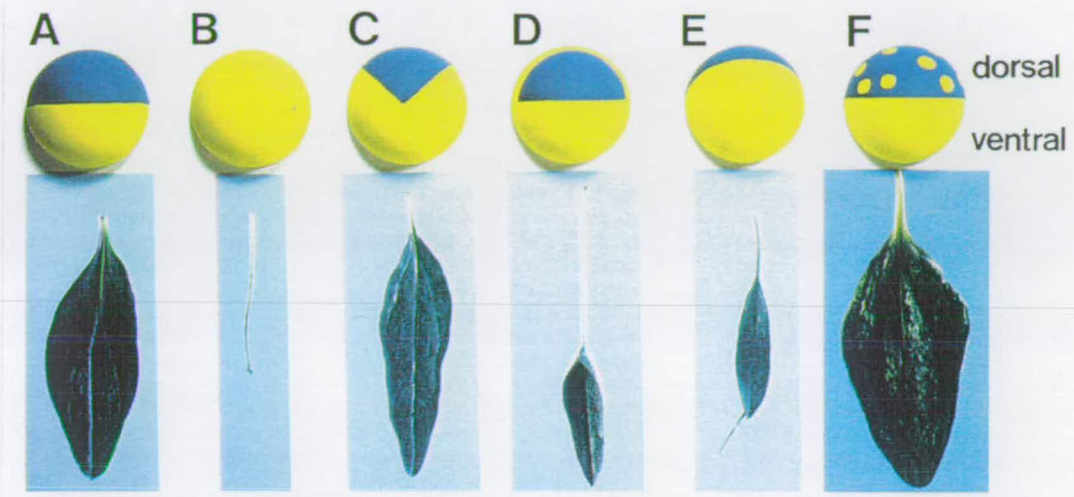

Figure 6.6 A model for the action of the dorsalising function in leaf development.

Early leaf primordia are depicted as yellow hemispheres viewed from a distal position. Dorsal regions of the primordia experiencing DF expression are coloured blue. Different leaf morphologies are shown below the patterns of expression that are proposed to have given rise to them. Mature leaves are viewed from above, with their distal ends towards the bottom of the page. (**A**) A wild-type leaf; (**B**) a needle-like *phan* mutant leaf; (**D**, **E**) mosaic mutant leaves; (**F**) an early *phan* mutant leaf showing ectopic patches of ventral cell types.

The other leaf forms could also be explained by reductions in the domain of DF expression. If expression was confined to a dorsal region this would have three effects (Figure 6.6 C). Firstly, the laminae would arise on a more dorsal position on the midrib because the boundary has been shifted to a more dorsal position. Secondly, the domain of DF has been reduced in size resulting in less cells developing with a dorsal identity. As a result more cells develop with a ventral identity and the midrib becomes more pronounced. Thirdly, the boundary has been shifted to a position where the primordium is narrower. This is reflected by a narrower leaf because of the loss of laminal initials. Narrow leaves, with more prominent midribs and lamina in a more dorsal position are characteristic of intermediate leaves of *phan* mutants and are therefore consistent with the domain of DF being reduced to a more dorsal position.

In other primordia DF could be restricted to a more proximal or distal position with a corresponding region lacking DF (Figure 6.6 D and E). In such cases regions that develop lacking DF expression would have a needle-like morphology and those with DF expression would have laminal characteristics. In each example the boundary of DF expression would be shifted to a novel position on the dorsal surface of the primordium. As a result the lamina would develop on an ectopic axis where this novel boundary is now positioned. The mosaic leaves of *phan* mutants showed morphologies consistent with this prediction.

The early heart-shaped leaves of the *phan* mutants were broader than wild-type and had ectopic patches of ventral cell types. The morphology of these leaves could have been the result of localised loss of DF relatively late in leaf development (Figure 6.6 F). Such a lack of DF would prevent the determination of dorsal cell types and also introduce a new boundary of DF expression where ectopic proliferations of laminal tissue would occur. Proliferation at the novel boundaries might also contribute to the increased lateral growth. Because the ventral

patches are more common in the proximal region of the leaf this would move the widest point of the leaf nearer the petiole resulting in a more the heart-shaped leaf.

CHAPTER 7 RESULTS

Further aspects of the *phan* mutant morphology

7.1 Introduction

Other lateral organs; cotyledons, bracts and floral organs, can be considered homologous to leaves. Like leaves they may be both flattened dorsoventrally and show dorsoventral differences in cell type. These features are most obvious in the cotyledons, bracts, sepals and petals, but also in the pollen sacs of anthers and in the gynoecium. To determine whether *phan* was required for development of these organs in *Antirrhinum*, the effect of the *phan* mutation was examined.

7.2 Results

7.2.1 Effects on petal development

The flower corolla consists of five petals which, over the proximal part, are united to form the corolla tube. Distally the petals diverge into individual lobes. The lobes are formed from primordia on the flanks of the floral meristem and the tube is formed by a proliferation of a more proximal ring of cells which includes regions between the lobe primordia. The inner surface of the petal is considered dorsal, and the outer surface ventral. There are morphological differences in the epidermal cells of these surfaces. The most obvious is in the colour of the red wild-type flowers. The dorsal surfaces appear more strongly pigmented than the ventral surfaces (Figure 7.1 A). This is due to distinct dorsoventral differences in cell type. The dorsal epidermal cells are conical in shape and the ventral flatter. The proportion of incident reflecting from epidermal cells is decreased by the angle of conical cells (Noda *et al.*, 1994).

The five *phan* mutations were found to affect the petal lobes to different degrees. In the most extreme case, *phan*-250G, the lobes were reduced to needles of tissue (Figure 7.1 B). The two upper petals and the lowest petal formed one needle each, and the two lateral petals are reduced to two needles each. The surface of the needles appeared smooth, suggesting that the

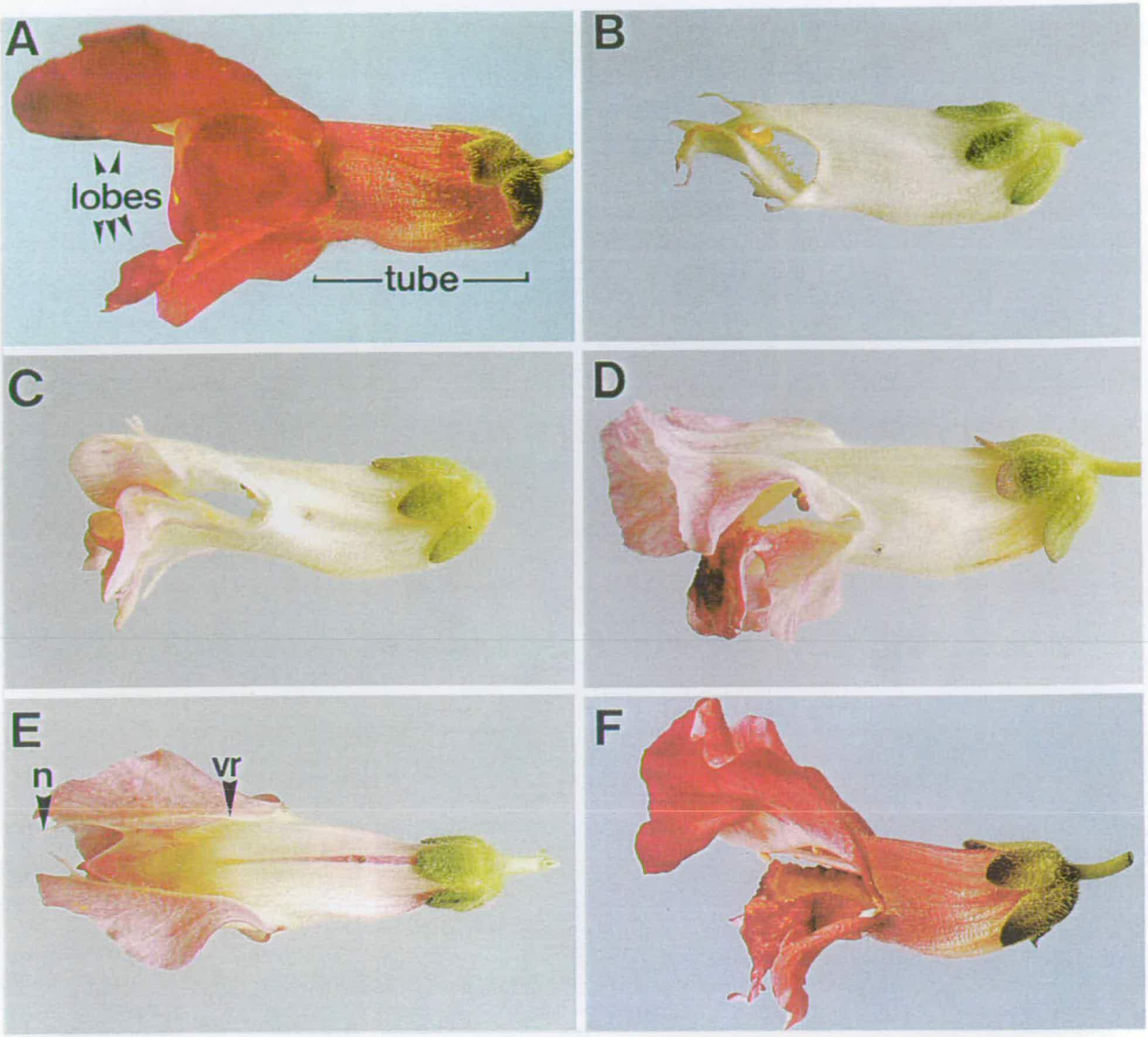

Figure 7.1 Effects of the *phan* mutations on flower morphology.

The wild-type flower (**A**) consists of five petals that are united proximally to form the corolla tube, but separate distally into five petal lobes. (**B**) A flower of the *phan*-250G mutant where petal lobes have been reduced to needles. Progressively lesser reductions in lobe tissue are shown by the *phan*-249G (**C**) and *phan*-552 (**D**) mutants. (**E**) The needles in these mutants (n) form the most distal part of ridge of ventral tissue running across the ventral surface of the corolla. This ventral ridge (vr) can be seen as lighter coloured tissue. (**F**) A flower of the *phan*-607 mutant. Differences in corolla pigmentation result from different combinations of alleles affecting anthocyanin synthesis in the inbred lines.

epidermis was ventralised. Therefore, this phenotype appeared analogous to the needle-like leaf of *phan* mutants.
The distal parts of the petal lobe of the *phan*-249G mutant were typically reduced to needles and the more proximal region formed a reduced lobe (Figure 7.1 C and E). The boundary between the two tissue types formed an ectopic petal lobe across the dorsal surface of the needle. These petals therefore appeared homologous to spoon leaves of *phan* mutants.

Characteristically, the petal lobes of the *phan*-607 mutant appeared slightly tattered and creased (Figure 7.1 F). This may have been due to lighter patches of ventral petal epidermis which were noticeable on the red dorsal surface of the lobe. These patches were surrounded by small proliferations or ridges resembling the edge of a wild-type petal. Again, this was an analogous situation to that identified in early *phan* mutant leaves.

7.2.2 Effects on the development of the other lateral organs

Flowers are produced in axils of bracts, the leaf-like structures of the inflorescence. In nearly every case, bracts of all five *phan* mutants were needle-like. Occasionally mosaics of laminal and needle-like bract tissue were identified.

In contrast, sepals, the bract-like organs of the first whorl of the flower were unaffected in *phan* mutants. The third and fourth whorls, the stamens and carpels also had no detectable mutant phenotype.

Mutant *phan* cotyledons had an extreme morphology (Figure 7.2). They were wider than wild-type and on either lateral side of the midrib there were two large bumps which appeared to be the result of buckling of the cotyledon laminae. The cotyledons also had frequent patches of ectopic ventral tissue, surrounded by ectopic ridges, on the dorsal surface. These patches were similar to those found on early *phan* mutant leaves. The ectopic proliferations, which may add laterally to the early mutant

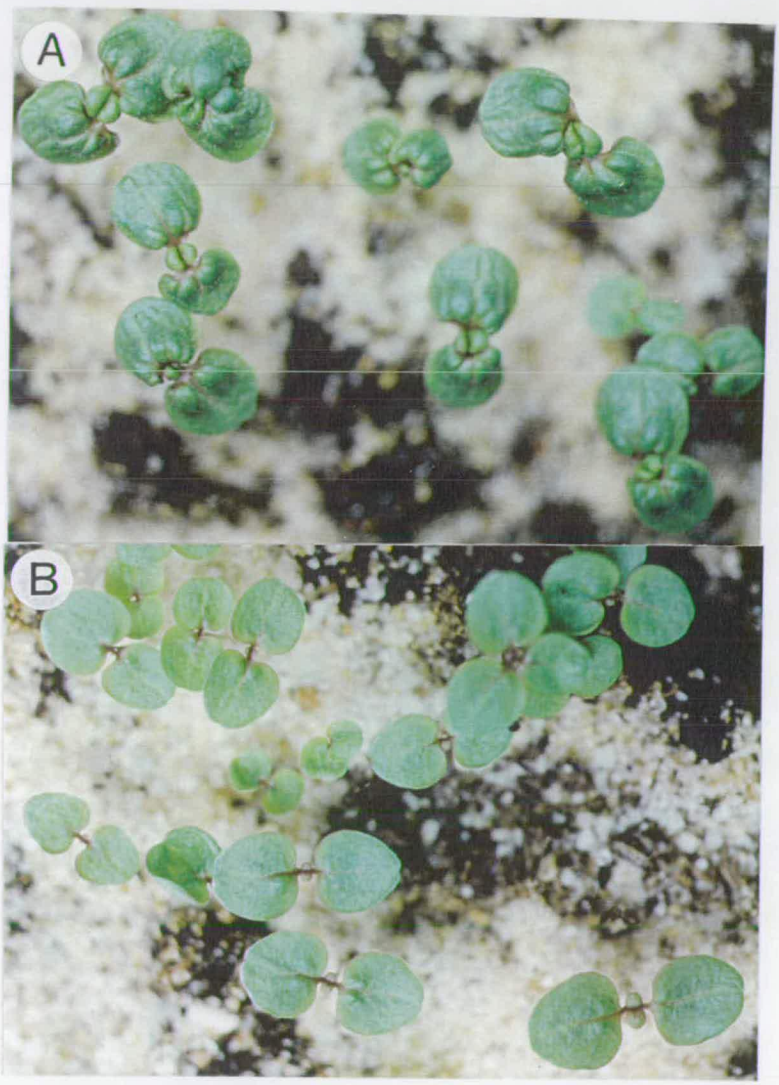

Figure 7.2 Effects of the *phan* mutation on cotyledon morphology.
phan-607 seedlings are shown (**A**) with Jl. 75 seedlings (**B**) for comparison.

leaves, may also cause mutant cotyledons to be wider than wild-type cotyledons and cause buckling of the cotyledon laminae.

7.2.3 Temperature sensitivity of the *phan* mutations

Another aspect of all the *phan* mutants was that their phenotypes were sensitive to temperature. The plants described previously had been grown at 20°C (Figure 7.3). The three stable *phan* mutant lines *phan*-249G, *phan*-250G and *phan*-607 were grown at a variety of temperatures and all showed more extreme phenotypes at lower temperatures.

At 25°C the *phan*-607 mutant had leaves which were more similar to wild-type in shape (Figure 7.4). However, the mutant leaves were slightly broader than wild-type and different in shape. The broadest region of wild-type leaves corresponds to a point about half way along their length. The broadest region of the wider mutant leaves was found to be nearer the proximal end of the leaf and these leaves therefore appeared heart-shaped. Only about one needle-like leaf was observed on every three plants and leaves with a mosaic needle and laminal tissue occurred at a similarly low frequency. Patches of ectopic ventral epidermis on dorsal surfaces were present on most leaves.

phan-250G and *phan*-249G mutants showed similar effects of temperature, except that both needle-like and mosaic leaves were slightly more common than in the *phan*-607 mutant. Also, the lower leaves of *phan*-249G and *phan*-250G were slightly wider than those of *phan*-607 as well as being much wider than wild-type plants grown at the same temperature (Figure 7.5).

The lowest temperature at which plants were grown was 15°C. At this temperature *phan*-607 seeds did not germinate whereas *phan*-250G and *phan*-249G, and the wild-type plants all germinated successfully (Figure 7.5). A slightly higher temperature of 17°C was required before *phan*-607 mutants could be grown. This produced the most extreme effect of the *phan* mutation seen (Figures 7.4 and 7.6). Only the cotyledons

Figure 7.3 Effects of temperature on the phenotype of *phan* mutants.
A plant of the mutant line *phan*-607 grown at 20°C, with a plant of its progenitor line Jl. 75 for comparison, also grown at 20°C.

Figure 7.4 Effects of temperature on the phenotype of *phan* mutants.
Plants of the mutant line *phan*-607 were grown at 25°C, 20°C and 17°C. Those at higher temperatures more closely resemble wild-type. All plants are the same age.

Figure 7.5 Effects of temperature on the phenotype of *phan* mutants.

Plants of the mutant line *phan*-249G were grown at 25°C, 20°C and 15°C. Those at higher temperatures more closely resemble wild-type. All plants are the same age.

Figure 7.6 Effects of temperature on the phenotype of *phan* mutants.
A plant of the mutant line *phan*-607 grown at 17°C.

had laminae that were very broad and had many ectopic patches of ventral epidermis. All the subsequent leaves were needle-like. Mutant plants had a similar number of leaves to wild-type plants at 17°C. However, the internode length of the mutant was significantly reduced. Initially, the *phan*-607 mutants did not flower at 17°C. Eventually, lateral shoots developed from the lowest part of the stem. These shoots were more vigorous and had an internode length similar to wild-type but still had only needle-like leaves. Often patches of cells, particularly at the distal ends of the leaves died. Occasionally the same was true of lateral shoots which did not grow further. Viable lateral shoots eventually flowered.

When *phan*-249G and *phan*-250G were grown at 15°C only the first and second sets of leaves had laminal tissue and these were very broad. All other leaves were needle-like. Internode lengths of these mutants was not affected (Figure 7.5).

The petal phenotype of *phan* mutants was also sensitive to temperature. The petals of the *phan*-607 mutant had a less severe phenotype at 25°C than at 20°C. The shape of the petal lobes was more complete and less creased. As with early leaves of this mutant, ectopic patches of ventral epidermis on the dorsal petal surface were more common at the higher temperature. At 20°C petals of *phan*-250G were completely reduced to needles of ventral tissue and *phan*-249G petals to needles with ectopic petal lobes. At 25°C, both petal phenotypes were less severe. The flowers of *phan*-250G resembled those of *phan*-249G grown at 20°C and in *phan*-249G the petal lobes were larger and the proportion of needle-like tissue reduced relative to plants grown at 20°C. The flower phenotypes were more extreme at lower temperatures. The petal lobes of *phan*-607 flowers at 17°C were smaller and more tattered. Also, the corolla face was less well defined and the lobes almost continuous with the tube. The upper petals had small needles. In both *phan*-249G and *phan*-250G the petals were completely reduced to needles. Neither mutant showed any petal lobes.

Interestingly, there was no identifiable effect of mutations on sepals, stamens or carpels at low temperature, even though other organs were drastically affected.

One explanation for the effect of temperature on the phenotype of the *phan* mutants was that DF was temperature sensitive: being reduced or absent at low temperature and increased at high temperature. Therefore, growing mutant plants in a cycle of low and high temperature might have been expected to switch DF expression from low to high. If this occurred repeatedly, patches of a few cells either expressing or not expressing DF with numerous ectopic DF boundaries might have been introduced across the developing leaf. The model for the action of *phan* suggests that such boundaries lead to proliferation, and therefore alternating the temperature in this way might have been expected to produce broader leaves in *phan* mutants than in mutant plants grown under constant temperatures.

To test this, *phan*-607 mutants and wild-type plants were grown in an alternating temperature cycle of 15°C from midnight to noon and 25°C for the rest of the day. The plants were illuminated from 6am to 10pm, and therefore experienced equal periods of light at each temperature. Plants were examined after ten weeks of this regime. The leaves of wild-type plants were unaffected, but mutant leaves were slightly broader than those of the *phan*-607 mutant grown at a constant temperature of 25°C (Figure 7.7).

7.3 Discussion

7.3.1 Role of *phan* in bract and cotyledon development

The effect of all five *phan* mutations on bract development is similar to that on later leaves. The organs are typically needle-like. This is not unexpected since bracts can be considered modified leaves. In a similar way, cotyledons are affected in a similar way to early leaves on all *phan* mutants. Both have ventral clones of epidermis on the dorsal surfaces and increased

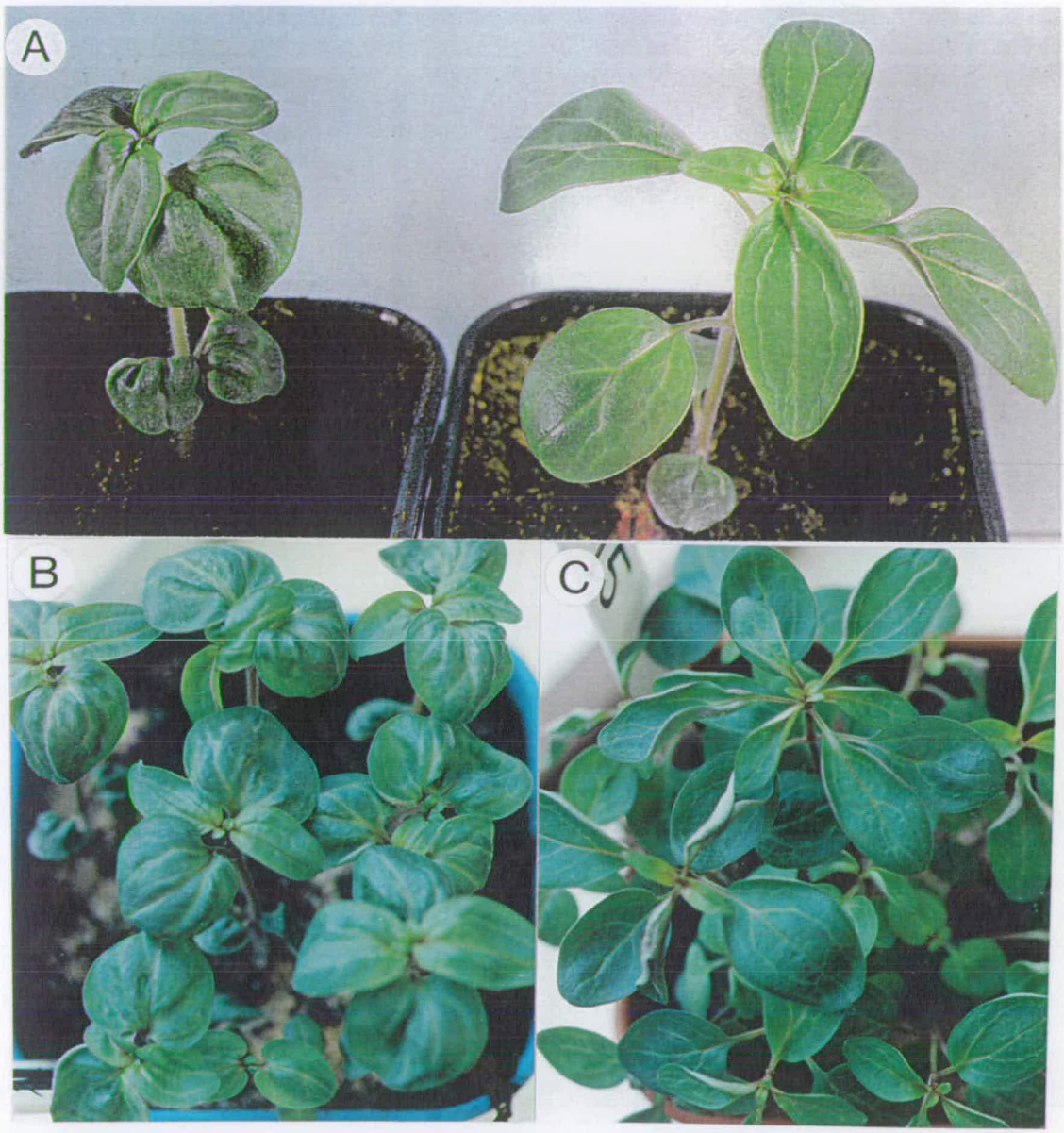

Figure 7.7 Morphology of the leaves of *phan* mutants grown in the alternating temperature cycle between 15°C and 25°C.

A wild-type (right) and a *phan*-607 mutant (left) grown in the alternating temperature cycle (**A**). For comparison *phan*-607 mutant plants (**B**) and wild-type plants (**C**) grown at 25°C. All plants are a similar age.

lateral proliferation. Again this is expected since cotyledons are considered equivalent to leaves. The model proposed to explain the action of DF in leaves is therefore equally applicable to bracts and cotyledons.

7.3.2 Role of *phan* in petal development

The petal lobes are affected in all *phan* mutants. The mutant phenotypes are similar to those of mutant leaves. In extreme cases radially symmetrical needles develop, in less severe examples ectopic petal lobes also occur. Patches of ventral epidermis were also identified on the dorsal surfaces of petals. These phenotypes can be explained by the same model proposed for leaf development. As the width of the DF domain is reduced it is shifted dorsally and the boundary is moved to a more proximal position. As a result the distal part of the primordium becomes a spike and a novel axis ofgrowth, forming an ectopic petal lobe, induced at the boundary. The petal phenotypes characteristic of each mutant are compatible with different degrees of reduction in the domain of DF. *phan*-250G typically has petals lobes reduced to needles and no ectopic lobes suggesting the greatest reduction in the DF domain. This may even be equivalent to the complete loss of DF. *phan*-607 would have the domain of DF nearest to wild-type because nearly complete petal lobes develop and the other mutants would show intermediate levels of DF. This suggests that different mutations cause different reductions in the domain of DF. This view is supported by the effects of temperature which can make one mutant phenotype at high temperature similar to that of a normally less severe mutant grown at low temperature.

Because petals are homologous to leaves they might be expected to retain the same system of DF. However, the corolla tube is unaffected in all five mutants, despite its showing dorsoventral differences in morphology. Most notably, the ventral epidermis is smooth and the dorsal hairy. The possible reasons for the lack of a *phan* phenotype in the corolla tube will be discussed later.

7.3.3 The role of *phan* in sepal development

The sepals in all *phan* mutants are unaffected, even though they show a high degree of dorsoventral flattening and dorsoventral differences in cell type. This is particularly surprising since sepals closely resemble bracts, which are strongly ventralised in *phan* mutants and also considered modified leaves. One explanation is that the level of *phan* expression is still sufficient for wild-type levels of DF in sepals, but not in bracts. However, this seems unlikely because sepals remain unaffected in the most severe mutants at low temperature when all other affected organs show extremely ventralised phenotypes. An alternative explanation is that DF in sepals does not require *phan*. Since sepals are considered modified leaves and are obviously dorsoventral, this implies that the requirement of *phan* has been lost, and perhaps been replaced by the expression of another gene. These same explanations apply to the corolla tube.

7.3.4 Role of *phan* in development of the sex organs

Despite obvious differences in morphology, the sex organs are believed to be derived from modified leaves, or sporophylls, bearing either male or female sporangia. The gynoecium has a bilocular ovary and can therefore be considered to consist of two united carpels each of which was derived from a female sporophyll. The outer, visible surface of the gynoecium can be regarded as ventral and the inner surface of the ovary, and the conductive tissue of the style, dorsal. Therefore the gynoecium appears to retain a high degree of dorsoventrality. The ovary wall is both flattened perpendicular to the floral axis and also has dorsoventral differences in cell type along the dorsoventral axis. The ventral epidermis is dark green and hairy, while the dorsal epidermis of the ovary wall is much lighter in colour and is smooth.

The sporophyll origins of stamens are not as clear. In particular, the structure and anatomy of the anther filaments suggest that they may be derived from a condensed stem and that only pollen

sacs represent modified sporophylls. Interestingly, this is consistent with the observation that the anther filaments show little dorsoventral asymmetry whereas the pollen sacs are both flattened and show differences between the dorsal (inner) and ventral (outer) surfaces. Although the sex organs are therefore considered to be at least partly homologous to leaves, and appear to retain dorsoventral asymmetry characteristic of leaves, they are unaffected in all five *phan* mutants even at low temperature. Assuming the interpretation of the origin of organs from the leaves is correct this would again suggest that there is either insufficient reduction of DF to affect these organs in *phan* mutants or that their development involves a *phan*-independent DF.

7.3.5 Is the *phan* mutation lethal?

Two observations suggested that the a *phan* mutation may in certain circumstances be lethal. First, *phan*-607 mutants failed to germinate at 15°C but did at 17°C, and secondly death of leaf tissue and meristems was observed in mutants at 17°C. One possible explanation is that *phan* expression is required for normal meristematic function. In this case, all the characterised mutants must retain some expression, otherwise they would not have been recovered. This hypothesis would be best tested by determining the effects of the mutations on *phan* expression at the molecular level.

CHAPTER 8 DISCUSSION

8.1 Introduction

8.1.1 Development from a single cell

Perhaps one fundamental question in biology is how a multicellular organism develops from a single totipotent cell. This question is particularly applicable to plants that not only develop from fertilised eggs but may also regenerate from what might have been considered a terminally differentiated cell. The zygote appears to develop through a programmed pattern of cell growth, cell division and differentiation of cell types to achieve the final form of the plant. Therefore, a further question might be, how is the complex form of a plant achieved through these mechanisms.

8.1.2 Importance of positional information in plant development

One possibility is that the lineage of cells could direct the development of plant form. New daughter cells are linked by a common cell wall and adjacent cells are therefore clonally related. However, clonal boundaries are not predictable and run across specific organ structures. Therefore, cell lineage appears not to be solely responsible for plant form (Poethig and Sussex, 1985ab; Scheres *et al.*, 1994; Dolan *et al.*, 1994).

An alternative explanation is that plant cells respond to their position. Because plants develop in three dimensions, cell identity could be determined from the positional information specified by co-ordinates in three axes. This might then allow determination of cell identity and subsequently pattern of cell division and differentiation of cell type.

Studying positional information in the whole plant would be complex, but can be more easily addressed in the development of a single organ, such as a leaf. In this thesis the role of the dorsoventral axis in leaf development has been examined. However, before the leaf develops aspects of positional

information have been established in other parts of the plant and these factors may also have a role in leaf development. Positional information appears to established in the primary organisation of the embryo and then maintained in the developing plant. Therefore embryogenesis, which has been most extensively studied in *Arabidopsis,* will be discussed briefly (Mansfield and Briarty, 1991).

A number of shape specific stages have been identified as the embryo develops. Initially the fertilised zygote expands and then divides asymmetrically. Each cell, as well as having a different fate, is a different size. The smaller apical cell forms the proembryo from which develops most of the embryo proper: cotyledons, shoot meristem, hypocotyl and radicle. The larger basal cell divides into a file of cells, the suspensor, connecting the embryo to the maternal tissues and also contributes to the root meristem. The embryo passes through the globular stage, and acquires bilateral symmetry at the heart shaped stage, at which point the basic body is believed to be established with development of the primordia for the seedling structures. Embryonic development continues through the characteristic torpedo-shape stage and then through the curled-cotyledon stage.

8.1.3 Apical-basal axis

Possibly the primary aspect of positional information to be considered is the apical-basal axis. The first zygotic division is oriented asymmetrically on this axis, suggesting that it may be present at the earliest stages of embryogenesis. Later evidence for existence of apical-basal polarity is apparent embryonic morphology where the shoot and root meristems appear arranged at opposite ends of this apical-basal pattern. Other morphological features of the embryo, such as the cotyledons and radicle, also appear arranged on the same axis.

Evidence for the apical-basal axis has also been derived from regular cell division patterns of the embryo. Slightly different

patterns of cell division have been identified in three embryonic domains along this axis. Apical and central domains represent the upper and lower regions of the proembryo and a basal region the suspensor.

However, despite this distinction the domains do not correspond to the seedling primordia. The shoot meristem and most of the cotyledons are derived from the apical region. The hypocotyl, root, root meristem initials and the rest of the cotyledons develop from the central region and the basal region contributes the remainder of the root meristem. This could be taken as evidence that there is no morphological significance of the domains.

However, compelling evidence for the domains has been derived from morphological mutants. The phenotypes appear to be domain-specific and result in the elimination of seedling structures. For example, *monopteros (mp)* mutants have an abnormal pattern of division in the central and basal domains that results in the loss of the hypocotyl, root and root meristem (Berleth and Jürgens, 1993). Cotyledons do develop but their position is altered.

Conversely, only the apical domain is affected in *gurke (gk)* mutants resulting in the loss of the shoot meristem and the cotyledons (Mayer *et al.*, 1991). A third mutant *fackel (fk)* is altered in the central domain and mutant seedlings develop with cotyledons attached directly to the root, with the hypocotyl absent (Mayer *et al.*1991). For a complete root meristem to develop in *fk* mutants it has been suggested that some of the apical domain must be acquired. Therefore, despite being genetically distinct, communication between cells of different domains may occur.

Interestingly, in mutants with affected domains, the remaining cells in the other unaffected domains still appear to respond to the apical-basal axis. Therefore, *gk*, *fk*, and *mp* appear not to be involved in axis determination but in specifying the domains in

response to apical-basal polarity. Another mutant *fass (fs)* confirms that the normal cell division is not required for determination of apical-basal pattern (Torres-Ruiz and Jürgens, 1994). In heart shaped *fs* mutant embryos the body pattern is unrecognisable, but still differentiates by the time the embryo has developed into a seedling. The first division of *fs* mutant zygotes is still asymmetrical indicating that the polarity of early cell division is unaffected. Also, *fs* mutants appear to be defective in cell elongation and the orientation of new cell walls.

If cell division and the action of domain-defining genes do not define the apical-basal axis, a further possibility is that this polarity is established before the first asymmetric division and maintained for later development. There is evidence for this: previously random microtubules become aligned perpendicular to the presumptive axis as the zygotic cell elongates (Webb and Gunning, 1991). Perhaps more compelling evidence has been derived from the morphology of the *gnom (gn)* mutant. The asymmetry of the first division is virtually lost as the mutant zygote fails to elongate properly (Mayer *et al.*, 1991). Therefore *gn* may have a role is establishing or maintaining the apical-basal axis. The further development of the mutant embryo is highly abnormal. Mutant plants do develop and flower but are greatly compressed along the apical-basal axis.

Interestingly, the action of *mp* is affected in *gn* mutants suggesting that *mp* might respond to the apical-basal axis. *gn* has been cloned as *emb30* (Shevell *et al.*, 1994). *emb30* encodes a domain that is shared amongst a number of gene products including that of the *sec7* gene of yeast. However, comparisons of predicted functions do not, as yet, appear to aid any interpretation of the role of *gn* in the apical-basal axis. Interestingly *gn* is expressed almost constitutively suggesting that it has a role in maintaining the apical-basal axis throughout development.

There is morphological evidence for the apical-basal axis in later development. For example, cell types such as the vascular tissue differentiate progressively from the apex of the stem downwards. Similarly, specific cell types in the root, such as root hair cells, differentiate at set distances away from the root tip. The site of initiation of lateral organs may also be partly determined by the apical-basal axis. All lateral organs are initiated sequentially at specific points at defined distances from the apex.

There is also physiological evidence, through the action of auxin, for the apical-basal axis. Auxin might act as a morphogen originating from the apex and forming a gradient along the apical-basal axis.

8.1.4 Radial axis

The second element of positional information important to plant development might be a radial axis. This radial axis is thought to be arranged perpendicular to the apical-basal axis. Again, much of the evidence for this axis has been determined from embryonic development.

When the embryo has reached the eight cell stage new cell divisions are possible in two orientations: periclinal divisions will give rise to a new layer of cells and anticlinal divisions will increase the number of cells in a layer. As cell divisions occur, a distinctive radial pattern of cell layers develops from before the globular stage, is established by the heart shaped stage and persists throughout development. The radial array of cells is particularly obvious in the central domain but much less so in the apical and basal domains (Jürgens, 1995; Scheres *et al.*, 1995). The morphological differences between cells along this radial axis are clear: in the middle of this radial array, presumptive vascular tissues are determined, on the outside of the array the epidermis is defined and in-between, the outer cortex and the endodermis are defined.

Again, compelling evidence for the radial axis has been identified in morphological mutants in which the radial-layer specific defects are apparent in the hypocotyl, roots and secondary roots suggesting that the radial axis does have a role throughout development. For example, only the epidermal cells of *keule* mutants are enlarged (Mayer *et al.*, 1991). The endodermis and cortex are affected in three mutants; *short root*, *scarecrow* and *pinocchio* (Scheres *et al.*, 1995). Similarly, only the vascular tissue of the mutants *wooden leg* and *gollum* are affected (Benfey *et al.*, 1993).

Interestingly, after the root meristem has been established clonal boundaries reflect the basic organisation of the radial pattern (Dolan *et al.*, 1994; Scheres *et al.*, 1994). However, there is evidence to suggest that cell ancestry is not required for determination of the radial axis. Oriented cell division and the radial pattern are both lost in *fs* mutant embryos but mutant seedlings display all wild-type tissue types (Torres-Ruiz and Jürgens, 1994). This apparent flexibility might be due to the radial axis and cell communication determining cell identity and differentiation. This may be confirmed by the phenotype of a mutant where the radial axis is disturbed. The epidermis of *knolle* mutant proembryos is not separated by periclinal divisions from the inner cell mass and consequently mutant seedlings appear to lack a normal epidermal layer (Mayer *et al.*, 1991).

The radial axis appears to occur in other parts of the plant. The shoot apex also shows a radial pattern of three cell layers. Like the cells of the root meristem the lineage distinction between the apex cell layers appears to be strong. At the apex the L1 layer reflects the single layer of epidermal cells, the L2 layer a single layer of cells below the epidermis and L3 the remaining core cells. Interestingly, certain factors reflect these layer distinctions and may also respond to a radial axis.

The *lateral suppresser* mutant of tomato fails to develop petal primordia. Chimeras of mutant and wild-type tissue layers have shown that gene function is necessary in L2 and L3 layers but not L1 (Szymkowiak and Sussex, 1993). In contrast only epidermal cells of the *fiddlehead* mutant of *Arabidopsis* are affected and result in epidermal fusions of floral and sometimes vegetative organs (Lolle *et al.*, 1992).

The radial axis has also been identified through layer specific gene expression. For example, the *ltp* gene is specifically expressed in the epidermis of the embryo and seedling of *Arabidopsis* (Thoma *et al.*, 1994).

8.1.5 Importance of the apical-basal and radial axes in plant development

Both the apical-basal and radial axes appear to determine patterns of growth and cell division. These axes also appear to be reflected in position-specific gene expression. Therefore there is strong evidence to suggest that they represent part of the positional information required for plant development.

8.2 Discussion

8.2 1 Apical-basal and radial axes in leaf development

Interestingly, the apical-basal and radial axes could specify a ring of cells around the stem or apex and might specify where leaves are initiated. However, this is not enough positional information to specify the exact site of leaf initiation. A specific point on the ring of cells needs to be defined. Despite a large amount of experimental evidence (Steeves and Sussex, 1989: Medford, 1992, for a review) the mechanism for the determination of the initiation site is as yet unclear.

8.2.3 A third axis for leaf initiation

One way in which the site of initiation could be determined is through a third axis specifying a third co-ordinate in combination with the radial and apical-basal axes. The third axis might be a marginocentric axis arranged perpendicular to both the radial and apical-basal axes so distinguishing this new

axis from the two established axes (Figure 8.1). The co-ordinates from the three axes might be enough to define a specific site for leaf initiation.

One possibility is that this new axis is maintained by the position of existng structures. For example the cotyledon primordia may determine the site of the first leaf primordia and existing leaf primordia might determine the site of new primordia creating a perpetuating pattern of phyllotaxy.

8.2.4 New axes for leaf development

The pattern of leaf growth after initiation appears to be defined by at least two new axes specific to the leaf. These new axes would account for growth proximodistally adding length to the leaf, and laterally, adding width. However, the leaf grows laterally from the stem and is also flattened perpendicular to the stem. Therefore, the growth of the leaf appears to be influenced by the axes of the stem. One way in which this could occur is by the established axes of the stem defining the new axes of the leaf.

8.2.5 Proximodistal axis

The proximodistal axis would reflect the pattern of the leaf from its tip to its base. This axis may be derived from a combination of the radial andmarginocentricaxes of the stem. The proximodistal axis is probably determined at or soon after initiation because the first growth of the primordium occurs along this axis and it might also have a role in determining the pattern of the proximodistal growth and orientation of cell division that add length to the developing leaf. The morphologies of *phan* mutant phenotypes suggest that *phan* is not required for determination of the proximodistal axis.

8.2.6 Dorsoventral axis

From the morphology of *phan* mutant leaves the dorsoventral axis appears to determine the lateral expansion of the leaf and the pattern from the dorsal to the ventral surface. Wild-type leaves appear to attain dorsoventrality soon after initiation

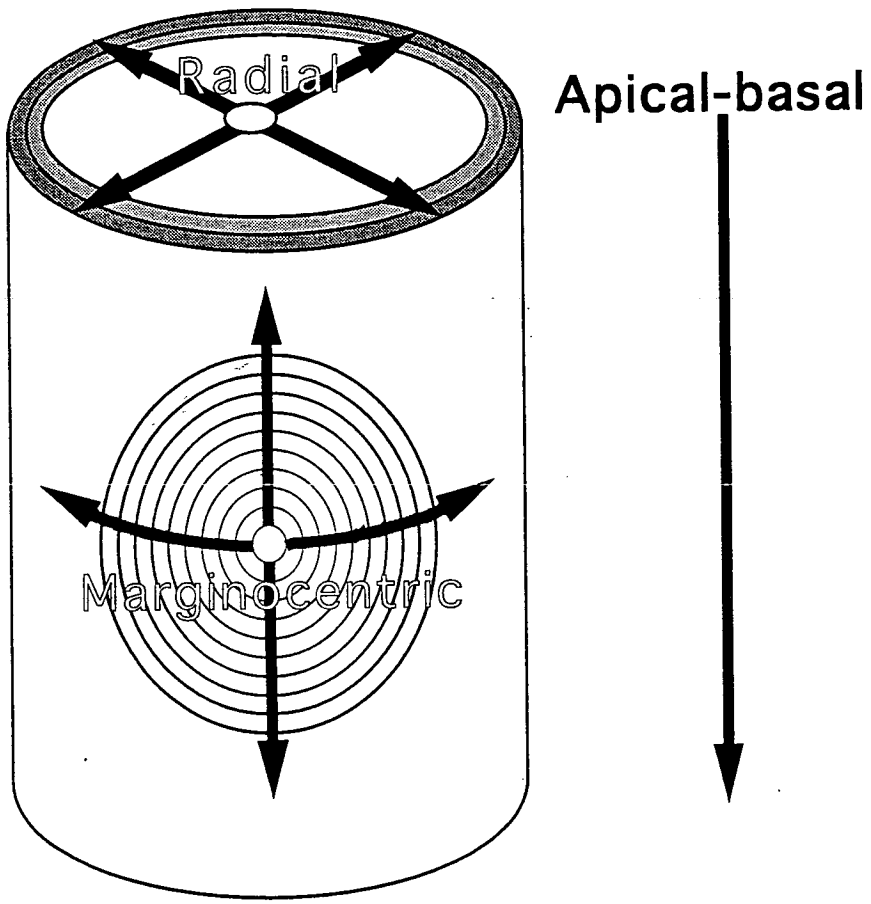

Figure 8.1 Representation of the axes required for leaf initiation.

A region of the stem is illustrated diagrammatically. A combination of the co-ordinates from each of three axes shown may be sufficient to determine the site of leaf initiation.

suggesting that this is the earliest point at which the axis is required. The dorsoventral axis could be determined by a combination of the apical-basal and radial axes of the stem. There is evidence that the axis is defined from the apex (Sussex, 1955; Snow and Snow, 1959; Hanawa, 1961). If leaf initials are isolated from the apex by surgical incisions they develop as radial leaves, similar to the needle-like leaves of *phan* mutants.

The dorsoventral axis appears, like the proximodistal axis, have a role in cell division. Anticlinal divisions that add to the width of the leaf appear to be directed by the dorsoventral axis. A further early example of dorsoventrality of the leaf is that the developing primordia curves over the apex soon after initiation presumably due to more cell divisions occurring in the ventral portion of the leaf than in the dorsal portion. This axis requires *phan* and may be established and maintained by DF.

8.2.7 The third axis of the leaf

The pattern of leaf growth is dominated by two dimensions, width and length. However, it would be naive to assume that only two axes are involved in leaf growth because the leaf does have depth and the importance of the dorsoventral axis is revealed by *phan* mutants. The possible involvement of the proximodistal and dorsoventral axes in leaf development have already been discussed. The question of what is the third axis in the leaf remains. Interestingly, this might be revealed by the needle-like *phan* mutant leaves. These leaves appear to have lost the dorsoventral axis but show a radial pattern that might reflect a radial axis. In combination with the dorsoventral axis,the radial axis may specify the fate of cells across the width of the leaf, for example defining the leaf edge and midrib. The leaf edge is defined relatively early in development before lateral expansion begins and may have a role in directing proliferation acting as an organiser. Alternatively, the radial axis might also have a role in combination with dorsoventral axis in directing lateral cell proliferation directly. Because the radial axis of the leaf is unaffected in *phan* mutants, it would

appear to be independent of the dorsoventral axis of the leaf. It may therefore be derived from a combination of the radial and mediolateral axes of the stem.

8.2.8 Dorsoventral lineage restrictions in the leaf

The model proposed to explain the role of DF in leaf development assumes that its expression is established in dorsal leaf initials cells (probably in response to apical-basal polarity in the stem) and that it persists in dorsal cells of the developing lamina as they grow in a new lateral axis through anticlinal divisions. One way in which DF expression could persist is by inheritance of expression. For example, the PHAN protein may stimulate expression of the *phan* gene. After cell division, daughter cells would inherit PHAN, and therefore *phan* expression. Therefore, cells expressing DF would be clonally related.

To prevent daughter cells expressing DF being included in ventral regions of a leaf as a result of periclinal divisions there would have to be a lineage restriction between dorsal and ventral domains that is established before lateral expansion of the leaf begins. This would involve divisions in cells adjacent to the boundary between dorsal and ventral domains being limited to anticlinal divisions. Little evidence for lineage restrictions in plant development has, as yet, been presented. However, it is possible to reinterpret the clonal analysis of Poethig and Sussex (1985a and 1985b) in this light. A lineage restriction appears to exist between the palisade and spongy mesophyll that might reflect a division of dorsal and ventral domains from leaf initiation onwards. Firstly, clones that were induced after leaf initiation are restricted to either the spongy or palisade cell types suggesting that these tissues are formed only by anticlinal divisions. Secondly, clones induced before leaf initiation occur across both cell types and therefore appear to have been induced before the lineage restriction.

However, periclinal cell layer chimeras suggest that part of the spongy mesophyll and part of the palisade mesophyll may be

derived from the same clone in either the LII or LIII layer of the meristem although their fates are independent of this origin. This could be explained if DF expression is established early in primordial development and irrespective of LII and LIII origins that, as a result, become irrelevant.

There is evidence that throughout leaf development LI remains distinct from the other layers undergoing only anticlinal divisions. In the leaf, DF is proposed to persist in dorsal cells of the LI layer. Unlike internal cells, it is difficult to envisage how a lineage restriction between dorsal cells with DF expression and ventral cells without expression might be maintained in LI because all LI cells divide anticlinally. However, there is evidence that such a lineage restriction may occur. The epidermal cells of the presumptive leaf edge appear to differentiate early, before lateral expansion of the leaf (R. F. Lyndon, pers. comm.). This might be a response to the coincidence of the LI layer with the boundary of the DF domain. These cells would form a barrier preventing displacement of dorsal cells into the ventral domain by anticlinal divisions.

It therefore appears possible that DF maintains two distinct domains between which daughter cells cannot be displaced across a dorsoventral boundary. This may have important implications for maintaining dorsoventrality and the lateral expansion of the leaf.

8.3 Dorsoventrality in the leaf of *Antirrhinum* and the wing of *Drosophila*

Development of the leaf of *Antirrhinum* and the wing of *Drosophila* show several similarities. Both organs develop in a novel axis to the main body: the stem or the body wall. In both cases, the pattern of growth results in lateral organs that develop from small groups of cells and come to show a high

degree of dorsoventrality. Both organs are only a few cells thick and both have a defined edge or margin.

The structure of the leaf has already been described. In comparison, the wing is thinner than the leaf: when fully developed it is only two cells thick. Distributed over the wing margin, are several sets of bristles that differ depending whether they are on the upper or lower surface. There are also crucial differences between leaves and the wings. For example, unlike leaves, wings have no bilateral symmetry.

Leaf development has been described but before comparing it to the formation of the wing, wing development will be discussed.

8.3.1 Development of the *Drosophila* wing

A *Drosophila* wing develops from an imaginal disc formed during embryogenesis from an invagination of the epidermis. The early disc consists of a cluster of about 20-40 cells (Madhaven and Scneiderman, 1977; Bate and Martinez-Arias, 1991; Cohen *et al.*, 1991) that do not participate in embryonic development but proliferate to over 50,000 cells during the three larval stages or instars (Garcia-Bellido and Merriam, 1971). In the wing disc, the cells of the prospective dorsal layer are arranged adjacent to the cells of the prospective ventral cell layer and are separated by the prospective margin. During pupation, the wing disc everts and cells of the upper and lower cell layers become opposed. The wing blade develops distally and the proximal region forms a large proportion of the dorsal thorax.

Development of the *Drosophila* embryo has been explained by a combination of patterns along the anterior/posterior and dorsoventral axes. The anterior/posterior and dorsoventral axes appear to be present in the wing disc, and together with a novel proximodistal axis, can account for wing growth.

The anterior/posterior axis appears to be established first in wing discs. A combination of *engrailed* and *invected* is expressed in the posterior portion of the disc (Kornberg *et al.*,

1985; Simmonds *et al.*, 1995). These two genes are homologues that appear to establish posterior cell fate.

Dorsoventral identity of cells appears to be established next. *wingless (wg)* is expressed ventrally followed by *apterous (ap)* that is expressed dorsally. The boundary between the expression of these two genes corresponds to the prospective margin of the wing (Diaz-Benjumea and Cohen, 1993). The expression of two genes *vestigal (vg)* and *scalloped (sd)* is detected in narrow domains spanning the prospective dorsoventral boundary where expression of *ap* and *wg* is juxtaposed (Williams *et al.*, 1993 and 1994). This suggests that both *vg* and *sd* respond to dorsoventral positional information. Subsequently, *fringe (fng)* is expressed in dorsal cells under the control of *ap* (Irvine and Wieschaus, 1994). The mutant phenotypes of *ap, wg, vg sd* and *fng* suggest that they are involved in wing proliferation because mutations in these genes typically block wing development (Butterworth and King, 1965; James and Bryant, 1981; Irvine and Wieschaus, 1994; Williams *et al,* 1993 and 1994).

However, *vg* and *sd* are not expressed in the cells adjacent to the wing margin that proliferate during wing growth. Therefore, signalling may occur between cells expressing *vg* and *sd* at the prospective margin and cells in a more dorsal or ventral position. *fng* is a candidate signalling gene because when *fng*- patches are induced ectopically the dorsoventral cell identity is not changed but an ectopic margin is produced at the boundaries of *fng*- clones (Irvine and Wiechaus, 1994). Also, the predicted *fng* protein includes a motif that suggests that it may be secreted. Interestingly, the pattern of bristles at the novel margins is symmetrical suggesting that *fng* is not involved in dorsoventral determination but in communication between the two compartments.

After the anterior/posterior and dorsoventral axes have been established a third axis, the proximodistal axis of the wing is established. Two genes have been identified that may have roles in the proximodistal axis. *nubbin (nub)* is expressed throughout

the wing disc but genetic mosaics with patches of *nub*$^-$ cells suggest that *nub* activity is localised to the hinge region and may be necessary for a lineage restriction between the wing blade and the notum (Ng *et al.*, 1995). *nub* mutants also result in almost a complete deletion of the wing. Further evidence for the proximodistal axis has been identified. *aristaless (al)* is expressed at the extreme distal end of the wing (Schneitz, 1993). Ectopic *al* expression can induce a duplication of the proximodistal axis and therefore *al* may be involved in axis specification.

8.3.2 Dorsoventrality in leaf and wing development

There are striking similarities between the mutant phenotypes of *ap* and *phan*, and for the proposed roles of DF and *ap*. The limit of dorsally restricted *ap* expression coincides with the dorsoventral compartment boundary suggesting that *ap* defines the dorsal compartment of the wing (Diaz-Benjumea and Cohen, 1993). Without *ap,* the wing does not develop (Butterworth and King, 1965). However, experiments were designed where expression of *ap* has been lost from small clones of cells. These *ap*$^-$ clones revealed more subtle defects and the roles of *ap* in wing development as the dorsal and ventral compartments are defined in the imaginal disc. For example, when *ap*$^-$ patches were induced in the dorsal region of the disc, small clones of cells with ventral identity developed on the dorsal surface of the wing indicating that *ap* is required for determining dorsal cell identity (Diaz-Benjumea and Cohen, 1993). The patches of ventral cells were surrounded by cell proliferations that appeared to be similar to wing margins suggesting that *ap* has a role in cell proliferation. The arrangement of bristles at the ectopic proliferations resembled those at the wing margins indicating that ectopic margins had been induced. Therefore *ap* is believed to have a further role in specifying where the margin will be determined. In a similar experiment, the fate of *ap*$^-$ clones induced in the dorsal region was followed (Blair *et al.,* 1994). Those induced before the third instar and close to the dorsoventral boundary crossed into the ventral compartment.

Whereas clones induced later or further from the margin did not cross and caused ectopic proliferations. Late clones close to the boundary could not cross because a lineage restriction had occurred between the dorsal and ventral compartments.

In comparison, the expression of DF is believed to dorsally restricted and the limit of the expression also to coincide with the leaf edge. Therefore DF may not only define the dorsal region of the leaf but also its edge. Evidence for these roles has been determined from the phenotypes of *phan* mutants. Examples have been described where, as a consequence of a mutation in the *phan* gene, DF may have been lost from small patches of cells. This appears to result in a patch of cells that has a ventral identity indicating that DF has a role in defining the identity of dorsal cells. These patches are surrounded by proliferations that suggests that DF also has a role in proliferation.

8.3.3 Further implications for leaf development

ap interacts with other genes. The interaction with *wg* may define the boundary between the dorsal and ventral compartments. In analogy, one or more genes that represents a ventralising function may also have a role in leaf development and perhaps act in combination with DF.

Two genes, *sd* and *vg* are expressed coincidentally with the boundary established by *wg* and *ap*. Therefore *sd* and *vg* may interpret their expression pattern from *wg* and *ap*. Further, ectopic patches of ap^- cells show expression of *vg* and *sd* at the patch boundaries. Interestingly, the mutant phenotypes of *vg* and *sd* involve no proliferation of the wing, suggesting that the proliferation associated with *ap* may be due to the action of *vg* and *sd*. Again in analogy, DF may have associated factors acting downstream of DF and their expression may be limited to the edge.

However there are obviously major differences between the proposed functions of DF in leaf development and those of *ap* in

the wing. In the wing, loss of *ap* expression abolishes formation of the distal wing structures, indicating that the proximodistal axis of the wing is dependent on *ap.* However, in leaves, even the most extreme, needle-like leaves of *phan* mutants develop along the proximodistal axis, suggesting that formation of this axis is independent of *phan.*

8.3.4 Other candidate genes for the dorsoventral axis in the leaf

The *graminifolia (gram)* mutant may show a disruption to the dorsoventral axis. Epidermal cells on the dorsal surface of the leaf have identities that more closely resemble ventral epidermal cells, and dorsal-like epidermal cell-types are also present on the ventral surface (A. Hudson pers. comm.). Therefore, *gram* may also have a role in establishing the dorsoventral axis or may respond to this axis. Further, the double mutant, *phan/gram* appears to have a higher proportion of leaves with the most extreme needle-like phenotype (A. Hudson pers. comm.) suggesting that *phan* and *gram* act independently in the same process.

Another candidate is the gene *filiformis (fili)* (Schiemann, 1926), appears to interact with *gram*: The phenotype of plants mutant for *fili* is only revealed in a *Gram* mutant background. Interestingly *fili* was recorded to have a phenotype remarkably similar to *phan.*

8.3.5 *phan* gene function

ap is predicted to encode a transcription factor containing both a LIM type domain and a homeodomain (Cohen *et al.*, 1992). The identity of its product is therefore consistent with its role in directing expression of other genes involved in establishing the identity of dorsal cell-types in the wing.

The *phan* gene and cDNA have been sequenced (H. Selvadurai and A. Hudson, pers. comm.). *phan* appears to encode a *myb*-related transcription factor that may regulate expression of

downstream genes involved in dorsal cell identity and lateral expansion of the leaf.

REFERENCES

Almeida, J., Carpenter, R., Robbins, T. P., Martin, C. and Coen, E. S. (1989). Genetic interactions underlying flower colour patterns in *Antirrhinum majus*. *Genes Dev.* **3**, 1758-1767.

Bate, M. and. Martinez.-Arias., A. (1991). The embryonic origin of imaginal discs in *Drosophila*. *Development* **112**, 755-761.

Baur, E. (1926). Untersuchungen über Faktormutationen. I. *Antirrhinum majus* mut. *phantastica*, eine neue, dauernd zum dominanten Typ zurückmutierende rezessive Sippe. *Z. f. indukt. Abst. u. Vererbungsl.* **41**, 47-53.

Baur, E. (1933). Artungrenzung und Artbildung in der Gattung Antirrhinum, Sektion Antirrhinastrum. *Z. f. indukt. Abst. u. Vererbungsl.* **63**, 256-302.

Berleth, T., and Jürgens, G. (1993). The role of the *monopteros* gene in organizing the basal body region of the *Arabidopsis* embryo. *Development* **118**, 575-587.

Blair, S. S., Brower, D. L., Thomas, J. B. and Zavortink, M. (1994). The role of *apterous* in the control of dorsoventral compartmentalization and PS integrin gene expression in the developing wing of *Drosophila*. *Development* **120**, 1805-1815.

Bureau, T. E., and Wessler, S. R. (1994). stowaway- a new family of inverted repeat elements associated with the genes of both monocotyledonous and dicotyledonous plnats. *Plant Cell.* **6**, 907-916.

Butterworth, F. M. and King, R. C. (1965). The developmental genetics of *apterous* mutants in *Drosophila melanogaster*. *Genetics* **52**, 1153-1174.

Buvat, R. (1952). Structure, evolution et fonctionnement du meristeme apical de quelques dicotyledones. *Am. des Sci. Nat. Bot.* **13**, 199-300.

Carpenter, R., Martin, C. and Coen, E. S. (1987). Comparison of genetic behaviour of the transposable element Tam 3 at two unlinked pigment loci in *Antirrhinum majus*. *Mol. Gen. Gen.* **207**, 82-89.

Catesson, A.-M. (1953). Structure, evolution et fonctionement du point vegetatif d'une monocotyledone: *Luzula pedemontana*. *Am. des Sci. Nat. Bot.* **14**, 253-291.

Coen, E. S., Robbins, T. P., Almeida, J., Hudson, A. and Carpenter, R. (1989). Consequences and mechanisms of transposition in *Antirrhinum majus*. *Mobile DNA*. Washington DC, American Society for Microbiology.

Coen, E. S. and Carpenter, R. (1990). Floral homeotic mutations produced by transposon-mutagenesis in *Antirrhinum majus*. *Genes Dev.* **4**, 1483-1493.

Cohen, B., Wimmer, E. A. and Cohen, S. M. (1991). Early development of leg and wing primordia in the *Drosophila* embryo. *Development* **33**, 229-240.

Cohen, B., McGuffin, M. E., Pfeifle, C., Segal, D. and Cohen, S. M. (1992). *apterous*, a gene required for imaginal disc development in *Drosophila*, encodes a member of the LIM family of developmental regulatory proteins. *Genes Dev.* **6**, 715-729.

Delong, A., Calderon-Urea, A. and Dellaporta, S. L. (1993). Sex determination gene *tasselseed2* of maize encodes a short-chain alcohol dehydrogenase required for stage-specific floral organ abortion. *Cell* **74**, 75-768.

Dermen, H. (1953). Periclinal cytochimeras and origin of tissues in stem and leaf of Peach. *Am. J. Bot.* **40**, 154-168.

Diaz-Benjumea, F. J. and Cohen, S. M. (1993). Interaction between dorsal and ventral cells in the imaginal disc directs wing development in *Drosophila*. *Cell* **75**, 741-752.

Dolan, L., Janmaat, K., Willemsen, V., Linstead, P., Poethig, S., Roberts, K., and Scheres, B. (1993). Cellular-organization of *Arabidopsis thaliana* root. *Development* **119**, 71-84.

Dolan, L., Duckett, C. M., Grierson, C., Linstead, P., Schneider, K., Lawson, E., Dean, C., Poethig, S., and Roberts, K.,. (1994). Clonal relationships and cell patterning in the root epidermis of *Arabidopsis*. *Development* **120**, 2465-2474.

Dubuc-Lebreux, M. A. and Sattler, R. (1980). Development des organes foliaces chez *Nicotiana tabacum* et le probleme des meristemes marginaue. *Phyto.* **30**, 17-32.

Essau, K. (1977). *Anatomy of Seed Plants.* New York, John Wiley and Sons.

Foard, D. E. (1971). The initial protrusion of a leaf can form without concurrent periclinal cell divisions. *Can. J. Bot.* **49**, 1601-1603.

Galway, M. E., Masuci, J. D., Lloyd, A.M., Walbot, V., Davis, R. W. and Schiefelbein, J. W. (1994). The *ttg* gene is required to specify epidermal-cell fate and cell patterning in the *Arabidopsis* root. *Dev. Biology.* **166**, 740-754.

Garcia-Bellido, A. and Merriam, J. R. (1971). Parameters of the wing the imaginal disc development of *Drosophila melanogaster. Dev. Biology.* **26**, 264-276.

Goodrich, J., Carpenter, R. and Coen, E. S. (1992). A common gene regulates pigmentation pattern in diverse plants species. *Cell* **68**, 955-964.

Green, P. B. and Linstead, P. (1990). A procedure for SEM of complex structures applied to the inflorescence of snapdragon (*Antirrhinum*). *Protoplasma.* **63**, 44-54

Harrison, B. J. and Carpenter, R. (1979). Resurgence of genetic instability in *Antirrhinum majus. Mut. Res.* **63**, 47-69.

Harrison, B. J. and Fincham, J. R. S. (1964). Instability at the *pal* locus in *Antirrhinum majus.* I: Effects of environment on frequencies of somatic and germinal mutation. *Heredity* **19**, 237-258.

Hudson, A., Carpenter, R. and Coen E. S. (1990). Phenotypic effects of short-range and aberrant transposition in *Antirrhinum majus. Pl. Mol. Biology* **14**, 835-844.

Hudson, A., Carpenter, R., Doyle, S. and Coen, E. S. (1993). *olive*: a key gene required for chlorophyll synthesis in *Antirrhinum majus. EMBO J.* **12**, 3711-3719.

Inagaki, Y., Hisatomi, Y., Suzuki, T., Kasahara, K., and Iida, S. (1994). Isolation of a suppressor-mutator enhancer-like transposable element, Tpn1, from Japanese morning glory bearing variegated flowers. *Plant Cell.* ***3***, 375-383.

Irvine, D. I. and Wiechaus, E. (1994). *fringe*, a boundary-specific signalling molecule, mediates interactions between dorsal and ventral cells during *Drosophila* wing development. *Cell* **79**, 595-606.

James, A. A. and Bryant, P. J. (1981). Mutations causing pattern deficiencies and duplications in the imaginal wing disk of *Drosophila melanogaster. Dev. Biology.* **85**, 39-54.

Jürgens, J. (1995). Axis formation in plant embryogenesis: cues and clues. *Cell* **81**, 467-470.

Kelly-Dawe, R. and Freeling, M. (1991). Cell lineage and its consequences in higher plants. *Plant. J.* **1**, 3-8.

Kornberg, T., Siden, I., O'Farrell, P. and Simon, M. (1985). The *engrailed* locus of *Drosophila*: *In situ* localization of transcripts reveals compartment-specific expression. *Cell* **40**, 45-53.

Lolle, S. J., Cheung, A. Y., and Sussex, I. M. (1992). *fiddlehead* - an *Arabidopsis* mutant constitutively expressing an organ fusion program that involves interactions between epidermal cells. *Dev. Biology* **152**, 383-392.

Luo, D., Coen, E. S., Doyle, S. and Carpenter, R. (1991). Pigmentation mutants produced by transposon mutagenesis in *Antirrhinum majus. Plant. J.* **1**, 59-69.

Lyndon, R., F. (1990). *Plant Development: The Cellular Basics.* Winchester, MA, Unwin Hyman Inc.

Lyndon, R. F. (1970). Rates of cell division in the shoot apical meristem of *Pisum. Ann. Bot.* **34**, 1-17.

Madhaven, M. M. and Scheiderman., H. A. (1977). Histological analysis of the dynamics of growth of imaginal discs and histoblast nests during the larval development of *Drosophila* embryo. *Development* **103**, 157-170.

Maksymowych, R. (1963). Cell division and cell elongation in leaf development of *Xanthium penyslvanium*. *Am. J. Bot.* **50**, 891-901.

Mansfield, S. G., and Briarty, L. G. (1991). Early embryogenesis in *Arabidopsis thaliana*. 2. The developing embryo. *Can. J. Bot.* **69**, 461-476.

Martin, C., Carpenter, R., Sommer, H., Saedler, H. and E. S. Coen. (1985). Molecular analysis of instability in flower pigmentation of *Antirrhinum majus* following isolation of the *pallida* locus by transposon tagging. *EMBO J.* **4**, 1625-1630.

Mayer, U., Torres-Ruiz, R. A., Berleth, T., Miséra, S., and Jürgens, G. (1991). Mutations affecting body organization in the *Arabidopsis* embryo. *Nature* **353**, 402-407.

Mayer, U., Buttner, G., and Jürgens, G.,. (1993). Apical-basal pattern formation in the *Arabidopsis* embryo- studies on the role of the *gnom* gene. *Development* **117**, 149-162.

Medford, J. I. (1992). Vegetative apical meristems. *Plant Cell* **4**, 1029-1039.

Ng, M., Diaz-Benjumea, F. J., and Cohen, S. M. (1995). *nubbin* encodes a pou-domain protein required for proximal-distal patterning in the *Drosophila* wing. *Development* **121**, 589-599.

Noda, K., Glover, B., Linstead, P. and Martin, C. (1994). Flower colour intensity depends on specialised cell shape controlled by a Myb-related transcription factor. *Nature* **369**, 661-664.

Nourarede, A. and. Rembur, J. (1978). Variations in the cell cycle phases in the shoot apex of *Chrysanthemum segetum L. Z. Pflanzenphys.* **81**, 173-179.

Poethig, R. S. (1984). Cellular parameters of leaf morphogenesis in maize and tobacco. *In Contemporary Problems in Plant Anatomy.* New York, Macmillan.

Ruth, J., Klekowski, E. J., Jnr, and Stein, O. L. (1985). Impermanent initials of the shoot apex and diplontic selection in a juniper chimera. *Am. J. Bot.* **72**, 1127-1135.

Sachs, T. (1991). *Pattern formation in plant tissues.* Cambridge, Cambridge University Press.

Satina, S., Blakeslee, A. F., and Avery, A. G. (1940). Demonstration of the three germ layers in the shoot apex of *Datura* by means of induced polploidy in periclinal chimeras. *Am. J. Bot.* **27**, 895-905.

Satina, S., and Blakeslee, A. F. (1941). Periclinal chimeras in *Datura stramonium* in relation to development of leaf and flower. *Am. J. Bot.* **28**, 862-871.

Scheres, B., Wolkenfelt, H., Wilemsen V., Terlouw, M., Lawson, E., Dean, C., and Weisbeek, P. (1994). Embryonic development of the *Arabidopsis* primary root and root meristem initials. *Development* **120**, 2475-2487.

Scheres, B., Dilaurenzio, L., Willemsen, V., Hauser, M. T., Janmaat, K., Weisbeek, P., and Benfey, P. N. (1995). Mutations affecting the radial organization of the *Arabidopsis* root display specific defects throughout the embryonic axis. *Development* **121**, 53-62.

Schiemann, E. (1926). Eine mutation in der *graminifolia*-Sippe von *Antirrhinum majus. Z. f. indukt. Abst. u. Vererbungsl* . **41**, 53-55.

Schneitz, K., Spielmann, P., and Noll, M. (1993). Molecular genetics of *aristaless*, a prd-type homeobox gene involved in the morphogenesis of proximal and distal pattern elements in a subset of appendages in *Drosophila. Genes. Dev.* **7**, 114-129.

Shepherd, N. (1988). Transposable elements and gene tagging. *Plant molecular biology, a practical approach.* Oxford, IRL Press.

Shevell, D. E., Leu, W. M., Gillmor, C. S., Xia, G. X, Feldmann, K. A., and Chua, N. H. (1994). *emb30* is essential for normal- cell division, cell expansion, and cell adhesion in *Arabidopsis* and encodes a protein that has similarity to *sec7. Cell* **77**, 1051-1062.

Simmonds, A. J., Brook, W. J., Cohen, S. M. and Belle, J. B. (1995). Distinguishable functions for *engrailed* and *invected* in anterior patterning in the *Drosophila* wing. *Nature* **376**, 424-427.

Smith, L., Green, B., Veit, B. and Hake, S. (1992). A dominant mutation in the maize homeobox gene *Knotted*1 causes its ectopic expression in leaf cells with altered fates. *Development* **116**, 21-30.

Snow, M., and Snow, R. (1959). The dorsiventrality of leaf primordia. *New Phytol.* **58**, 188-207.

Sommer, H., Carpenter, R., Harrison, B. J. and Saedler, H. (1985). The transposable element Tam 3 of *Antirrhinum majus* generates a novel type of sequence alteration upon excision. *Mol. Gen. Genetics.* **199**, 225-231.

Sommer, H., Bonas, U. and Saedler, H. (1988a). Transposon-induced alterations in the promoter region affect transcription of chalcone synthase gene of *Antirrhinum majus*. *Mol. Gen. Genetics.* **211**, 49-55.

Sommer, H., Hehl, R., Krebbers, E. , Piotraviak, R., Lonning, W. and Saedler, H. (1988b). Transposable elements of *Antirrhinum majus*. *Plant transposable elements.* New York, Plenum Publishing Corp.

Steeves, T. A. and Sussex., I. M. (1989). *Patterns in Plant Development.* New York, Cambridge University Press.

Stewart, R. N., and Dermen, H. (1975). Flexibility of ontogeny as shown by the contribution of the shoot apical layers to leaves of periclinal chimeras. *Am. J. Bot.* **62**, 935-947.

Stewart, R. N. and Burk, L. G. (1970). Independence of tissues derived from apical layers in ontogeny of the tobacco leaf and ovary. *Am. J. Bot.* **57**, 1000-1016.

Stubbe, H. (1966). *Genetik and Zytologie von Antirrhinum L. sect. Antirrhinum.* Jena, Germany, V. E. B. Gustav Fischer.

Sussex, I. M. (1954). Experiments on the cause of dorsiventrality in leaves. *Nature* **174**, 351-352.

Sussex, I. M. (1955). Experimental investigation of leaf dorsoventrality and orientation in the juvenile shoot. *Phyto.* **5**, 286-300.

Szymkowiak, E. J. and Sussex, I. M. (1993). Effect of *lateral suppressor* on petal initiation in tomato. *Plant. J.* **4**, 1-7.

Thoma, S., Hecht, U., Kippers, A., Botella, J., de Vries, S. C., and Sommerville, C. (1994). Tissue-specific expression of a gene encoding a cell wall-localized lipid transfer protein from *Arabidopsis. Plant Physiol.* **105**, 34-45.

Torres-Ruiz, R. A., and Jürgens, G. (1994). Mutations in the *fass* gene uncouple pattern formation and morphogenesis in *Arabidopsis* development. *Development* **120**, 2967-2978.

Upadyaya, K., Sommer, H., Krebbers, E. and Saedler, H. (1985). The paramutagenic line *niv*44 has a 5kb insert of Tam 2 in the chalcone synthase gene of *Antirrhinum majus. Mol. Gen. Genetic.* **199**, 201-207.

Vollbrecht, E., Veit, B., Sinha, N. and Hake, S. (1991). The developmental gene *Knotted*1 is a member of a maize homeobox gene family. *Nature* **503**, 241-243.

de Vries, H. (1910). *The Mutation Theory 2.* Peru, Open Court Publishing Co.

Webb, M. C. and Gunning, B. E. S. (1991). The microtubular cytoskeleton during development of the zygote, in *Arabidopsis thaliana* L. Heynh. *Planta* 187-195.

Weigle, D. and Meyerowitz, E. M. (1994). The ABCs of floral homeotic genes. *Cell* **78**, 203-209.

Williams, J. A., Paddock, S. W., and Carroll, S. B. (1993). Pattern formation in a secondary field: a hierarchy of regulatory genes subdivides the *Drosophila* wing into discrete subregions. *Development* **117**, 571-584.

Williams, J. A., Paddock, S. W., Vorwerk, K. and Carroll, S. B. (1994). Organisation of wing formation and induction of a wing-patterning gene at the dorsal/ventral compartment boundary. *Nature* **368**, 299-305.

Development 121, 2143-2154 (1995)
Printed in Great Britain © The Company of Biologists Limited 1995

phantastica: a gene required for dorsoventrality of leaves in *Antirrhinum majus*

Fichard Waites and Andrew Hudson*

Institute of Cell and Molecular Biology, University of Edinburgh, King's Buildings, Mayfield Road, Edinburgh EH9 3JH, UK

*Author for correspondence

SUMMARY

To understand better the mechanisms that lead to dorsoventrality in the lateral organs of plants, mutants at the *phantastica* (*phan*) locus of *Antirrhinum majus* have been identified and characterised. The leaves, bracts and petal lobes of *phan* mutants show varying degrees of reduction in dorsal tissues, indicating that *phan* is required for establishing dorsal cell identity. Each *phan* mutant produces a variety of different leaf morphologies, but has a characteristic and relatively constant floral phenotype. In several different forms of *phan* mutant leaves and petal lobes, novel boundaries between dorsal and ventral cell types form ectopic axes of growth, suggesting that *phan*-dependent dorsal cell identity is required for lateral growth of the wild-type leaf and petal lobe. Comparisons between the development of wild-type and mutant petals or leaves reveal that *phan* acts early in development of these lateral organs. The possible role of the *phan* gene in evolution of different leaf forms is discussed.

Key words: *Antirrhinum majus*, leaf development, dorsoventrality, transposon mutagenesis, *phantastica*

INTRODUCTION

The leaves of most plants have two striking morphological features: they are produced laterally from the stem axis, and they are considerably broader and longer than thick. Their flattened shape, which presents a large area to incident light, involves relatively little tissue and can be considered an adaptation to their photosynthetic role. In dicotyledonous plants with entire leaves, the characteristic leaf shape results from two major shifts in the pattern of growth early in development (Avery, 1933; Dubuc-Lebreux and Sattler, 1980; Foster, 1936; Jeune, 1981; Poethig and Sussex, 1985a,b). The first occurs in a group of initial cells on the flanks of the vegetative meristem (Fig. 1A) which divide and expand to form a leaf primordium with a novel axis of growth away from that of the stem (Fig. 1B). This axis, the proximodistal axis of the leaf, is represented in the mature organ by a line along the midrib. The second occurs in cells towards the dorsal (adaxial) side of the leaf primordium which continue to contribute to proximodistal growth, but also undergo a shift in polarity of division to form the leaf laminae laterally (Fig. 1C). The more ventral part of the primordium shows little or no lateral growth and forms the ventral midrib of the mature leaf (Fig. 1D). The difference in the pattern of division between dorsal and ventral cells of the leaf primordium suggests that dorsoventrality is defined early in organ development. Further dorsoventral differences within the leaf become apparent later, as specialised cell types differentiate in layers perpendicular to the dorsoventral axis.

Other lateral organs of the plant, including bracts and floral organs are considered at least in some parts homologous to leaves (discussed by Hagemann, 1984). Their initiation from inflorescence or floral meristems is similar to the production of leaf primordia at the vegetative apex, and may also be followed by lateral proliferation which leads to flattening (e.g. Green and Linstead, 1990; Tepfer, 1953). They also show dorsoventral differences in cell type. Dorsoventrality is most obvious in bracts, sepals and petals, where a flattened shape is associated with roles in protecting the developing flower or attracting pollinators, but it is also apparent in the pollen sacs of stamens and the the ovary wall of the gynoecium (Goebel, 1905). The mechanisms that define dorsoventrality may therefore be similar in all lateral organs of the plant.

At the developmental stage when dorsoventrality becomes apparent, leaf primordia are small and consist of relatively few cells. They are therefore not ideally suited to surgical studies or to biochemical analysis. As a result, relatively little is known of the mechanisms that determine the form of lateral organs, including their dorsoventrality. An alternative method of study is to characterise mutants in which early development has been disrupted. This has been successfully applied to studies of determination in meristems and floral organ primordia of maize (DeLong et al., 1993; Smith et al., 1992; Vollbrecht et al., 1991), *Antirrhinum* (reviewed by Coen and Carpenter, 1993) and *Arabidopsis* (reviewed by Weigel and Meyerowitz, 1994). One major advantage of these species is that they allow genes which have been identified by mutation to be isolated. In the case of *Antirrhinum* and maize, this approach has exploited transposon-induced mutations, which provide the basis for gene isolation by transposon tagging (Shepherd, 1988). Subsequent detection of transcripts by in situ hybridisation has

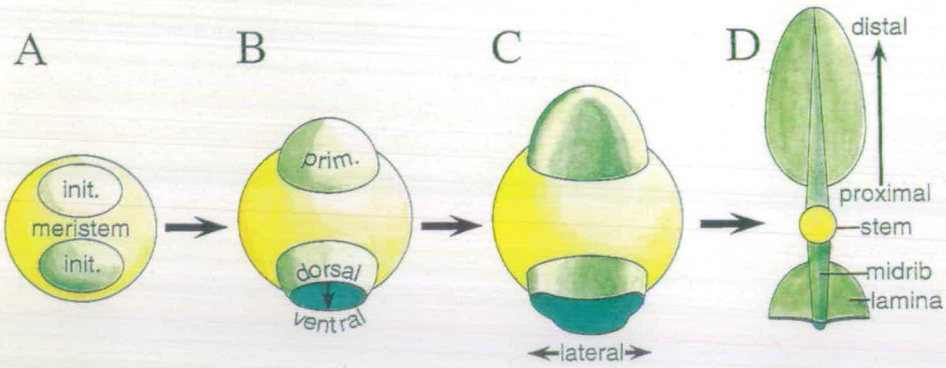

Fig. 1. Leaf initiation. Successive stages in leaf initiation at the vegetative apex are represented as viewed from above. (A) Two groups of leaf initials (init.) destined to form leaf primordia are shown within the flanks of the vegetative meristem. (B) Each groups of initials subsequently forms a primordium (prim.) with an axis of growth away from that of the apical meristem. (C) Lateral proliferation in the dorsal part of the primordium forms the laminae, and the leaf therefore shows dorsoventral asymmetry which becomes more pronounced in mature leaves (D).

revealed that many of the isolated genes show patterned expression in meristems and organ primordia consistent with their roles in determining the developmental fates of these tissues.

Here we describe the variable effects of four mutations at the *phantastica* (*phan*) locus of *Antirrhinum majus*. Mutant phenotypes suggest that *phan* expression is involved in all aspects of dorsoventrality in leaves, bracts and petals: from specifying the position of laminal initiation early in organ development, to determination of dorsal cell types at a later stage. They also suggest that subtle changes in the level or pattern of *phan* activity can give rise to a variety of organ morphologies. At least one of the *phan* mutant alleles shows the genetic instability characteristic of transposon-induced mutations, which should allow its isolation by transposon-tagging.

MATERIALS AND METHODS

Origin of *phan* mutants

The wild-type line, JI.75, was produced at the John Innes Institute, Norwich, UK (Harrison and Carpenter, 1979). The mutants $phan^{ambigua}$ (*phan*-250G) and $phan^{antiqua}$ (*phan*-249G), originally isolated by Baur (1926) were obtained from Zentralinstitut für Genetik und Kulturflanzenforschung, Gatersleben, Germany, and inbred as homozygous stocks for at least a further three generations. The *phan*-607 mutant arose amongst families produced by self-pollination of line JI.75, in a programme designed to identify transposon-induced mutations (Carpenter and Coen, 1990), and was kindly provided by R. Carpenter and E. S. Coen, John Innes Centre, Norwich, UK. It was shown to carry a single recessive mutation which was unable to complement the *phan*-249G and *phan*-250G mutant alleles. A fourth mutant allele, *phan*-552, was obtained in a screen for new mutations at the locus, when plants of the mutant line, *phan*-249G, were crossed as female parent to the transposon-rich, wild-type line, JI.75. The resulting F_1 seeds were germinated on moist vermiculite, and seedlings examined for alterations in the morphology of cotyledons and the first pair of leaves. A single *phan* mutant seedling was identified amongst approx. 18,000 wild-type siblings. Because this mutant showed the floral pigmentation phenotype expected of an F_1 plant, it appeared not to be the result of accidental self-pollination of the mutant parent. Therefore, the simplest explanation for the leaf phenotype of the new mutant was that this plant carried a newly mutated allele, *phan*-552, heterozygous with the *phan*-249G allele. Alterations to petal morphology in the new mutant were less severe that those in its mutant parent, *phan*-249G (see Results), suggesting that the *phan*-552 allele was dominant to *phan*-249G and responsible for the new phenotype. This was supported by analysis of plants produced by self-pollination of the new mutant, approximately one quarter of which resembled line 249G and were assumed to be *phan*-249G/*phan*-249G homozygotes, while the remainder resembled their parent and were assumed to consist of both heterozygotes and *phan*-552/*phan*-552 homozygotes. In order to obtain plants that were homozygous for the *phan*-552 allele, the new mutant was back-crossed to its wild-type parent, JI.75, to give F_1 progeny carrying either the *phan*-249G or *phan*-552 allele. One quarter of the progeny of each F_1 plant consisted of either severe *phan* mutants, assumed to be homozygous for the *phan*-249G allele, or plants that resembled the new *phan* mutant in morphology, suggesting that they were homozygous for the *phan*-552 allele. Plants assumed to be *phan*-552/*phan*-552 homozygotes were subsequently maintained by inbreeding.

Because the *phan*-552 allele arose in line JI.75, which carries active transposons, it was potentially transposon-induced. This was further supported by the observation that the allele was germinally unstable: 10% of the progeny resulting from self-pollination of the *phan*-552/*phan*-249G mutant had a wild-type $Phan^{+}$ phenotype. In contrast, *phan*-607, which was also obtained from line JI.75, and *phan*-249G and *phan*-250G produced only *phan* mutant progeny on self-pollination, suggesting that the mutant alleles in these lines did not carry active transposons.

Plant culture

Plants used for morphological analysis were grown at 20°C in a 16 hour light - 8 hour dark cycle, with illumination of 50 μmol m^{-2} s^{-1} from metal halide lamps. Those for genetic analysis were grown as described by Carpenter et al. (1987).

Microscopy

Wax embedded leaf material for histological sectioning was fixed and dehydrated using the method described by Jackson et al. (1994). 5-10 μm sections were stained with toluidine blue using the method of Sakai (1973), and the wax removed with Histoclear (CellPath plc, Hemel Hempstead, UK) before mounting. Alternatively, tissue was prepared as described by Roland and Vian (1991), embedded in Agar 100 epoxy resin (Agar Scientific Ltd., Stansted, UK) and 1 μm sections stained with toluidine blue. Scanning electron microscopy of apices was carried out on resin replicas made using a modification of the method described by Green and Linstead (1990). Specimens of plant material were coated in Extrude vinylsiloxane dental impression medium (Kerr UK Ltd., Peterborough, UK), which polymerised to form moulds. After about 30 minutes, the moulds were removed and infiltrated with Agar 100 epoxy embedding resin for 15 minutes at 70°C under vacuum. The vacuum was then released, the moulds drained of excess resin, and the remaining resin allowed to polymerise at 65°C for 16-24 hours. Resin replicas were gold coated before examination at ambient temperature in a scanning electron microscope.

RESULTS

Dorsoventrality in the wild-type *Antirrhinum* leaf

The wild-type *Antirrhinum* leaf shows dorsoventral asymmetry

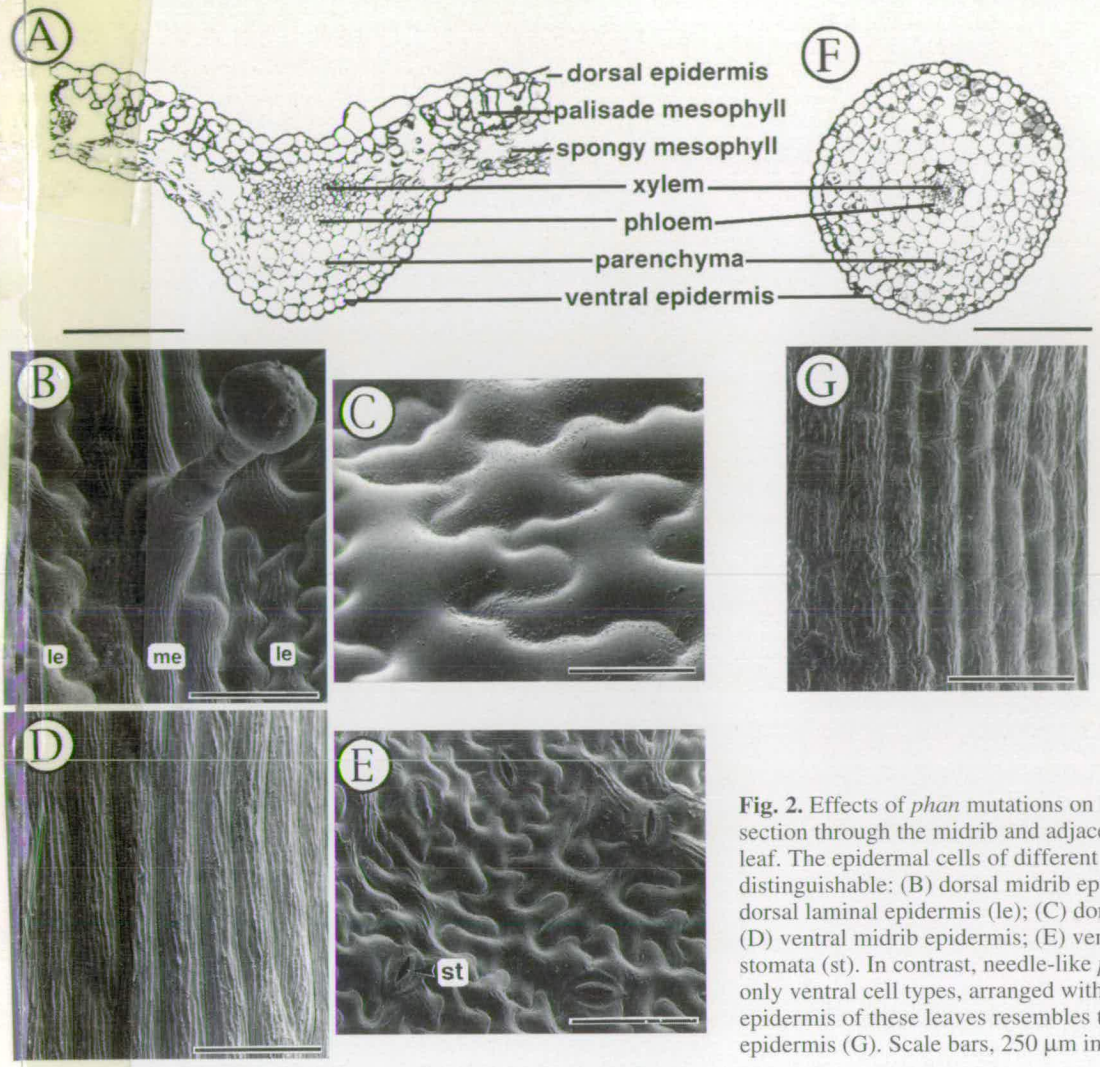

Fig. 2. Effects of *phan* mutations on leaf anatomy. (A) Transverse section through the midrib and adjacent laminal regions of a wild-type leaf. The epidermal cells of different regions are morphologically distinguishable: (B) dorsal midrib epidermis (me) and neighbouring dorsal laminal epidermis (le); (C) dorsal laminal epidermis; (D) ventral midrib epidermis; (E) ventral laminal epidermis, including stomata (st). In contrast, needle-like *phan* mutant leaves consist of only ventral cell types, arranged with radial symmetry (F). The epidermis of these leaves resembles that of wild-type ventral epidermis (G). Scale bars, 250 μm in A and F; 50 μm in B-E and G.

in two respects. First, the laminae, which make the leaf considerably wider than it is thick, arise towards the dorsal side of the midrib (Fig. 2A). Therefore the dorsal and ventral parts of the leaf are not mirror images of each other and the mature leaf possesses only one plane of symmetry, oriented vertically and running along the midrib. Secondly, both the laminae and midrib show a distinct arrangement of tissue layers. In regions of the lamina between veins, four distinct cell types are recognisable along the dorsoventral axis: dorsal epidermis, palisade mesophyll, spongy mesophyll and ventral epidermis. The ventral epidermis, shown in Fig. 2E, consists of cells which are smaller and more complex in outline than those of the dorsal epidermis (Fig. 2C) and is further characterised by the presence of stomata, which are absent from the dorsal surface of the leaf. Dorsoventral differences are also apparent in major veins, including the midrib. Here the vascular tissue consists of an arc of xylem on the dorsal side of an arc of phloem which together are surrounded by parenchyma (Fig. 2A). The epidermal cells which make up the ventral surface of the midrib are elongated along the proximodistal axis and are therefore distinct from the epidermal cells of the lamina (compare Fig. 2D,E). They can also be distinguished from the cells at the dorsal surface of the midrib, which are shorter and include hair cells (Fig. 2B). The petiole shows the same dorsoventral differences as the leaf, although it contains a much lower proportion of laminal tissue (data not shown).

Effects of *phantastica* mutations on leaf anatomy

The four *phantastica* (*phan*) mutants show similar vegetative phenotypes, although leaf morphology varies with the developmental stage of each plant. Leaves produced at, and above, the fifth node of *phan* mutants are typically needle-like and show no evidence of dorsoventrality (Figs 3B,D, 4A) They lack laminae and all cell-types associated with the dorsal region of the wild-type leaf. Internally, they consist entirely of ventral tissue types: parenchyma, phloem and xylem, which are arranged in concentric cylinders (Fig. 2F). They are therefore radially symmetrical in transverse section. The epidermis of these needles, shown in Fig. 2G, resembles that of the ventral midrib of a wild-type leaf, except that it also shows some laminal characters, in that the cells are shorter than those of the ventral midrib and occasional stomata are present, distributed evenly over the leaf surface. The phenotype of needle-like leaves suggests that *phan* is necessary for a dorsalising function which determines all aspects of dorsoventrality in leaves, including initiation of the laminae and development of dorsal cell types.

In contrast, the cotyledons and first three pairs of leaves of

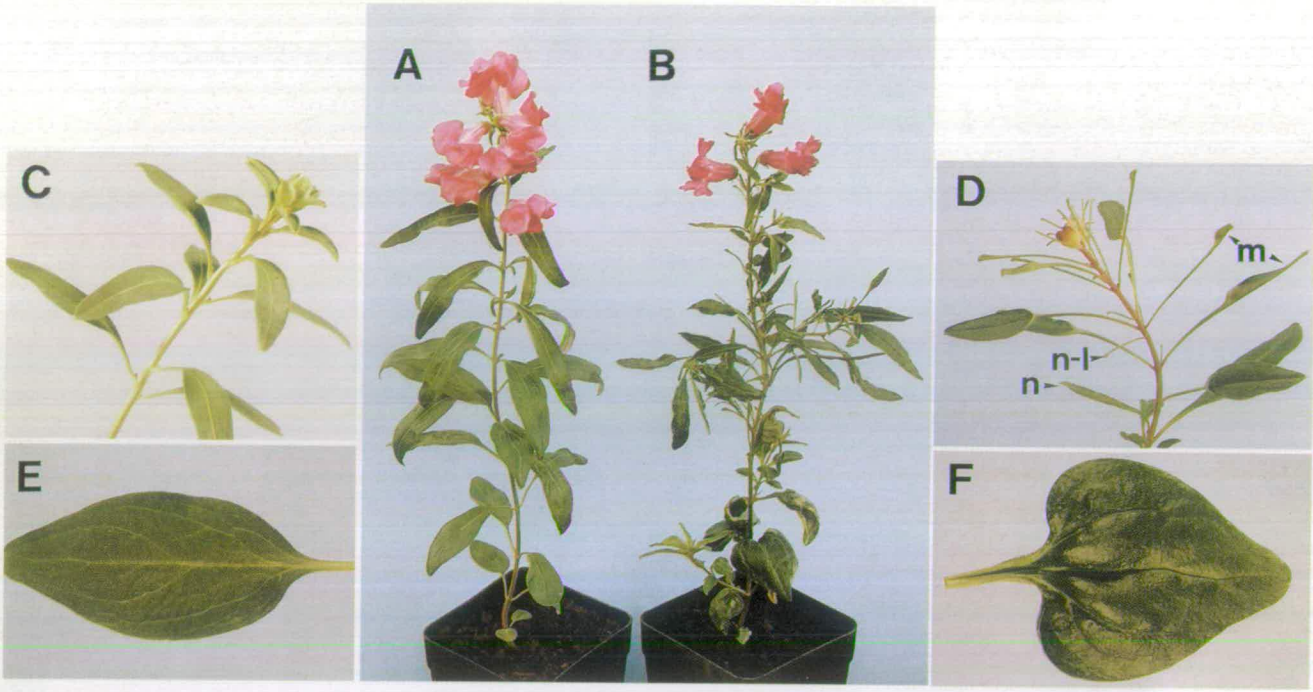

Fig. 3. Effects of *phan* mutations on morphology. (A) A wild-type plant and (B) the *phan*-607 mutant. (C) The vegetative shoot of a wild-type plant, and (D) the corresponding region of a *phan* mutant with narrow (n), needle-like (n-l) and mosaic (m) leaves. (E) A leaf from the second node of a wild-type plant, and (F) a broad, heart-shaped leaf typical of the equivalent node of a *phan* mutant.

phan mutants are broader and more heart-shaped than the corresponding leaves of wild-type plants (Fig. 3F), containing more cells in transverse section (data not shown). They are further characterised by patches of ventral epidermal tissue, which include stomata, on their dorsal surfaces (Fig. 5A,C). The boundary between these regions of ectopic ventral epidermis and the surrounding dorsal epidermis forms a ridge in an axis perpendicular to the leaf surface (Fig. 5B). In section, these ridges resemble the edges of a wild-type leaf, containing palisade mesophyll on the side covered by dorsal epidermis, and spongy mesophyll covered by ventral epidermis on the other (compare the ridges in Fig. 5D with the leaf margins in Fig. 6A). Within the ridges, the leaf lamina consists of ventral epidermal tissue on both upper and lower surfaces, with only spongy mesophyll between. Larger patches of ventral epidermis tend to be elongated in an axis parallel to the leaf venation, while smaller patches are more isodiametric. Patches are also larger and more frequent in the proximal part of the leaf where their size, shape and distribution resemble those of clones showing altered levels of chlorophyll in both *Antirrhinum* (Hudson et al., 1993) and tobacco (Poethig and Sussex, 1985b). This suggests that each may consist of clonally related cells, initiated relatively late in leaf development.

The transition between early heart-shaped leaves and later needle-like leaves of *phan* mutants is rarely abrupt. Leaves at intermediate nodes are typically narrower than those of wild-type or are mosaics of needle-like and laminal tissues (Fig 3D). Narrower leaves contain fewer cells in transverse section than wild-type and their laminae arise from more dorsal positions on the midrib (Fig. 6A). The most common form of mosaic leaf is one in which the proximal region is needle-like and the distal region laminal (Fig. 3D), although leaves with needle-like tissue distal to laminal tissue also occur. In both cases, the lamina forms an additional dorsal axis at the junction with needle-like tissue (Fig. 6B). The morphology of the boundary between ventralised (needle-like) tissue and dorsal (laminal) tissue therefore resembles that found at the boundary of patches of ventral epidermal cells in earlier, broad leaves of *phan* mutants.

Effects of *phan* mutations on leaf morphogenesis

The morphogenesis of needle-like leaves was compared with that of wild-type. Leaf primordia first become visible as bulges on the flanks of the apical meristem. At this early stage, mutant and wild-type primordia are indistinguishable (compare Fig. 7A,C). The proximal region of each primordium, the leaf buttress, extends laterally around the circumference of the apex, and therefore appears flattened. The distal region is also flattened, though less so. The dorsal flanks of the wild-type primordium in this region grow both distally and laterally to accentuate the flattened shape soon after initiation (Fig. 7A,B). In contrast, growth in the equivalent part of the *phan* mutant primordium is limited to the distal axis, and this produces a needle-like leaf (Fig. 7C). Only the very proximal part of the mutant leaf, produced from the leaf buttress, retains any flattening (Fig. 4A,D). Early developmental stages of mosaic leaves were also observed. In these, initiation of the laminae occurred at a more dorsal position on the primordium than in wild-type (Fig. 7D).

Development of the early, broader leaves of *phan* mutants was also characterised. The apical meristem at this stage of development is larger than that of more mature plants. Mature mutant leaves are broader than those of wild-type, containing more cells in transverse section, and mutant primordia appear

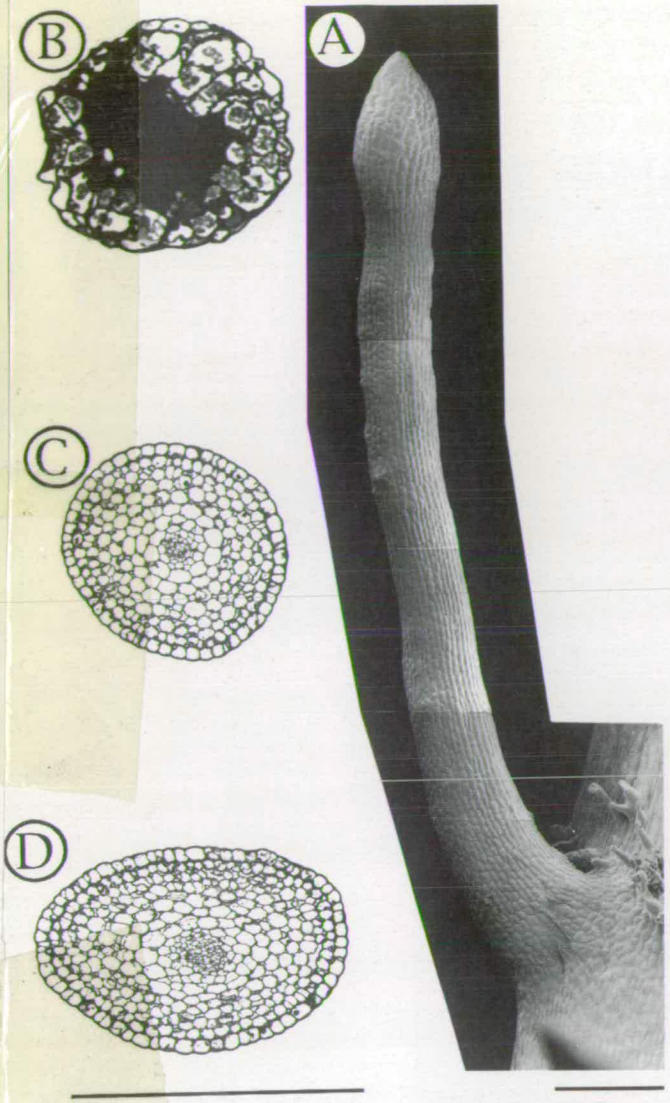

Fig. 4. A needle-like *phan* mutant leaf. (A) A mature needle-like leaf from a *phan* mutant, and transverse sections cut from the distal (B), middle (C) and proximal (D) parts of the same leaf. Only the most proximal region, derived from the leaf buttress, shows dorsoventral flattening, although it consists of only ventral cell types and has radially symmetrical vascular tissue. The darkly staining cells, of unknown function, in the distal region are also found in the tips of wild-type leaves. Scale bars, 250 μm.

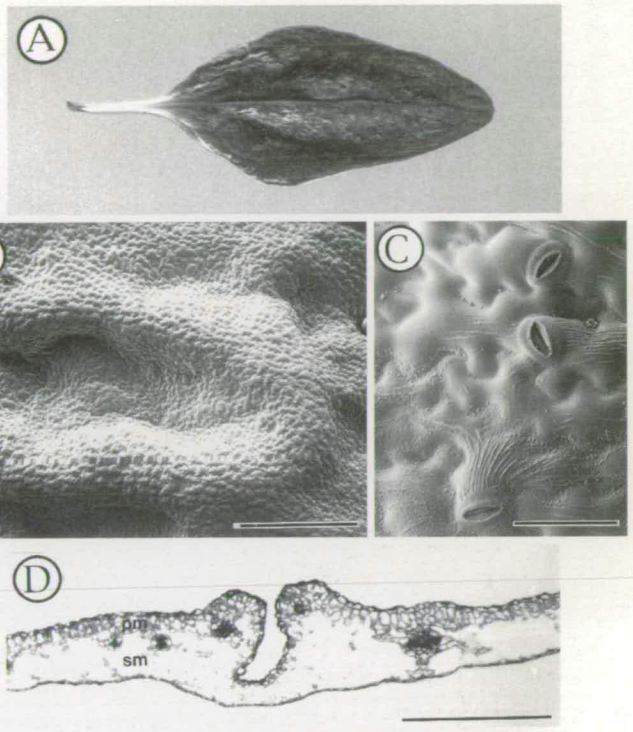

Fig. 5. Ectopic patches of ventral cell types in *phan* mutant leaves. (A) A leaf from the third node of a *phan* mutant plant. Patches of ventral epidermal tissue appear lighter than the surrounding dorsal epidermis and the leaf surface is uneven due to the presence of frequent ectopic laminal ridges. (B) Scanning electron micrograph of an ectopic patch of ventral tissue and the surrounding ectopic ridge. (C) Numerous stomata, characteristic of ventral epidermis, are present within the patches. (D) A transverse section through a patch of ventral tissue. The region within the ridges lacks palisade mesophyll cells (pm) but retains cells of the spongy mesophyll (sm). Scale bars, 500 μm in A, B and D; 50 μm in C.

slightly broader than those of wild-type soon after initiation (Fig. 7E,F). The initiation of ectopic laminal tissue, which surrounds patches of ventral cells in early mutant leaves, was not observed, suggesting that it occurs later in leaf development.

Effects of *phan* mutations on corolla morphology

Although the four *phan* mutants are virtually identical in vegetative development, each shows a characteristic floral morphology which does not vary between individual flowers of the same mutant line. Only development of the corolla is affected, and the remaining organs (sepals, stamens and carpels) are indistinguishable from those of wild-type flowers.

The wild-type corolla consists of five petals: two upper, two lateral and one lower. All are united over the proximal part of their length to form the corolla tube, at the distal end of which, the upper pair are separated from the lower three in the hinge region. The lower three petals remain further united forming the corolla face, before separating into distinct petal lobes (Fig. 8A). In analogy to the leaf, the outer (abaxial) surface of the corolla can be considered ventral, and the inner (adaxial) surface dorsal. As in leaves, the epidermal cells which form the two surfaces show different morphologies. In the petal lobes and corolla face, cells of the dorsal epidermis are characterised by conical projections, while ventral epidermal cells form a smooth surface, although this is punctuated by hairs (Noda et al., 1994).

Of the four mutations, *phan*-250G has the most severe effect on corolla morphology. The petal lobes are reduced to needles consisting of cell types characteristic of the ventral part of a wild-type petal (Fig. 8B) This ventralised morphology can therefore be considered homologous to that of needle-like leaves. Although the upper and lowest petal lobes are each reduced to a single needle, each lateral petal lobe is represented by a pair of needles.

Whereas petals of the *phan*-250G mutant are reduced to needles, those of the *phan*-249G and *phan*-552 mutants consist of reduced petal lobes with needles arising from their ventral

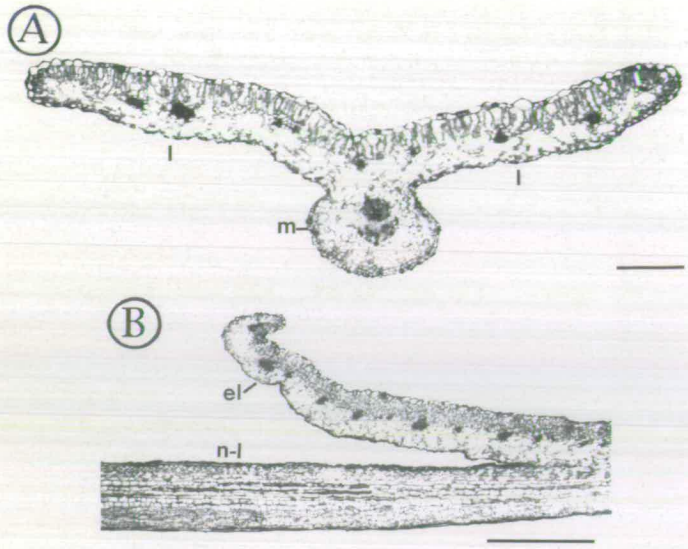

Fig. 6. Anatomy of *phan* mutant leaves with laminae. (A) Transverse section of a narrow *phan* mutant leaf. The laminae (l) are produced at a more dorsal position on the midrib (m) than in wild-type (compare with Fig. 2A). (B) A longitudinal section through a mosaic *phan* mutant leaf at the boundary between laminal and needle-like tissue. In this region, the lamina forms an ectopic dorsal axis (el), distinct from that of the needle-like tissue (n-l). The distal part of the leaf is to the left. Scale bars, 250 μm in A and 500 μm in B.

surfaces (Fig. 8C,D). Each needle is the most distal part of a ridge of ventral tissue which extends between the points where the petal lobe joins its neighbours (Fig. 8E).

To determine the relationship between the needles and petal lobes in these mutants, floral development of the mutant *phan*-249G was compared with that of wild type. In wild-type flowers, five petal primordia, initiated on the flanks of the floral meristem, give rise to the petal lobes (Fig. 9A-E). A more proximal group of cells, which encircles the floral meristem in a continuous band, divides to displace the lobes distally and form the corolla tube. Only the ventral surface of the corolla is visible until the petal lobes expand and reflex to reveal their dorsal surfaces.

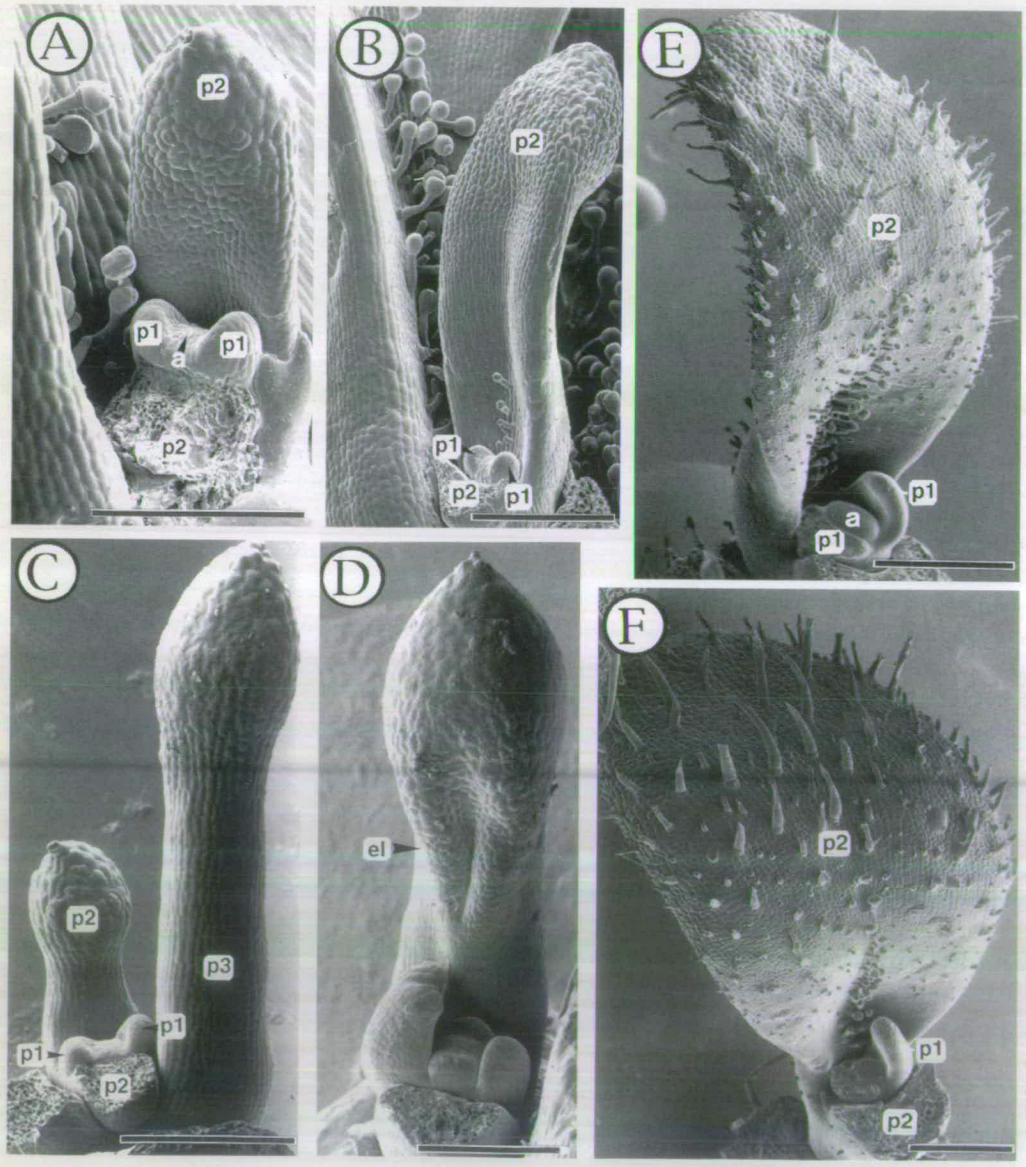

Fig. 7. Morphogenesis of wild-type and *phan* mutant leaves. (A) A wild-type apex late in vegetative development. Two newly initiated leaf primordia (p1) flank the apical meristem (a). One of the older pair of leaves (p2) has been removed. At this stage, p2 shows obvious dorsoventral flattening. Subsequent growth rapidly extends the leaf axis and also increases flattening to the stage shown in B. The equivalent region of a *phan* mutant shoot is shown in C. Newly initiated primordia (p1) are indistinguishable from those of wild-type, but fail to undergo lateral expansion and therefore extend into needle-like leaves (p2 and p3). (D) Formation of a mosaic leaf. The oldest leaf shown is needle-like in its proximal region but forming an ectopic lamina (el) at its distal end. The lamina is at a more dorsal position than in wild-type (compare with B) and extends across the primordial axis. (E) A wild-type apex early in development. The the first true leaf of the plant is the largest shown (p2). The equivalent *phan* mutant leaf (F) is slightly broader than wild-type, but has yet to show ectopic laminal tissue characteristic of early mutant leaves. All scale bars, 250 μm.

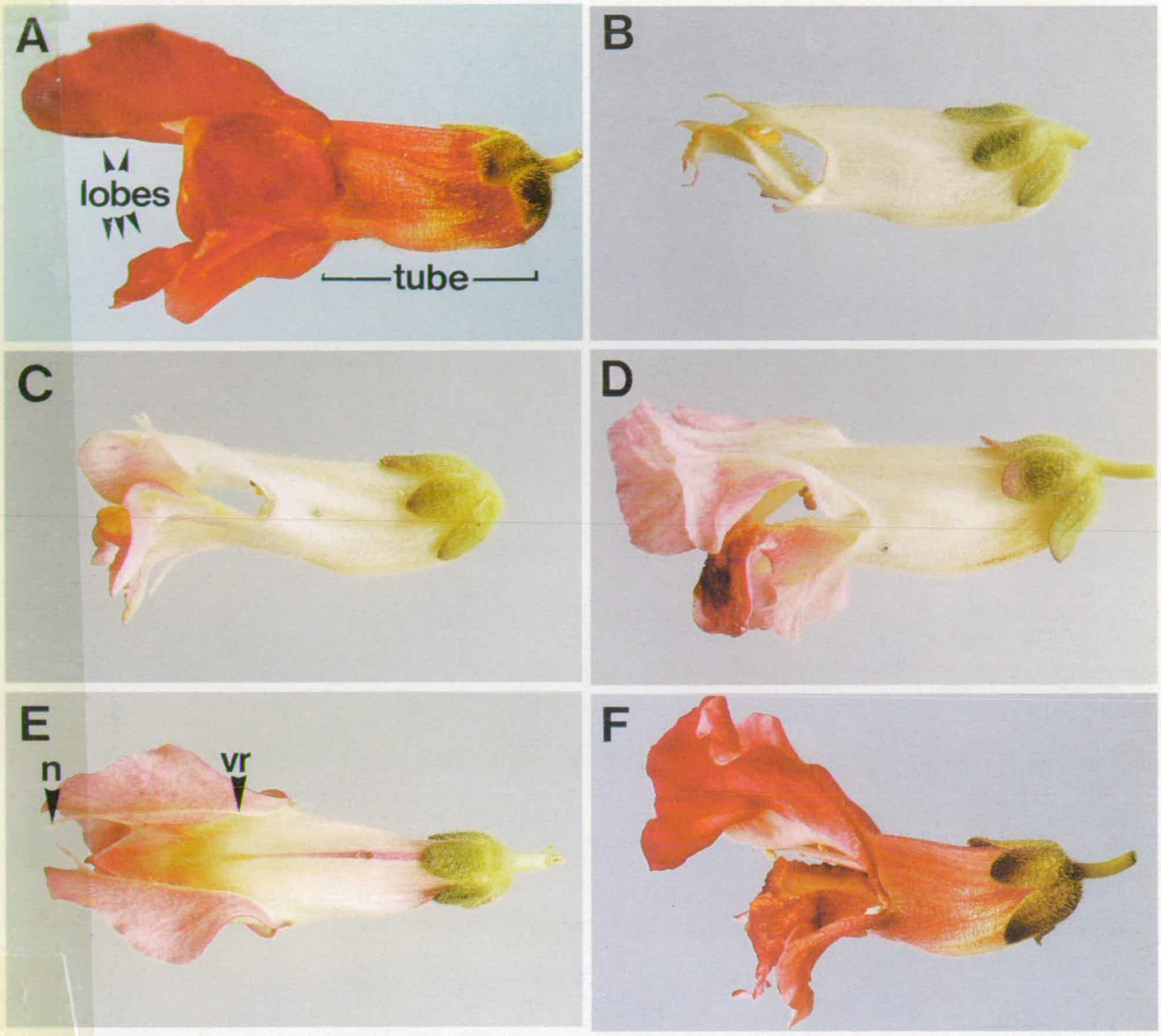

Fig. 8. Effects of *phan* mutations on flower morphology. The wild-type flower (A) consists of five petals which are united proximally to form the corolla tube, but separate distally into five petal lobes. (B) A flower of the *phan*-250G mutant in which petal lobes have been reduced to needles. Progressively lesser reductions in lobe tissue are shown by the *phan*-249G (C) and *phan*-552 (D) mutants. (E) The needles in these mutants (n) form the most distal part of a ridge of ventral tissue running across the ventral surface of the corolla. This ventral ridge (vr) can be seen as lighter coloured tissue. (F) A flower of the *phan*-607 mutant. Differences in corolla pigmentation result from different combinations of alleles affecting anthocyanin synthesis in the inbred lines.

At initiation, the petal primordia of the *phan*-249G resemble those of wild-type flowers (Fig. 9F,G). However, their distal regions fail to grow laterally and extend only distally to form needles (Fig. 9H-J). A novel axis of growth is initiated on the dorsal slope of each primordium, and this produces a reduced petal lobe (Fig. 9J). The ridge of ventral tissue associated with the needles represents the lateral edges of the early petal primordia. The lobes remain relatively inconspicuous until the flower opens, when they expand and reflex to displace the needles ventrally. The morphology of these petals can therefore be considered homologous to that of mosaic mutant leaves with needle-like tissue distal to laminal tissue. In both cases, the most distal part of the primordium develops without dorsoventrality, to form needle-like tissue, while a novel dorsal axis of growth is initiated at the boundary between dorsal and ventral tissue types.

The effect of the *phan*-607 mutation on corolla morphology is similar, but less severe than those of the other mutations. The petal lobes are larger and needles are rarely formed (Fig. 8F). The ridge of ventral tissue may remain united with the petal lobes as far as their distal edges. Because the lobes undergo more lateral expansion than the ridge, they become folded. A further characteristic of all mutants, except *phan*-250G, is that patches of ventral epidermis are seen on the dorsal surfaces of their petal lobes and corolla face. As is the case with patches of ventral epidermis in heart-shaped mutant leaves, the boundary between dorsal and ventral epidermis forms a ridge (Fig. 10A). This ridge has a similar morphology

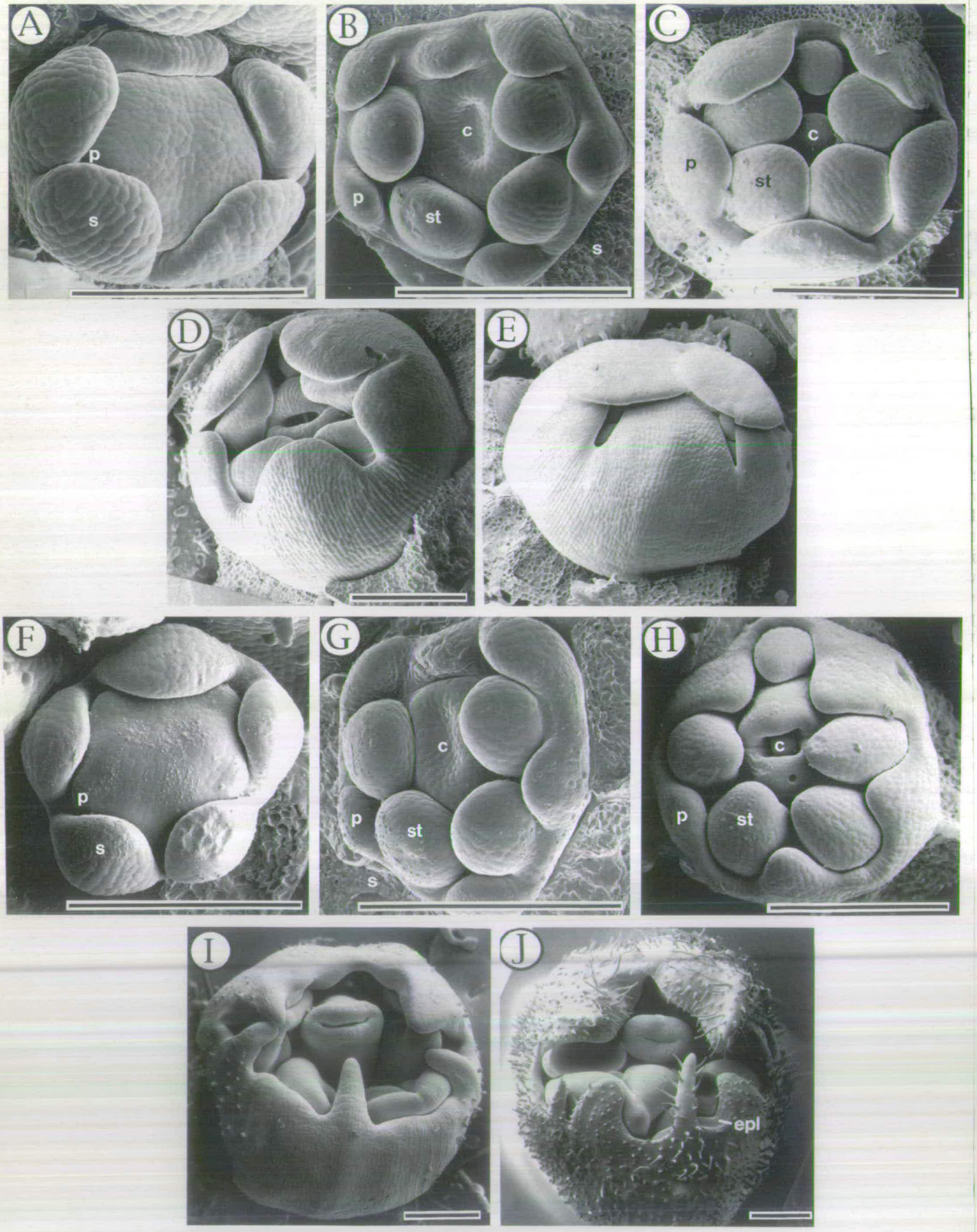
A
p
s
B
c
p
st
s
C
c
p
st
D
E
F
p
s
G
c
p
st
s
H
c
p
st
I
J
epl

to the edge of a wild-type petal (Fig. 10B), and can therefore be considered an additional petal axis.

Effects of temperature on *phan* mutant phenotypes

All four mutants are more similar to wild-type when grown at higher temperatures. For example, the *phan*-607 mutant grown at 17°C produces large cotyledons with frequent patches of ventral epidermis and ectopic leaf edges on their dorsal surfaces. Subsequent leaves are almost all needle-like (Fig. 11). In marked contrast, leaves of the same line grown at 25°C are similar in outline to those of wild-type and rarely show patches of ectopic ventral epidermis. A similar response to temperature is shown by the other three *phan* mutants. One explanation for this effect is that all four mutants retain some degree of *phan* expression and that this is greater at higher temperatures. Alternatively, the effect of the *phan* mutations may be to reveal the temperature sensitivity of one or more other genes which are also involved in determining dorsoventrality.

DISCUSSION

Although each *phan* mutant shows a variety of leaf phenotypes, they suggest a relatively simple model for the determination of dorsoventrality. This involves a dorsalising function, DF, which is expressed in the most dorsal cells of the wild-type leaf primordium (Fig. 12A). Soon after primordial initiation, a plate of cells near the ventral boundary of the expression domain is induced to change division pattern and so form the laminae by lateral proliferation. DF expression persists in the dorsal part of the lamina where it is necessary to specify the identity of dorsal cell types (dorsal epidermis, palisade and spongy mesophyll).

Needle-like leaves of *phan* mutants lack laminae and dorsal cell types: a phenotype suggesting complete loss of DF (Fig. 12B). Other leaf forms produced by *phan* mutants can be explained by reductions in the domain of DF expression. Expression confined to a more dorsal region, as depicted in Fig. 12C, is predicted to have two effects. First, the laminae will be formed at a more dorsal position and a larger part of the primordium will develop with ventral identity. Secondly, because the primordium is widest at its midpoint, the shifted margin of the expression domain will contain fewer laminal initial cells and the leaf may therefore be narrower. Such narrow leaves with laminae at more dorsal positions are characteristically produced at intermediate nodes of *phan* mutants. In other primordia, the DF domain could be restricted to either a more distal or a more proximal position (Fig. 12D,E). In these cases, the region lacking expression would develop a needle-like morphology. Cells at the boundary of the domain would form laminal tissue, and because the boundary crosses the dorsal side of the primordium, the lamina would form a novel axis of growth in this region. The mosaic leaves of *phan* mutants show morphologies consistent with this prediction. Early leaves of *phan* mutants are broader than wild type and show ectopic patches of ventral cell types. This morphology could result from localised loss of DF relatively late in leaf development (Fig. 12F). Lack of DF would prevent differentiation of dorsal cell types, and the newly introduced boundary of DF expression around each patch of cells would induce formation of ectopic laminal tissue. Proliferation at the introduced boundaries might also contribute to increased lateral growth. Because patches of ventral cells are more frequent in the proximal region, this would produce a heart-shaped mutant leaf with its widest point closer to the petiole than in wild type.

One explanation for the general decrease in dorsal tissues in successive *phan* mutant leaves is that the dependence of DF on *phan* expression increases during vegetative development. Alternatively, it might reflect a gradual loss of *phan* activity remaining in mutants.

Leaf morphogenesis shows a number of similarities to development of insect wings. The wing is formed from a group of

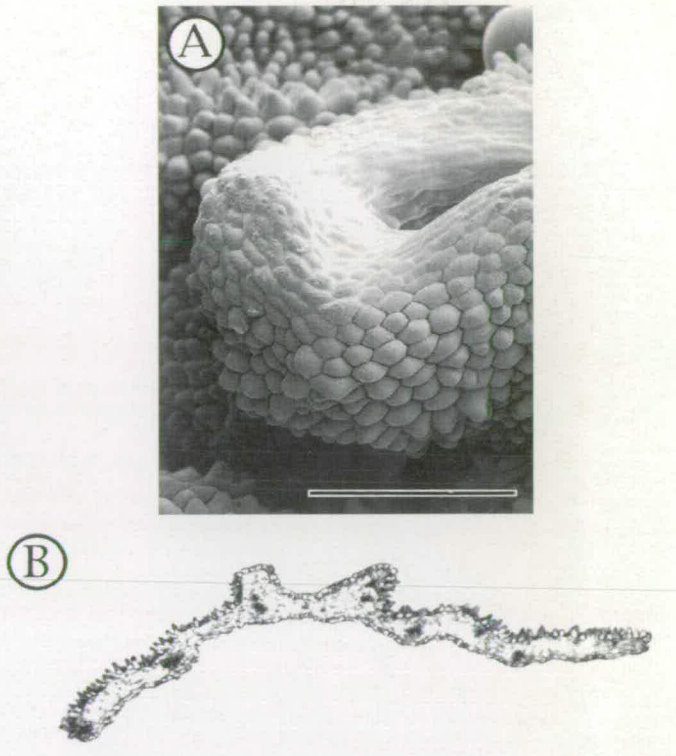

Fig. 10. Ectopic ventral tissue in *phan* mutant petals. (A) A ridge of tissue has formed at the boundary between dorsal epidermis (conical cells) and ectopic ventral epidermis (flatter cells) in a *phan*-607 mutant petal lobe. (B) Transverse section through a mutant petal lobes containing an equivalent patch of ectopic ventral epidermis. The ectopic dorsal ridges resemble the lateral margins of the petal. Scale bars, 250 μm.

Fig. 9. The effects of *phan* mutations on floral development. (A-E) Stages in the development of wild-type flowers. In (A) petal primordia (p) are visible between sepal primordia (s). Sepals have been removed in subsequent stages to reveal development of the corolla. The petal primordia grow in length and laterally to cover the developing stamens (st) and carpels (c), by the stage shown in E. In flowers of the *phan*-249G mutant, petal primordia resemble those of wild-type in early developmental stages (F-G), but subsequently show reduced lateral growth (H). They therefore form spikes at the distal end of the corolla tube (I). Ectopic petal lobes (epl) are formed on the dorsal side of these spikes later in development (J). The epidermal hairs on the corolla of the flower in J are a sepaloid character occasionally seen in both mutant and wild-type plants and therefore not characteristic of *phan* mutant flowers. All scale bars, 250 μm.

Fig. 11. Effects of temperature on the phenotype of *phan* mutants. Plants of the mutant line *phan*-607 were grown at 25°C, 20°C and 17°C. Those at higher temperatures more closely resemble wild type. All plants are the same age.

initial cells, the imaginal disc, present within the larval body. In both wings and leaves, localised cell proliferation leads to growth in a new axis, away from the insect body or stem, and lateral growth produces a dorsoventrally flattened organ (García-Bellido and Mirriam, 1971; Milner and Muir, 1987). Wings, like leaves, also show differences between dorsal and ventral cell types. In *Drosophila*, a transcription factor encoded by the *apterous* (*ap*) gene is necessary both for dorsoventrality and for production of the wing axis (Cohen et al., 1992). Expression of *ap* becomes established within a dorsal domain of the wing imaginal disc during larval development. Juxtaposition of *ap*-expressing and *ap*-nonexpressing cells leads to activation of a number of genes in domains running along the ventral boundary of the *ap* expression domain (Diaz-Benjumea and Cohen, 1993; Williams et al., 1993, 1994) As a result, cells adjacent to the boundary form the wing margin, while cells dorsal and ventral to the margin initials proliferate to form the wing blade. Expression of *ap* persists in dorsal cells of the developing wing, and is necessary for determination of dorsal cell type. The roles of *ap* in wing development therefore appear similar to those proposed for DF in the leaf. This is illustrated by the effect of removing *ap* expression from clones of dorsal initial cells. These ap^- cells develop as patches of ventral tissue surrounded by ectopic wing axes (Diaz-Benjumea and Cohen, 1993) and are therefore analogous to patches proposed to result from loss of DF in early leaves of *phan* mutants. However, *ap* and DF differ in one important respect. Wing discs that lack *ap* expression fail to grow in the proximodistal axis, indicating that *ap* is required for specification of this axis (Butterworth and King, 1965). In contrast, even an extreme needle-like leaf, which has shown no lateral growth, retains a proximodistal axis, suggesting that determination of this axis is independent of DF in leaves.

By analogy to the role of *ap* in wing development, the domain of DF expression in leaves may correspond to cells that express *phan* and other genes required for DF activity. Differences in cell fate within the domain may then be the result of interactions between DF and other functions with adjacent or partially overlapping domains. For example, overlap between the DF domain and that of a ventralising factor might activate localised expression of genes required for production of the lamina. The existence of potential target genes has been revealed by mutations in a number of dicot species which specifically reduce laminal proliferation, without affecting dorsoventrality of the leaf (e.g. McHale, 1992).

DF expression might be established in response to a morphogen which forms a gradient in the apical meristem. Support for the role of a gradient in establishing leaf dorsoventrality has been provided by surgical experiments carried out on vegetative meristems of potato (Sussex, 1955), *Epilobium* (Snow and Snow, 1959) and *Sesamum* (Hanawa, 1961). Incisions that isolated leaf initials from the apex frequently led to the production of leaves with radial symmetry (a phenocopy of the needle-like leaves of *phan* mutants). Smaller cuts, positioned so as to only partially isolate the initials, produced leaves with narrower laminae (Sussex, 1954) similar to those proposed to result from partial loss of DF in *phan* mutants. These results suggested that a gradient with a source originating in the apex was responsible for determination of dorsoventrality in leaf initials.

Wild-type leaf primordia become distinguishable from those of *phan* mutants when they begin to show lateral proliferation soon after initiation. For DF to be effective at this stage, its expression must have been established earlier, possibly prior to leaf initiation. In the case of the *Drosophila* wing, expression of *ap* begins in the imaginal disc (Cohen et al., 1992), presumably in response to dorsoventral polarity in the larval body (reviewed by St Johnstone and Nüsslein-Volhard, 1992). It therefore not only maintains dorsoventral polarity from the larval body to the wing, but also serves to translate it into formation of a new wing axis. By analogy, DF may allow apical-basal polarity in the vegetative meristem to specify dorsoventrality in leaves and to elaborate a new lateral axis as a result. While the potential nature of apical-basal polarity in the meristem remains obscure, its existence is revealed by patterned expression of a number of genes in this region (Fleming et al., 1993; Medford et al., 1991; Smith et al., 1992).

The model proposed to explain the effects of *phan* mutations on leaf morphogenesis is equally applicable to development of petal lobes. In wild-type flowers, expression of DF is proposed to occur in dorsal cells of the petal primordia. Lateral proliferation towards the boundary of expression forms the petal lobes, and the DF later specifies the identity of dorsal cell types. In the most extreme mutant, (*phan*-250G), the petal

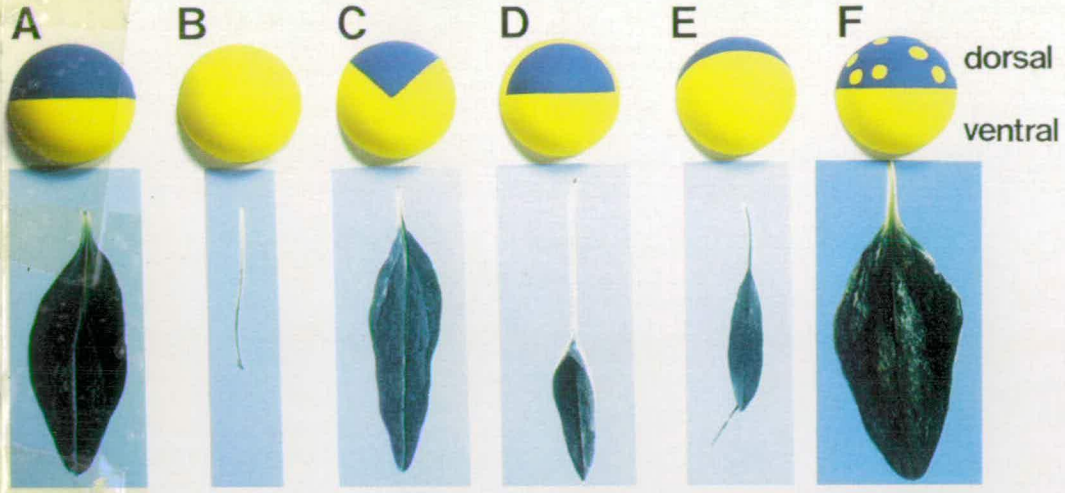

Fig. 12. A model for the action of the dorsalising function in leaf development. Early leaf primordia are depicted as yellow hemispheres viewed from a distal position. Dorsal regions of the primordia experiencing DF expression are coloured blue. Different leaf morphologies are shown below the patterns of expression which are proposed to have given rise to them. Mature leaves are viewed from above, with their distal ends towards the bottom of the page. (A) A wild-type leaf; (B) a needle-like *phan* mutant leaf; (C) a narrow leaf of a *phan* mutant; (D,E) mosaic mutant leaves; (F) an early *phan* mutant leaf showing ectopic patches of ventral cell types. See text for further explanation.

primordia develop as needles of ventral tissue. This morphology is similar to that of needle-like leaves and suggests absence of DF expression from petal primordia. The floral phenotypes of the remaining four mutants are consistent with reductions in the domain of DF expression to more dorsal positions. The regions without DF develop as needles or form part of a ridge of ventral tissue, and reduced petal lobes are formed at the shifted boundary of DF expression on their dorsal flanks: a morphology which is similar to that of the mutant leaf shown in Fig. 10E. The differences in floral phenotype between the four *phan* mutants suggest that each shows a characteristic reduction in the domain of DF expression. Those with stronger expression are predicted to produce larger petal lobes at more dorsal positions on the primordia. The final feature of *phan* mutant petal lobes is that they may show patches of ventral cell types surrounded by ectopic lobe tissue on their dorsal surfaces. This effect on petal development appears similar to that observed in early leaves of *phan* mutants, and can also be explained by loss of DF expression from groups of dorsal initial cells.

The similarity of the effects of *phan* mutations on leaves and petal lobes is consistent with the view that these are homologous structures. However, dorsoventrality in the corolla tube and in floral organs other than petals remains unaffected in the mutants. This is particularly striking in the case of sepals, which in wild-type are very similar in morphology to bracts. Whereas the bracts of *phan* mutants are commonly reduced to needle-like structures, their sepals invariably resemble those of wild-type. One explanation for this difference is that dorsoventrality in floral organs other than petal lobes may be independent of *phan* expression. Alternatively, the level of DF expression in *phan* mutants may be limiting in leaves, bracts and petal lobes, but sufficient for determination of dorsoventrality in other organs.

Leaves of *phan* mutants may resemble those characteristic of other plants. For example, needle-like mutant leaves have a similar morphology to tendrils and spines, which in many species are considered to be modified leaves or leaflets (Goebel, 1905). Likewise, peltate leaves with laminal tissue which completely surrounds the petiole, as in nasturtium (*Tropaeolum majus*), resemble those of *phan* mutants in which the proximal region lacks dorsoventrality and the distal region is laminal. The development of peltate leaves also mirrors that of a mosaic mutant leaf, in that the proximal part of the lamina which forms an axis distinct from the petiole, is formed by proliferation on the dorsal surface of the primordium after initiation (Hagemann, 1984; Troll, 1932). In *phan* mutants, these differences in leaf morphology are proposed to result from relatively small changes in the strength or position of DF expression. Equally subtle changes may therefore be responsible for evolution of a number of leaf forms.

At least one of the *phan* mutant alleles is germinally unstable and able to revert to wild type at a frequency characteristic of other transposon-induced mutations in *Antirrhinum* (Carpenter and Coen, 1990). This mutant should therefore allow the *phan* locus to be isolated by transposon tagging, and the role of the gene in determination of dorsoventrality to be examined further.

We thank Des Bradley, Rosemary Carpenter and Enrico Coen for constructive comments on the manuscript. This work was supported by BBSRC.

REFERENCES

Avery, G. S. (1933). Structure and development of the tobacco leaf. *Am. J. Bot.* **20**, 565-592.

Baur, E. (1926). Untersuchungen über Faktormutationen. I. *Antirrhinum majus* mut. *phantastica*, eine neue, dauernd zum dominanten Typ zurückmutierende rezessive Sippe. *Z. f. indukt. Abst. u. Vererbungsl.* **41**, 47-53.

Butterworth, F. M. and King, R. C. (1965). The developmental genetics of apterous mutants in *Drosophila melanogaster*. *Genetics* **52**, 1153-1174.

Carpenter, R. and Coen, E. S. (1990). Floral homeotic mutations produced by transposon-mutagenesis in *Antirrhinum majus*. *Genes Dev.* **4**, 1483-1493.

Carpenter, R., Martin, C. and Coen, E. S. (1987). Comparison of genetic behaviour of the transposable element Tam3 at two unlinked pigment loci in *Antirrhinum majus*. *Mol. Gen. Genet.* **207**, 82-89.

Coen, E. S. and Carpenter, R. (1993). The metamorphosis of flowers. *Plant Cell* **5**, 1175-1181.

Cohen, B., McGriffin, M. E., Pfeifle, C., Segal, D. and Cohen, S. M. (1992). *apterous*: a gene required for imaginal disc development in *Drosophila*

encodes a member of the LIM family of developmental regulatory proteins. *Genes Dev.* **6**, 715-729.

DeLong, A., Calderon-Urrea, A. and Dellaporta, S. L. (1993). Sex determination gene *TASSELSEED2* of maize encodes a short-chain alcohol dehydrogenase required for stage-specific floral organ abortion. *Cell* **74**, 757-768.

Diaz-Benjumea, F. J. and Cohen, S. M. (1993). Interaction between dorsal and ventral cells in the imaginal wing disc directs wing development in Drosophila. *Cell* **75**, 741 - 752.

Dubuc-Lebreux, M. A. and Sattler, R. (1980). Développment des organes foliacés chez *Nicotiana tabacum* et le problème des méristèmes marginaux. *Phytomorphology* **30**, 17-32.

Fleming, A. J., Mandel, T., Roth, I. and Kuhlemeier, C. (1993). The patterns of gene expression in the tomato shoot apical meristem. *Plant Cell* **5**, 297-309.

Foster, A. S. (1936). Leaf differentiation in angiosperms. *Bot. Rev.* **2**, 349-372.

García-Bellido, A. and Merriam, J. R. (1971). Parameters of the wing imaginal disc development of *Drosophila melanogaster*. *Dev. Biol.* **24**, 61-87.

Goebel, K. (1905). *Organography of Plants*. (trans. I. B. Balfour). Oxford: Clarendon Press.

Gottschalk, W. (1970). Possibilities of leaf evolution through mutation and recombination. A model for the evolution and further evolution of leguminous leaves. *Z. Pflantzenphysiol.* **63**, 44-54.

Green, P. B. and Linstead, P. (1990). A procedure for SEM of complex structures applied to the inflorescence of snapdragon (*Antirrhinum*). *Protoplasma* **158**, 33-38.

Hagemann, W. (1984). Morphological aspects of leaf development in ferns and angiosperms. In *Contemporary problems in plant anatomy*. (eds. R. A. White and W. C. Dickison) pp. 301-349. Orlando: Academic Press.

Hanawa, J. (1961). Experimental studies of leaf dorsiventrality in *Sesamum indicum L. Bot. Mag. Tokyo* **74**, 303-309.

Harrison, B. J. and Carpenter, R. (1979). Resurgence of genetic instability in *Antirrhinum majus. Mut. Res.* **63**, 47-69.

Hudson, A., Carpenter, R. and Coen, E. S. (1993). *Olive*: a key gene required for chlorophyll synthesis in *Antirrhinum majus. EMBO J.* **12**, 3711-3719.

Jackson, D., Veit, B. and Hake, S. (1994). Expression of maize *KNOTTED1* related homeobox genes in the shoot apical meristem predicts patterns of morphogenesis in the vegetative shoot. *Development* **120**, 405-413.

Jeune, B. (1981). Position et orientation des mitoses dans la zone organogène des jeunes feuilles de *Fraxinus excelsior*, *Glechoma hederacea* et *Lycopus europaeus*. *Can. J. Bot.* **62**, 2861-2864.

McHale, N. A. (1992). A nuclear mutation blocking initiation of the lamina in leaves of *Nicotiana sylvestris. Planta* **186**, 355-360.

Medford, J. I., Elemer, J. S. and Klee, H. J. (1991). Molecular cloning and characterisation of genes expressed in shoot apical meristems. *Plant Cell* **3**, 359-370.

Milner, M. J. and Muir, J. (1987). The cell biology of *Drosophila* wing metamorphosis *in vitro*. *Roux's Arch. Dev. Biol.* **196**, 191-201.

Noda, K., Glover, B., Linstead, P. and Martin, C. (1994). Flower colour intensity depends on specialised cell shape controlled by a Myb-related transcription factor. *Nature* **369**, 661-664.

Poethig, R. S. and Sussex, I. M. (1985a). The developmental morphology and growth dynamics of the tobacco leaf. *Planta* **165**, 158-169.

Poethig, R. S. and Sussex, I. M. (1985b). The cellular parameters of leaf development in tobacco: a clonal analysis. *Planta* **165**, 170-184.

Roland, J. C. and Vian, B. (1991). General preparation and staining of thin sections. In *Electron Microscopy of Plant Cells* (ed. Hall, J. L. and Hawes, C.), pp. 1-66. London: Academic Press.

Sakai, W. S. (1973). Simple method for differential staining of paraffin embedded plant material using toluidine blue O. *Stain Technol.* **48**, 247-249.

Shepherd, N. (1988). Transposable elements and gene tagging. In *Plant Molecular Biology, A Practical Approach* (ed. C. H. Shaw), pp. 187-220. Oxford: IRL Press.

Smith, L., Green, B., Veit, B. and Hake, S. (1992). A dominant mutation in the maize homeobox gene, *Knotted-1*, causes its ectopic expression in leaf cells with altered fates. *Development* **116**, 21-30.

Snow, M. and Snow, R. (1959). The dorsiventrality of leaf primordia. *New Phytol.* **58**, 188-207.

St Johnstone, D. and Nüsslein-Volhard, C. (1992). The origin of pattern and polarity in the Drosophila embryo. *Cell* **68**, 201-219.

Stubbe, H. (1966). *Genetik und Zytologie von* Antirrhinum *L. sect.* Antirrhinum. Jena: Gustav Fischer.

Sussex, I. M. (1954). Experiments on the cause of dorsiventrality in leaves. *Nature* **174**, 351-352.

Sussex, I. M. (1955). Experimental investigation of leaf dorsiventrality and orientation in the juvenile shoot. *Phytomorphology* **5**, 286-300.

Tepfer, S. S. (1953). Floral anatomy and ontogeny in *Aquilegia formosa* var. *truncata* and *Ranunculus repens*. *Univ. Calif. Pub. Bot.* **25**, 513-648.

Troll, W. (1932). Morphologie der schildförmigen Blätter. *Planta* **17**, 153-314.

Vollbrecht E., Veit, B., Sinha, N. and Hake, S. (1991). The developmental gene *knotted-1* is a member of a maize homeobox gene family. *Nature* **503**, 241-243.

Weigle, D. and Meyerowitz, E. M. (1994). The ABCs of floral homeotic genes. *Cell* **78**, 203-209.

Williams, J. A., Paddock, S. W. and Carroll, S. B. (1993). Pattern formation in a secondary field: a hierarchy of regulatory genes subdivides the *Drosophila* wing into discrete subregions. *Development* **117**, 571-584.

Williams, J. A., Paddock, S. W., Vorwerk, K. and Carroll, S. B. (1994). Organisation of wing formation and induction of a patterning gene at the dorsal/ventral compartment boundary. *Nature* **368**, 299-305.

(Accepted 4 April 1995)